TRANSNUCLEAR

July 6, 2004
NUH03-04-61

Mr. L. Raynard Wharton
Spent Fuel Project Office, NMSS
U. S. Nuclear Regulatory Commission
11555 Rockville Pike M/S O13-D-13
Rockville, MD 20852

Subject: Response to Request for Additional Information (RAI) and Submittal of Revision 1 of Application for Amendment No. 8 to the NUHOMS® Certificate of Compliance No. 1004 (TAC NO. L23653)

References:
1. NRC Request for Additional Information Regarding Approval To Add NUHOMS® -24PTH System to the Standardized NUHOMS® System (TAC NO. L23653), Dated May 3, 2004.
2. Revision 0 of Application for Amendment No. 8 to the NUHOMS® Certificate of Compliance (CoC), No. 1004, Submitted September 19, 2003.

Dear Mr. Wharton:

Transnuclear, Inc. (TN) herewith submits our responses to the RAI (Reference 1) and Revision 1 of our application for Amendment No. 8 to the NUHOMS® CoC No. 1004.

This package is organized in the following format to facilitate your staff's review:

- Affidavit for Withholding Proprietary Information (Enclosure 1),
- Ten Copies of Revision 1 of Application for Amendment No. 8 to the NUHOMS® CoC No. 1004, Proprietary Version (Replacement Pages Only, Enclosure 2),
- Three Copies of Revision 1 of Application for Amendment No. 8 to the NUHOMS® CoC No. 1004, Non-Proprietary Version (Replacement Pages Only, Enclosure 3), and
- Response to the RAI (Enclosure 4).

An overview of the Revision 1 changes is provided in Attachment A of Enclosure 2. Besides addressing the RAI Questions, TN has also addressed staff's verbal questions in a subsequent telecon on Chapter P.9.

NMSS01

This submittal includes proprietary documents which may not be used for any purpose other than to support your staff's review of the application. In accordance with 10 CFR 2.390, Transnuclear, Inc. is providing an affidavit (Enclosure 1) specifically requesting that you withhold this proprietary information from public disclosure.

Please replace the affected pages of the Revision 0 application (Reference 1) with the changed pages submitted herewith.

Should you or your staff require additional information to support review of this application, please do not hesitate to contact me at 510-744-6053 or Mr. Jayant Bondre at 510-744-6043.

Sincerely,

James W. Ayler for UBCHOPRA

U. B. Chopra

Licensing Manager

Docket 72-1004

Enclosures:

1. Affidavit for withholding proprietary information.
2. Ten Copies of Revision 1 of Application for Amendment No. 8 to the NUHOMS® CoC No. 1004, Proprietary Version (Replacement Pages Only).
3. Three Copies of Revision 1 of Application for Amendment No. 8 to the NUHOMS® CoC No. 1004, Non-Proprietary Version (Replacement Pages Only).
4. Response to the RAI.

AFFIDAVIT PURSUANT TO 10 CFR 2.390

Transnuclear, Inc.)
State of California) SS.
County of Alameda)

I, Jayant Bondre, depose and say that I am the Manager of Engineering and Licensing of Transnuclear, Inc., duly authorized to make this affidavit, and have reviewed or caused to have reviewed the information which is identified as proprietary and referenced in the paragraph immediately below. I am submitting this affidavit in conformance with the provisions of 10 CFR 2.390 of the Commission's regulations for withholding this information.

The information for which proprietary treatment is sought is contained in Enclosure 2, as listed below:

1. Attachment C of the Application for Amendment No. 8 to the NUHOMS® CoC 1004 (Proprietary Version).

This section of the document has been appropriately designated as proprietary.

I have personal knowledge of the criteria and procedures utilized by Transnuclear, Inc. in designating information as a trade secret, privileged or as confidential commercial or financial information.

Pursuant to the provisions of paragraph (b) (4) of Section 2.390 of the Commission's regulations, the following is furnished for consideration by the Commission in determining whether the information sought to be withheld from public disclosure, included in the above referenced document, should be withheld.

1) The information sought to be withheld from public disclosure is a proprietary Safety Analysis Report relating to the analysis of the NUHOMS® Cask, which is owned and has been held in confidence by Transnuclear, Inc.

2) The information is of a type customarily held in confidence by Transnuclear, Inc. and not customarily disclosed to the public. Transnuclear, Inc. has a rational basis for determining the types of information customarily held in confidence by it.

3) The information is being transmitted to the Commission in confidence under the provisions of 10 CFR 2.390 with the understanding that it is to be received in confidence by the Commission.

4) The information, to the best of my knowledge and belief, is not available in public sources, and any disclosure to third parties has been made pursuant to regulatory provisions or proprietary agreements which provide for maintenance of the information in confidence.

5) Public disclosure of the information is likely to cause substantial harm to the competitive position of Transnuclear, Inc. because:

   a) A similar product is manufactured and sold by competitors of Transnuclear, Inc.

b) Development of this information by Transnuclear, Inc. required expenditure of considerable resources. To the best of my knowledge and belief, a competitor would have to undergo similar expense in generating equivalent information.

c) In order to acquire such information, a competitor would also require considerable time and inconvenience related to the development of a design and analysis of a dry spent fuel storage system.

d) The information required significant effort and expense to obtain the licensing approvals necessary for application of the information. Avoidance of this expense would decrease a competitor's cost in applying the information and marketing the product to which the information is applicable.

e) The information consists of description of the design and analysis of a dry spent fuel storage and transportation system, the application of which provides a competitive economic advantage. The availability of such information to competitors would enable them to modify their product to better compete with Transnuclear, Inc., take marketing or other actions to improve their product's position or impair the position of Transnuclear, Inc.'s product, and avoid developing similar data and analyses in support of their processes, methods or apparatus.

f) In pricing Transnuclear, Inc.'s products and services, significant research, development, engineering, analytical, licensing, quality assurance and other costs and expenses must be included. The ability of Transnuclear, Inc.'s competitors to utilize such information without similar expenditure of resources may enable them to sell at prices reflecting significantly lower costs.

Further the deponent sayeth not.

SHANNON L. CHRISTENSEN
COMM. #1485004
Notary Public-California
ALAMEDA COUNTY
My Comm. Exp. May 18, 2008

Jayant Bondre
Manager of Engineering/Licensing
Transnuclear, Inc.

Subscribed and sworn to me before this 2nd day of July, 2004, by Jayant Bondre.

Notary Public

ATTACHMENT A

Description, Justification, and Evaluation of COC Amendment Changes

NON-PROPRIETARY
FOR INFORMATION ONLY

ATTACHMENT A

DESCRIPTION, JUSTIFICATION AND EVALUATION OF AMENDMENT CHANGES

1.0 INTRODUCTION

The purpose of this amendment application is to add a new NUHOMS®-24PTH system to the Standardized NUHOMS® system described in the FSAR. The NUHOMS®-24PTH system is a modular canister based spent fuel storage and transfer system, similar to the Standardized NUHOMS®-24P system described in the FSAR. The NUHOMS®-24PTH system consists of the following new or modified components:

- A new dual purpose (Storage/Transportation) Dry Shielded Canister (DSC), with three alternate configurations, designated as DSC Type NUHOMS®-24PTH-S, -24PTH-L, and -24PTH-S-LC,

- A new 24PTH DSC basket design, which is provided with two alternate options: with aluminum inserts (Type 1) or without aluminum inserts (Type 2). In addition, depending on the boron content in the basket poison plates, each basket type is designated as Type A (low B10), Type B (moderate B10) or Type C (high B10) which results in six different basket types (Type 1A, 1B, 1C, 2A, 2B, or 2C),

- A modified version of the Standardized Horizontal Storage Module (HSM) Model 102 described in the FSAR, designated as HSM-H, equipped with special design features which provide enhanced shielding and heat rejection capabilities, and

- The OS197/OS197H Transfer Cask (TC) described in the FSAR, is provided with an optional modified top lid to allow air circulation through the TC/DSC annulus during transfer operations at certain heat loads when time limits for transfer operations cannot be satisfied. The OS197/OS197H TC with a modified top lid is designated as OS197FC TC.

The NUHOMS®-24PTH system is designed to store up to 24 intact (or up to 12 damaged and balance intact) B&W 15x15, WE 17x17, CE 15x15, WE 15x15, CE 14x14, and WE 14x14 class PWR fuel assemblies. The fuel to be stored is limited to a maximum assembly average initial enrichment of 5.0 wt. %, a maximum assembly average burn up of 62 GWd/MTU, and a minimum cooling time of 3.0 years. The 24PTH-S and 24PTH-L DSC types are the short and long cavity configurations of the 24PTH DSC designed for a maximum heat load of 40.8 kW. They are transferred to the ISFSI for storage in the HSM-H in either the OS197/OS197H or OS197FC TC depending upon the heat load.

To meet the capacity limits of the lifting crane at the Oconee Station, a third DSC type, designated 24PTH DSC-S-LC, is provided. This is a modified version of the 24PTH-S DSC, provided with thinner top and bottom lead shield plugs instead of steel, resulting in a longer cavity length. It is designed for a maximum heat load of 24 kW per DSC and may be stored in

either the currently licensed Standardized HSM Model 102, or in the new HSM-H, and is to used with the currently licensed Standardized TC (with a solid neutron shield) only for onsite transfer.

Fuel assemblies with Control Components (CCs) are to be stored only in 24PTH-L and 24PTH-S-LC DSC Types, due to their longer cavity length.

This section of the application provides (1) a brief description of the changes, (2) justification for the change, and (3) a safety evaluation for this change.

Revision 1 of this application is being submitted to reflect TN's response to the NRC Request for Additional Information (RAI) dated May 3, 2004 (TAC No. L23653).

2.0 BRIEF DESCRIPTION OF THE CHANGE

2.1 Significant Changes to the Technical Specifications of NUHOMS® CoC 1004, Amendment 7

The changes listed below are relative to CoC Amendment 7:

A complete mark up of the changes to the Technical Specifications due to the addition of the NUHOMS®-24PTH system to CoC 1004 is included as Attachment B in Enclosures 2 and 3 of this submittal. A few of the proposed changes listed here correct errors, inconsistencies and/or discrepancies within the existing Specifications. None of these corrections have any significant effect on safety. A brief justification for each of such suggested corrections to the Specifications is also provided herewith.

- Revise "Limit/Specification" and "Action" sections of Specification 1.2.1, "Fuel Specification", to add reference to Tables 1-11, and 1-1m. Table 1-11, and 1-1m specify the applicable parameters for each type of PWR fuel allowed to be stored in the NUHOMS®-24PTH system.

- Revise the "Surveillance" section of Specification 1.2.1, Fuel Specification", to say "*Prior to loading.....*" instead of "Immediately before insertion...". to allow operational flexibility to a Cask user. There is no change to the requirement of independent identification and verification of each assembly being placed into the DSC.

- Revise the "Bases" section of Specification 1.2.1, "Fuel Specification", to provide the supporting bases for storage of intact and/or damaged PWR fuel, with or without Control Components (CCs) in the NUHOMS®-24PTH DSC. Add a cross reference to Appendix P where the safety analyses for the 24PTH are provided.

- Add Table 1-11 to identify the acceptable parameters for each type of intact PWR fuel assembly class allowed to be stored in the NUHOMS®-24PTH DSC.

- Add Table 1-1m to specify PWR fuel assembly design characteristics for storage into NUHOMS®-24PTH DSC.

- Add Table 1-1n to specify the thermal and radiological characteristics for CCs authorized for storage in the NUHOMS®-24PTH DSC.

- Add Table 1-1p to specify the maximum assembly average initial enrichment for which each intact fuel assembly class (with or without CCs) is qualified as a function of soluble boron concentration and basket type (fixed boron).

- Add Table 1-1q to specify the maximum assembly average initial enrichment for which each damaged fuel assembly class (with or without CCs) is qualified as a function of soluble boron concentration and basket type (fixed boron) and the maximum number of damaged fuel assemblies allowed to be stored.

- Add Table 1-1r to specify the minimum B10 content of the poison plates as a function of the six NUHOMS®-24PTH basket types.

- Add Fuel Qualification Tables 1-3a, 1-3b, 1-3c, and 1-3d for the NUHOMS®-24PTH DSC (PWR Fuel without CCs).

- Add Fuel Qualification Tables 1-3e, 1-3f, 1-3g, and 1-3h for the NUHOMS®-24PTH DSC (PWR Fuel with CCs).

- Relocate the existing Figure 1-10 from its existing location (page A-65) to page A-63 as shown. This is an editorial change and represents a more logical location for this Figure in the Technical Specifications.

- Add Figures 1-11, 1-12, 1-13 and 1-14 to specify the four heat load zoning configurations analyzed for the 24PTH-S or 24PTH-L DSC. Add Figure 1-15 to specify the heat load zoning configuration analyzed for the 24PTH-S-LC DSC.

- Add Figure 1-16 to specify the location inside the NUHOMS®-24PTH DSC where up to 12 damaged fuel assemblies may be stored.

- *Revise the Limit/Specification of Specification 1.2.2 to delete the requirements of a "stepped" evacuation. The requirement of a stepped evacuation is a process detail which does not affect safety. As stated in the basis subsection, achieving a stable vacuum pressure of 3 mm Hg ensures that the 0.25 volume % oxidizing gases is met. This 3 mm limit may be achieved by the licensee in several ways without this additional restraint.*

- *Revise the Applicability subsection of Specification 1.2.2 to add the clarification that "the term 'inner top cover' used in this and other Technical Specifications means either the inner top cover plate or the top shield plug assembly." Accordingly replace the term "cover plate" with "cover" in Action Statement No. 4. This change avoids ambiguity in interpretation of the requirements of this Specification (and other Technical Specifications such as Specification 1.2.3, 1.2.3a, 1.2.4, 1.2.4a), since it is the DSC top cover which is welded to the DSC shell. The DSC "top cover" may be the top cover plate for DSC designs (such as 24PTH-S or 24PTH-L) or the "top shield plug assembly" for other DSC designs (such as 24PTH-S-LC). A similar change is also made to page A-2 of the Specifications.*

- Revise the Title and "Applicability" subsections of Specification 1.2.3a to extend the applicability of this specification to the 24PTH DSC.

- Revise Action Statement No. 5 of Specifications 1.2.3 and 1.2.3a to say "Check and repair the seal weld *between the inner top cover and the DSC shell*" instead of "Check and repair the seal weld on the DSC top shield plug". *See justification provided for Specification 1.2.2 above.*

- Revise the title ,"Applicability" and the "Bases" sections of Specification 1.2.4a to extend the applicability of this specification to 24PTH DSC.

- *Revise Specification 1.2.4 and 1.2.4a to replace the term "top cover plate" with "top cover" as marked. See justification provided for Specification 1.2.2 above.*

- Revise the Applicability Specification 1.2.5 to correct a spelling error of the term "siphon".

- Add a new Specification 1.2.7c, entitled "HSM-H Dose Rates with a Loaded 24PTH-S or 24PTH-L DSC Only", to specify the limiting doses rates due to the storage of a loaded 24PTH-S or 24PTH-L DSC inside the HSM-H.

- Add a new Specification 1.2.7d, entitled "HSM or HSM-H Dose Rates with a Loaded 24PTH-S-LC DSC Only", to specify the limiting doses rates due to the storage of a loaded 24PTH-S-LC DSC inside either the Standardized HSM or HSM-H.

- Revise the Title of Specification 1.2.8 to include 24PTH-S-LC DSC, since this DSC is authorized to be stored in the Standardized HSM. Also, revise the third sentence in the Action Statement of this Specification to say "...than the upper limit *in the Specification 1.2.1* ....." instead of "than the upper limit specified in Section 3 of the FSAR...". This is a betterment change.

- Add a new specification 1.2.8a, entitled "HSM-H Maximum Air Exit Temperature with a Loaded 24PTH DSC", to specify the limiting air exit temperature due to the storage of a NUHOMS®-24PTH DSC inside the HSM-H.

- Revise Specification 1.2.9 to reflect that the alignment requirements of the TC with the HSM as specified herein are also applicable to the HSM-H.

- *Revise the tile and Limit/Specification of Specification 1.2.10 to replace the words "Outside the Spent Fuel Pool Building" with "for all transfer operations". In addition, add a definition of the term "Transfer Operations" in the Basis section. There is no change to the currently specified 80" TC/DSC handling height limit which is based on a TC/DSC drop accident analysis as stated in the Basis section and presented in FSAR section 8.2.5. Addition of a definition of "Transfer Operations" provides clarity to the applicability of this Specification.*

- Add a new Specification 1.2.11b, entitled "Transfer Cask Dose Rates with a Loaded 24PTH-S or 24PTH-L DSC", to specify the limiting doses rates due to the transfer of a loaded 24PTH-S or 24PTH-L DSC inside the Transfer Cask.

- Add a new Specification 1.2.11c, entitled "Transfer Cask Dose Rates with a Loaded 24PTH-S-LC DSC", to specify the limiting doses rates due to the transfer of a loaded 24PTH-S-LC inside the Transfer Cask.

- Revise Specification 1.2.12, Surveillance section to delete the last 2 sentences related to decontamination of the transfer cask. This change makes the Specification consistent with its Applicability section.

- *Revise Specification 1.2.13 to delete Limits 1, 2, 3 and 4. Instead, add a new Limit to say "No lifts or handling or transfer of a loaded TC/DSC is permissible at DSC basket temperatures below 0°F". This change removes the 80" lifting/handling limit from this Specification, <u>since this handling height limit for transfer operations is controlled by Specification 1.2.10 as discussed above.</u> Hence, with this change this Specification limits the operation of a Loaded TC/DSC in a low temperature environment, while Specification 1.2.10 controls the Handling Heights of a Loaded TC/DSC.*

  Accordingly, the terms "Heights" or "and Height" are deleted from the title, Applicability, Objective, and Bases sections. The Bases section is also revised to delete the bases for the 80" drop height limit.

  The phrase "and Location" is also deleted, from the title of the Specification. The Applicability section is revised to delete the distinction between the locations where Part 50 or Part 72 requirements are applicable, since the requirements for Part 72 apply to both outside and also inside the spent fuel pool building (once the loaded TC/DSC is placed on the transfer trailer).

  Finally, the Action statement of this Specification is revised to correct an editorial error (the term "available" is replaced with the term "unavailable".

  The suggested revision of this Specification adds clarity but places additional operational constraints for the licensees, since it deletes the previous flexibility of allowing limited TC/DSC handling operations at temperatures between -20°F and 0°F. There is no change to the low temperature limit or the bases for this limit as currently specified in the Bases section. Hence, this is a betterment change and is more conservative.

- Revise the second sentence of the "Bases" section of Specification 1.2.14, entitled "TC/DSC Operations at High Ambient Temperatures" to state that the fuel cladding limits of ISG-11, Rev. 2 also apply to the 24PTH system. Also, Item No. 2 of the Limit/Specification is revised to delete the words "*up to 125°F*", since the upper ambient temperature limit is different for each canister type as stated in paragraph 1.1.1, item 2 of CoC.

- For Specifications 1.2.15, 1.2.15a, and 1.2.15b, revise the surveillance activities No. 1 and 2 to reflect a time requirement of 24 hours instead of 4 hours for determination of boron

concentration in the SFP water and the water inside DSC cavity. The current four hour requirement results in an increased exposure to the Cask user without providing a commensurate increase in public safety.

- Add a new Specification 1.2.15c, entitled "Boron Concentration in the DSC Cavity Water for the 24PTH Design Only", to specify the minimum boron concentration required during loading of the NUHOMS®-24PTH system.

- Revise the Limits/Specifications of Specification 1.2.16 to delete the additional constraint of "*and the fully loaded TC weight is less than 190 kips*" to make this Specification consistent with its Applicability statement. *In accordance with RAI 12-2 response, revise the Action Statement of this Specification to delete the words "...and determine if the cask weight is less than 190 kips". This revision corrects an omission from the original submittal.*

- Add a new Specification 1.2.17c, entitled "24PTH DSC Vacuum Drying Duration Limit", to specify the vacuum drying duration limit for the NUHOMS®-24PTH DSC.

- Add a new Specification 1.2.18, entitled "Time Limit for Completion of 24PTH DSC Transfer Operation" to specify the limits for completion of transfer of a loaded NUHOMS®-24PTH DSC.

- Revise the Surveillance and Monitoring requirements of Specification 1.3 to eliminate the mandatory requirements of implementing both 1.3.1 and 1.3.2 on a daily basis. Implementation of any one of the two surveillance requirements is sufficient to accomplish the specified objective of this specification. Implementation of both requirements adds to the exposure requirements of the Cask user without providing a commensurate increase in public safety. In addition, revise Specifications 1.3.1 and 1.3.2 to show that the requirements of these Specifications apply to "HSM or HSM-H".

- Update Table 1.3.1 to reflect the changes as described above as applicable.

- Revise the Captions of Tables and Figures to delete underline, as applicable. This is a format change which makes the appearance of the document consistent. No change to the contents of the Specification.

2.2 Changes to NUHOMS® FSAR, Revision 8

Attachment C of this submittal includes a new FSAR Appendix P which has been prepared in a format consistent with the Standard Review Plan for Dry Cask Storage (NUREG 1536). It provides a description of the design features and a comprehensive evaluation of the new 24PTH system. It also documents the changes where applicable to the existing safety analyses provided in the FSAR.

Revision 1 to Appendix P reflects the SAR changes due to RAI responses. Table 1 of this Attachment A provides a listing of some minor additional changes implemented in Revision 1 of this application.

3.0 JUSTIFICATION OF CHANGE

The NUHOMS®-24PTH System design has been developed based on research and development efforts driven by the needs of the commercial nuclear power industry. TN is in discussions with two utilities for dry storage systems using the 24PTH system. To support the needs of these utilities, fabrication of the 24PTH canisters is planned to begin in early 2004 to support initial use in mid 2005. Accordingly, TN requests that the staff assign appropriate priority for review of this application consistent with the issuance of an RAI, if needed, by February 2004.

4.0 EVALUATION OF CHANGE

TN has evaluated the NUHOMS®-24PTH system for structural, thermal, shielding, confinement and criticality adequacy and has concluded that the addition of the NUHOMS®-24PTH System to the standardized NUHOMS® System has no significant effect on safety. This evaluation is documented in Appendix P of the FSAR (Attachment C).

Table 1
List of Non RAI Changes to COC 1004 24PTH Amendment Application

SAR Section or Drawing No	Location	Description of Change	Reason for Change
Table P.1-1	Page P.1-13	"Shield walls" changed to "shield walls".	Editorial
Table P.1-1	Page P.1-13	In Note 2 "Under" changed to "Unless".	Editorial
P.2.5.2	Page P.2-17, 1st paragraph	Added a new sentence	Clarification to indicate that Table P.2-18 presents the HSM-H design criteria.
Table P.2-14	Page P.2-35	Changed Service Level for Non-Operational Load Cases NO-3 and NO-4 from Level A to Level B	This change is made for consistency with other NUHOMS DSCs. NO-3 and NO-4 Load Cases are one-time type, non operational (without fuel in the DSC) loads cases, and therefore, Service Level B designation is more appropiate.
Table P.2-18	Page P.2-43	Changed ACI Code Edition to ACI 318-95. Replaced "for installation" to "for construction"	Editorial Corrections. The Code Edition for construction of the HSM-H is ACI 318-95
P.3.6.1.3.1(D)	Page P.3.6-9, bottom paragraph	Added word "handling".	Editorial Clarification
P.3.6.1.3.1(E)	Page P.3.6-10, second paragraph	To correct misspelled word "paltes" to "plates"	Editorial corrections
P.4.10	Page P.4-66, Table P.4-40, Figure P.4-54	Page P.4-66 was revised to reflect the revised confirmatory analysis results, as summarized in Table P.4-40. Updated Figure P.4-54 to reflect refined modeling of the DSC shell to improve radiation modeling	Reanalysis was required due to refinements in the DSC modeling approach to account for surface-to-surface radiation modeling methodology and use of second order discretization solution technique.
P.4.2(16)	Page P.4.11	In Note 1 deleted references to HSM-H "floor".	Delete information not applicable to the HSM-H.
Table P.4-21	Page P.4-91	In Note 3 change the words "without" to "with"	Editorial correction
Chapter 9	Pages P.9-2, P.9-3, P.9.5, P.9-6, P.9-7, P.9-8, P.9-11,	To provide additional information for qualification of "equivalent" poison materials and to provide example calculations of nominal boron content.	To provide additional information to assist staff's review
Table P.10-7	Page P.10-15	To correct the header information in the of third and fourth columns of the table	Editorial correction

Table 1
List of Non RAI Changes to COC 1004 24PTH Amendment Application

SAR Section or Drawing No	Location	Description of Change	Reason for Change
Description of Changes to SAR DRAWINGS included in Section P.1.5. (NOTE: The changes listed below provide an overview of the changes shown on the drawings. It does not list all the detailed changes called out therein).			
Dwg NUH24PTH-1001-SAR, SHEETS 1 and 2	Parts List (sheet 1) and Views E-E and J-J (sheet 2)	Added Item 21, Reinforcing Pad for Lifting Lug, and revised Lifting Lug design to accommodate the reinforcing pad	To provide additional marging for the non-operational lift loads during basket insertion and retrieval into/from the DSC
Dwg NUH-03-7001-SAR, SHEETS 1 and 10	Parts List (sheet 1) and Views R-R and H-H (sheet 10)	Corrected Part Number for Side Heat Shield Connection Bracket shown in Sheet 10. This bracket is assigned Part 65 in Parts List.	Correction consistent with design
Description of Non RAI Changes to CoC 1004 Technical Specifications are described in Attachment A			

ATTACHMENT B

Suggested Changes to Technical Specifications of CoC 1004 Amendment No. 7

~~(CoC Changes implemented under CoC Amendment 7, which is currently in rule making, have been included as current configuration.)~~

3. The horizontal and vertical seismic acceleration levels of 0.25g and 0.17g, respectively.

4. The analyzed flood condition of 15 fps water velocity and a height of 50 feet of water (full submergence of the loaded HSM DSC).

5. The potential for fire and explosion should be addressed, based on site-specific considerations.

6. The HSM foundation design criteria are not included in the FSAR. Therefore, the nominal FSAR design or an alternative should be verified for individual sites in accordance with 10 CFR 72.212(b)(2)(ii). Also, in accordance with 10 CFR 72.212(b)(3), the foundation design should be evaluated against actual site parameters to determine whether its failure would cause the standardized NUHOMS® system to exceed the design basis accident conditions.

7. The potential for lightning damage to any electrical system associated with the standardized NUHOMS® system (e.g., thermal performance monitoring) should be addressed, based on site-specific considerations.

8. Any other site parameters or consideration that could decrease the effectiveness of cask systems important to safety.

In accordance with 10 CFR 72.212(b)(2), a record of the written evaluations must be retained by the licensee until spent fuel is no longer stored under the general license issued under 10 CFR 72.210.

1.1.2 Operating Procedures

Written operating procedures shall be prepared for cask handling, loading, movement, surveillance, and maintenance. The operating procedures suggested generically in the FSAR should provide the basis for the user's written operating procedure. The following additional procedure requested by NRC staff should be part of the user operating procedures:

> If fuel needs to be removed from the DSC, either at the end of service life or for inspection after an accident, precautions must be taken against the potential for the presence of damaged or oxidized fuel and to prevent radiological exposure to personnel during this operation. This can be achieved with this design by the use of the purge and fill valves which permit a determination of the atmosphere within the DSC before the removal of the inner top cover ~~plate~~ and shield plugs, prior to filling the DSC cavity with water (borated water for the 24P or 32PT or 24PHB *or 24PTH*). If the atmosphere within the DSC is helium, then operations should proceed normally with fuel removal either via the transfer cask or in the pool. However, if air is present within the DSC, then appropriate filters should be in place to preclude the uncontrolled release of any potential airborne radioactive particulate from the DSC via the purge-fill valves. This will protect both personnel and the operations area from potential contamination. For the accident case, personnel protection in the form of respirators or supplied air should be considered in accordance with the licensee's Radiation Protection Program.

1.2.2 DSC Vacuum Pressure During Drying

Limit/Specification:

Vacuum Pressure: ≤3 mm Hg

Time at Pressure: ≥30 minutes following ~~stepped~~ evacuation

Number of Pump-Downs: 2

Applicability: This is applicable to all DSCs. *The term "inner top cover" as used in this and other Technical Specifications means either the inner top cover plate or the top shield plug assembly.*

Objective: To ensure a minimum water content.

Action: If the required vacuum pressure cannot be obtained:

1. Confirm that the vacuum drying system is properly installed.
2. Check and repair, or replace, the vacuum pump.
3. Check and repair the system as necessary.
4. Check and repair the seal weld between the inner top cover ~~plate~~ and the DSC shell.

Surveillance: No maintenance or tests are required during normal storage. Surveillance of the vacuum gauge is required during the vacuum drying operation.

Bases: A stable vacuum pressure of ≤3 mm Hg further ensures that all liquid water has evaporated in the DSC cavity, and that the resulting inventory of oxidizing gases in the DSC is well below the 0.25 volume %.

1.2.4 24P and 52B DSC Helium Leak Rate of Inner Seal Weld

Limit/Specification:

$\leq 1.0 \times 10^{-4}$ atm · cubic centimeters per second (atm · cm^3/s) at the highest DSC limiting pressure.

Applicability: This specification is applicable to the inner top cover ~~plate~~ seal weld of the 24P and 52B DSCs only.

Objective:

1. To limit the total radioactive gases normally released by each canister to negligible levels. Should fission gases escape the fuel cladding, they will remain confined by the DSC confinement boundary.

2. To retain helium cover gases within the DSC and prevent oxygen from entering the DSC. The helium improves the heat dissipation characteristics of the DSC and prevents any oxidation of fuel cladding.

Action: If the leak rate test of the inner seal weld exceeds 1.0×10^{-4} (atm · cm^3/s):

1. Check and repair the DSC drain and fill port fittings for leaks.

2. Check and repair the inner seal weld.

3. Check and repair the inner top cover ~~plate~~ for any surface indications resulting in leakage.

Surveillance: After the welding operation has been completed, perform a leak test with a helium leak detection device.

Bases: If the DSC leaked at the maximum acceptable rate of 1.0×10^{-4} atm · cm^3/s for a period of 20 years, about 63,100 cc of helium would escape from the DSC. This is about 1% of the 6.3×10^6 cm^3 of helium initially introduced in the DSC. This amount of leakage would have a negligible effect on the inert environment of the DSC cavity. (Reference: American National Standards Institute, ANSI N14.5-1987, For Radioactive Materials—Leakage Tests on Packages for Shipment," Appendix B3).

1.2.4a 61BT, 32PT, 24PHB and *24PTH DSC* Helium Leak Rate of Inner Seal Weld

Limit/Specification:

$\leq 1.0 \times 10^{-7}$ reference cubic centimeters per second (cc/s).

Applicability: This specification is applicable to the inner top cover ~~plate~~ seal weld of 61BT, 32PT 24PHB and *24PTH* DSC only.

Objective:

1. To demonstrate that the top cover ~~plate~~ to be "leak tight", as defined in "American National Standard for Leakage Tests on Packages for Shipment of Radioactive Materials," ANSI N14.5 – 1997..

2. To retain helium cover gases within the DSC and prevent oxygen from entering the DSC. The helium improves the heat dissipation characteristics of the DSC and prevents any oxidation of fuel cladding.

Action: If the leak rate test of the inner seal weld exceeds 1.0×10^{-7} reference cc/s:

1. Check and repair the inner seal weld.

2. Check and repair the inner top cover ~~plate~~ for any surface indications resulting in leakage.

Surveillance: After the welding operation has been completed, perform a leak test with a helium leak detection device.

Bases: The 61BT, 32PT, 24PHB *and 24PTH* DSC will maintain an inert atmosphere around the fuel and radiological consequences will be negligible, since it is designed and tested to be leak tight.

1.2.10 *TC/*DSC Handling Height ~~Outside the Spent Fuel Pool Building~~*for All Transfer Operations*

Limit/Specification:

1. The loaded TC/DSC shall not be handled at a height greater than 80 inches ~~outside the spent fuel pool building~~*for all transfer operations.*

2. In the event of a drop of a loaded TC/DSC from a height greater than 15 inches: (a) fuel in the DSC shall be returned to the reactor spent fuel pool; (b) the DSC shall be removed from service and evaluated for further use; and (c) the TC shall be inspected for damage and evaluated for further use.

Applicability: The specification applies to handling the TC, loaded with the DSC, on route to, and at, the storage pad.

Objective:

1. To preclude a loaded TC/DSC drop from a height greater than 80 inches.

2. To maintain spent fuel integrity, according to the spent fuel specification for storage, continued confinement integrity, and DSC functional capability, after a tip-over or drop of a loaded DSC from a height greater than 15 inches.

Surveillance: In the event of a loaded TC/DSC drop accident, the system will be returned to the reactor fuel handling building, where, after the fuel has been returned to the spent fuel pool, the DSC and TC will be inspected and *evaluated* for future use.

Basis: *Transfer Operations include all activities from the time a loaded TC/DSC is disconnected from a crane until the DSC is in storage inside the HSM.* The NRC evaluation of the TC/DSC drop analysis concurred that drops up to 80 inches, of the DSC inside the TC, can be sustained without breaching the confinement boundary, preventing removal of spent fuel assemblies, or causing a criticality accident. This specification ensures that handling height limits will not be exceeded in transit to, or at the storage pad. Acceptable damage may occur to the TC, DSC, and the fuel stored in the DSC, for drops of height greater than 15 inches. The specification requiring inspection of the DSC and fuel following a drop of 15 inches or greater ensures that the spent fuel will continue to meet the requirements for storage, the DSC will continue to provide confinement, and the TC will continue to provide its design functions of DSC transfer and shielding.

1.2.13 TC/DSC Lifting/*Handling* ~~Heights~~ as a Function of Low Temperature ~~and Location~~

Limit/Specification: ~~1. No lifts or handling of the TC/DSC at any height are permissible at DSC basket temperatures below -20°F inside the spent fuel pool building.~~ *No lifts or handling or transfer of a loaded TC/DSC is permissible at DSC basket temperatures below 0°F.*

2. ~~The maximum lift height of the TC/DSC shall be 80 inches if the basket temperature is below 0°F but higher than -20°F inside the spent fuel pool building.~~

~~3. No lift height restriction is imposed on the TC/DSC if the basket temperature is higher than 0°F inside the spent fuel pool building.~~

~~4. The maximum lift height and handling height for all transfer operations outside the spent fuel pool building shall be 80 inches and the basket temperature may not be lower than 0°F.~~

Applicability: These temperature ~~and height~~ limits apply to lifting and transfer of all loaded TC/DSCs inside and outside the spent fuel pool building.

~~The requirements of 10 CFR Part 72 apply outside the spent fuel building. The requirements of 10 CFR Part 50 apply inside the spent fuel pool building.~~

Objective: The low temperature ~~and height~~ limits are imposed to ensure that brittle fracture of the ferritic steels, used in the TC trunnions and shell and in the DSC basket, does not occur during transfer operations.

Action: Confirm the basket temperature before transfer of the TC. If calculation or measurement of this value is *un*available, then the ambient temperature may conservatively be used.

Surveillance: The ambient temperature shall be measured before transfer of the TC/DSC.

Bases: The basis for the low temperature ~~and height~~ limits is ANSI N14.6-1986 paragraph 4.2.6 which requires at least 40°F higher service temperature than nil ductility transition (NDT) temperature for the TC. In the case of the standardized TC, the test temperature is -40°F; therefore, although the NDT temperature is not determined, the material will have the required 40°F margin if the ambient temperature is 0°F or higher. This assumes the material service temperature is equal to the ambient temperature.

The basis for the low temperature limit for the DSC is NUREG/CR-1815. ~~The basis for the handling height limits is the NRC evaluation of the structural integrity of the DSC to drop heights of 80 inches and less.~~

1.2.16 Provision of TC Seismic Restraint Inside the Spent Fuel Pool Building as a Function of Horizontal Acceleration and Loaded Cask Weight

Limit/Specification:

Seismic restraints shall be provided to prevent overturning of a loaded TC during a seismic event if a certificate holder determines that the horizontal acceleration is 0.40 g or greater~~ and the fully loaded TC weight is less than 190 kips~~. The determination of horizontal acceleration acting at the center of gravity (CG) of the loaded TC must be based on a peak horizontal ground acceleration at the site, but shall not exceed 0.25 g.

Applicability: This condition applies to all TCs which are subject to horizontal accelerations of 0.40 g or greater.

Objective: To prevent overturning of a loaded TC inside the spent fuel pool building.

Action: Determine what the horizontal acceleration is for the TC ~~and determine if the cask weight is less than 190 kips~~.

Surveillance: Determine need for TC restraint before any operations inside the spent fuel pool building.

Bases: Calculation of overturning and restoring moments.

AMENDMENT 8, REV. 1

APPENDIX P

CHANGED PAGES

ATTACHMENT C

NUHOMS® FSAR Revision *8* Changed Pages

Listed below are the affected NUHOMS® FSAR Revision *8* pages due to the addition of the NUHOMS®-24PTH System to the Standardized NUHOMS®System:

- Page 1.1-2
- Page 1.1-*2*a
- Page 1.1-3
- Appendix P

NUHOMS® storage system in selection of acceptable assemblies during loading. In addition, Amendment No. 2 authorizes the storage of Burnable Poison Rod Assemblies (BPRAs) in the NUHOMS®-24P long cavity DSC. A detailed description of the authorized contents and supporting analyses for the storage of PWR fuel with BPRAs is provided in Appendix J.

Amendment No. 3 to CoC 1004, approved on September 12, 2001, authorizes the addition of the NUHOMS®-61BT DSC to the standardized NUHOMS® system. The NUHOMS®-61BT DSC is designed to store 61 intact BWR fuel assemblies and meets the storage and transportation requirements of 10CFR72 and 10CFR71, respectively. A detailed description of the authorized contents and supporting safety analyses for this system are provided in Appendix K.

TN has added NUHOMS®-24PT2 DSC to the standardized NUHOMS® system. The NUHOMS®-24PT2 DSC is a modified version of the NUHOMS®-24P DSC, designed to store 24 intact PWR fuel assemblies with or without BPRAs. This DSC meets the storage and transportation requirements of 10CFR72 (CoC 1004) and 10CFR71 (CoC 9255), respectively. A detailed description of the authorized contents and supporting safety analyses for this system are provided in Appendix L.

Amendment No. 4 to CoC 1004, approved on February 12, 2002, authorizes the addition of low burn-up spent fuel in the NUHOMS®-24P DSC.

Amendment No. 5 to CoC 1004, approved on January 7, 2004, authorizes the addition of the NUHOMS®-32PT DSC to the standardized NUHOMS® system. The NUHOMS®-32PT DSC is designed to store 32 intact PWR fuel assemblies and meets the storage and transportation requirements of 10CFR72 and 10CFR71, respectively. A detailed description of the authorized contents and supporting safety analyses for this system are provided in Appendix M.

Amendment No. 6 to CoC 1004, approved on December 22, 2003, adds NUHOMS®-24PHB DSC to the standardized NUHOMS® system. The NUHOMS®-24PHB DSC is designed to store a total of 24 intact B&W 15x15 fuel assemblies with an assembly average burnup of up to 55,000 MWd/MTU and an initial enrichment of up to 4.5 weight % U-235. The 24PHB DSC is designed for storage in the existing Model 102 NUHOMS® HSM and for transfer in the existing standard, or OS197 or OS197H transfer cask. A detailed description of the authorized contents and supporting safety analyses for the 24PHB DSC are provided in Appendix N.

Amendment No. 7 to CoC 1004, approved on March 3, 2004, authorizes the addition of new fuel types and damaged fuel to the list of authorized contents for the Standardized NUHOMS®-61BT system (Appendix K).

Amendment No. 8 to CoC 1004 adds NUHOMS®-24PTH system to the standardized NUHOMS® system. The NUHOMS®-24PTH system is designed to store a total of 24 intact intact (or up to 12 damaged and balance intact) PWR fuel assemblies with a maximum assembly average initial enrichment of 5.0 wt. % U-235, a maximum assembly average burn up of 62 GWd/MTU, and a minimum cooling time of 3.0 years. Five heat load zoning configurations are authorized and the system is designed to accommodate a decay heat load of up to 40.8 kW per DSC depending upon the specific configuration selected.

The NUHOMS®-24PTH system adds a new canister with three alternate configurations (designated as DSC Type 24PTH-S, -24PTH-L, or -24PTH-S-LC), a new module designated as HSM-H, and a modified version of OS197/OS197H transfer cask designated as OS197FC.

A detailed description of the 24PTH system, including drawings, authorized payload contents and supporting safety analyses for this system are provided in Appendix P of this FSAR.

Chapters 1 though 8 and Appendices A through H of this FSAR provide the supporting licensing basis for the Standardized NUHOMS®-24P and -52B systems only.

A complete description of the new systems addressed by the above listed amendments, including supporting safety analysis, is located within self-contained Appendices to this FSAR as summarized in the following table:

Amendment No.	Description	Location of Supporting Licensing Basis
3	Addition of the NUHOMS®-61BT DSC to the contents of the Standardized NUHOMS® system	Appendix K
N/A	Addition of the NUHOMS®-24PT2 DSC to the contents of the Standardized NUHOMS® system	Appendix L
4	Addition of low burnup fuel to the contents of the NUHOMS®-24P DSC	Chapter 3
5	Addition of the NUHOMS®-32PT DSC to the Standardized NUHOMS® system	Appendix M
6	Addition of the NUHOMS®-24PHB DSC to the Standardized NUHOMS® system	Appendix N
7	Addition of damaged fuel to the contents of the NUHOMS®-61BT DSC	Appendix K
8	*Addition of the NUHOMS®-24PTH system to the Standardized NUHOMS® system*	*Appendix P*

TABLE OF CONTENTS

Page

P.1 General Discussion P.1-1
- P.1.1 Introduction P.1-3
- P.1.2 General Description of the NUHOMS®-24PTH System P.1-5
  - P.1.2.1 NUHOMS®-24PTH System Characteristics P.1-5
    - P.1.2.1.1 NUHOMS®-24PTH DSC P.1-5
    - P.1.2.1.2 NUHOMS®-HSM-H Module P.1-6
    - P.1.2.1.3 NUHOMS®-OS197FC Transfer Cask P.1-7
  - P.1.2.2 Operational Features P.1-7
    - P.1.2.2.1 General Features P.1-7
    - P.1.2.2.2 Sequence of Operations P.1-7
    - P.1.2.2.3 Identification of Subjects for Safety and Reliability Analysis P.1-8
  - P.1.2.3 Cask Contents P.1-8
- P.1.3 Identification of Agents and Contractors P.1-9
- P.1.4 Generic Cask Arrays P.1-10
- P.1.5 Supplemental Data P.1-11
- P.1.6 References P.1-12

P.2 Principal Design Criteria P.2-1
- P.2.1 Spent Fuel To Be Stored P.2-2
  - P.2.1.1 General Operating Functions P.2-5
- P.2.2 Design Criteria for Environmental Conditions and Natural Phenomena P.2-6
  - P.2.2.1 Tornado Wind and Tornado Missiles P.2-6
    - P.2.2.1.1 Applicable Design Parameters P.2-6
    - P.2.2.1.2 Determination of Forces on Structure P.2-6
    - P.2.2.1.3 Tornado Missiles P.2-7
  - P.2.2.2 Water Level (Flood) Design P.2-8
  - P.2.2.3 Seismic Design P.2-8
  - P.2.2.4 Snow and Ice Loading P.2-8
  - P.2.2.5 Combined Load Criteria P.2-8
    - P.2.2.5.1 NUHOMS®–24PTH DSC Structural Design Criteria P.2-8
    - P.2.2.5.2 NUHOMS® HSM-H Structural Design Criteria P.2-11
- P.2.3 Safety Protection Systems P.2-14
  - P.2.3.1 General P.2-14
  - P.2.3.2 Protection By Multiple Confinement Barriers and Systems P.2-14
  - P.2.3.3 Protection By Equipment and Instrumentation Selection P.2-14
  - P.2.3.4 Nuclear Criticality Safety P.2-14
    - P.2.3.4.1 Control Methods for Prevention of Criticality P.2-14
    - P.2.3.4.2 Error Contingency Criteria P.2-15
    - P.2.3.4.3 Verification Analysis-Benchmarking P.2-15

P.2.3.5 Radiological Protection P.2-15
P.2.3.6 Fire and Explosion Protection P.2-15
P.2.4 Decommissioning Considerations P.2-16
P.2.5 Summary of NUHOMS®-24PTH DSC and HSM-H Design Criteria P.2-17
P.2.5.1 24PTH DSC Design Criteria P.2-17
P.2.5.2 HSM-H Design Criteria P.2-17
P.2.6 References P.2-18

P.3 Structural Evaluation P.3.1-1
P.3.1 Structural Design P.3.1-1
P.3.1.1 Discussion P.3.1-1
P.3.1.1.1 General Description of the 24PTH DSC P.3.1-1
P.3.1.1.2 General Description of the HSM-H P.3.1-4
P.3.1.1.3 General Description of the HSM Model 102 ..... P.3.1-5
P.3.1.1.4 General Description of the OS197FC TC P.3.1-5
P.3.1.2 Design Criteria P.3.1-6
P.3.1.2.1 24PTH DSC Shell Assembly Confinement Boundary P.3.1-6
P.3.1.2.2 24PTH DSC Basket P.3.1-6
P.3.1.2.3 Alternatives to the ASME Code for the 24PTH DSC P.3.1-7
P.3.2 Weights and Centers of Gravity P.3.2-1
P.3.3 Mechanical Properties of Materials P.3.3-1
P.3.3.1 24PTH DSC Material Properties P.3.3-1
P.3.3.2 HSM-H Material Properties P.3.3-2
P.3.3.3 Materials Durability P.3.3-2
P.3.4 General Standards for Casks P.3.4-1
P.3.4.1 Chemical and Galvanic Reactions P.3.4-1
P.3.4.2 Positive Closure P.3.4-7
P.3.4.3 Lifting Devices P.3.4-7
P.3.4.4 Heat and Cold P.3.4-7
P.3.4.4.1 Summary of Pressures and Temperatures P.3.4-7
P.3.4.4.2 Differential Thermal Expansion P.3.4-8
P.3.4.4.3 Thermal Stress Calculations P.3.4-10
P.3.5 Fuel Rods P.3.5-1
P.3.6 Structural Analysis (Normal and Off-Normal Operations) P.3.6-1
P.3.6.1 Normal Operation Structural Analysis P.3.6-1
P.3.6.1.1 Normal Operating Loads P.3.6-1
P.3.6.1.2 Dry Shielded Canister Analysis P.3.6-3
P.3.6.1.3 NUHOMS®-24PTH Basket Structural Analysis P.3.6-6
P.3.6.1.4 NUHOMS® HSM-H Structural Analysis P.3.6-10
P.3.6.1.5 OS197/OS197H/OS197FC On-Site TC Analysis P.3.6-12
P.3.6.2 Off-Normal Load Structural Analysis P.3.6-13
P.3.6.2.1 Jammed DSC during Transfer P.3.6-14

P.3.6.2.2 Off-Normal Thermal Loads Analysis P.3.6-15
P.3.6.2.3 HSM-H Off-Normal Loads P.3.6-16
P.3.6.2.4 OS197/OS197H/OS197FC Off-Normal Loads P.3.6-16
P.3.6.3 Damaged Fuel Integrity Assessment for Normal and Off-Normal Loads P.3.6-17
P.3.7 Structural Analysis (Accidents) P.3.7-1
P.3.7.1 Tornado Winds/Tornado Missile P.3.7-2
P.3.7.1.1 Effect of DBT Wind Pressure Loads on HSM-H P.3.7-2
P.3.7.2 Earthquake P.3.7-4
P.3.7.2.1 DSC Seismic Evaluation P.3.7-4
P.3.7.2.2 Basket Seismic Evaluation P.3.7-6
P.3.7.2.3 HSM-H Seismic Evaluation P.3.7-6
P.3.7.2.4 TC Seismic Evaluation P.3.7-8
P.3.7.3 Flood P.3.7-8
P.3.7.3.1 HSM-H Flooding Analysis P.3.7-8
P.3.7.3.2 DSC Flooding Analyses P.3.7-10
P.3.7.4 Accidental TC Drop P.3.7-10
P.3.7.4.1 General Discussion P.3.7-11
P.3.7.4.2 24PTH DSC Shell Assembly Drop Evaluation P.3.7-12
P.3.7.4.3 24PTH Basket Assembly Drop Evaluation P.3.7-14
P.3.7.4.4 On-site TC Horizontal and Vertical Drop Evaluation P.3.7-17
P.3.7.4.5 Loss of Neutron Shield P.3.7-17
P.3.7.5 Lightning P.3.7-17
P.3.7.6 Blockage of HSM-H Air Inlet and Outlet Openings P.3.7-17
P.3.7.7 DSC Leakage P.3.7-18
P.3.7.8 Accident Pressurization of DSC. P.3.7-18
P.3.7.9 Reduced HSM Air Inlet and Outlet Shielding P.3.7-18
P.3.7.10 Fire and Explosion P.3.7-18
P.3.7.11 Load Combinations P.3.7-18
P.3.7.11.1 DSC Load Combination Evaluation P.3.7-18
P.3.7.11.2 DSC Fatigue Evaluation P.3.7-19
P.3.7.11.3 TC Load Combination Evaluation P.3.7-19
P.3.7.11.4 TC Fatigue Evaluation P.3.7-19
P.3.7.11.5 HSM –H Load Combination Evaluations P.3.7-19
P.3.7.11.6 HSM-H Stress Analysis P.3.7-20
P.3.8 References P.3.8-1

P.4 Thermal Evaluation P.4-1
P.4.1 Discussion P.4-1
P.4.2 Summary of Thermal Properties of Materials P.4-4
P.4.3 Specifications for Components P.4-12
P.4.4 Thermal Analysis of HSM Model 102 and HSM-H with 24PTH DSC P.4-13

P.4.4.1 Ambient Temperature Specification P.4-13
P.4.4.2 Thermal Analysis of HSM-H with 24PTH DSC P.4-13
P.4.4.3 HSM-H Air flow Analysis (Stack Effect Calculations) P.4-15
P.4.4.4 Description of the Thermal Model of HSM-H with 24PTH DSC P.4-18
P.4.4.5 Description of the HSM-H Blocked Vent Model P.4-21
P.4.4.6 Description of Cases Evaluated for the HSM-H P.4-22
P.4.4.7 HSM-H Thermal Model Results P.4-23
P.4.4.7.1 Normal and Off-normal Operating Condition Results P.4-23
P.4.4.7.2 Accident Condition Results P.4-23
P.4.4.8 Evaluation of HSM-H Performance P.4-23
P.4.5 Thermal Analysis of Transfer Casks with 24PTH DSC P.4-24
P.4.5.1 Thermal Analysis of the NUHOMS® Standardized Cask with 24PTH DSC P.4-24
P.4.5.2 Thermal Model of 24PTH DSC in the OS197FC TC P.4-24
P.4.5.2.1 SINDA/FLUINT™ Thermal Desktop® General Code Description P.4-25
P.4.5.2.2 OS197FC TC SINDA/FLUINT™ Thermal Model P.4-25
P.4.5.2.3 DSC Steady State and Transient Conditions Thermal Models P.4-26
P.4.5.2.4 Natural Convection Heat Transfer Coefficients P.4-26
P.4.5.2.5 Neutron Shield Effective Thermal Conductivity P.4-27
P.4.5.3 Analysis Cases for OS197FC TC with 24PTH DSC P.4-28
P.4.5.4 Standardized TC Thermal Model Results P.4-28
P.4.5.5 OS197FC TC Thermal Model Results P.4-28
P.4.5.5.1 Normal and Off-Normal Conditions Results P.4-28
P.4.5.5.2 Normal and Off-Normal Operations with Air Circulation Results P.4-30
P.4.5.5.3 Accident Conditions P.4-32
P.4.5.6 Evaluation of OS197FC TC Performance P.4-34
P.4.6 NUHOMS®-24PTH DSC Basket Thermal Analysis P.4-35
P.4.6.1 NUHOMS® 24PTH DSC Basket and Payload Model P.4-35
P.4.6.2 Mesh Sensitivity Study P.4-36
P.4.6.3 Boundary Conditions for the DSC Basket Model P.4-36
P.4.6.4 Heat Generation for the DSC Basket Model P.4-36
P.4.6.5 DSC Thermal Evaluation for Normal Conditions of Storage and Transfer P.4-37
P.4.6.5.1 Boundary Conditions, Storage P.4-37
P.4.6.5.2 Boundary Conditions, Transfer P.4-37
P.4.6.5.3 Maximum Temperatures P.4-38
P.4.6.5.4 Maximum Internal Pressures P.4-38
P.4.6.5.5 Maximum Thermal Stresses P.4-41

P.4.6.5.6 Evaluation of 24PTH DSC Performance for Normal Conditions P.4-41
P.4.6.6 DSC Thermal Evaluation for Off-Normal Conditions P.4-41
P.4.6.6.1 Off-Normal Ambient Temperatures during Storage P.4-41
P.4.6.6.2 Boundary Conditions, Off-Normal Storage P.4-41
P.4.6.6.3 Off-Normal Ambient Temperatures during Transfer P.4-41
P.4.6.6.4 Boundary Conditions, Off-Normal Transfer P.4-42
P.4.6.6.5 24PTH DSC Thermal Model Results for Off-Normal Conditions of Storage and Transfer P.4-42
P.4.6.6.6 Off-Normal 24PTH DSC Maximum Internal Pressure during Storage/Transfer P.4-42
P.4.6.6.7 Maximum Thermal Stresses P.4-43
P.4.6.6.8 Evaluation of 24PTH DSC Performance for Off-Normal Conditions P.4-43
P.4.6.7 DSC Thermal Evaluation for Accident Conditions P.4-43
P.4.6.7.1 Blocked Vent Accident Evaluation P.4-44
P.4.6.7.2 Transfer Accident Evaluation P.4-44
P.4.6.7.3 Hypothetical Fire Accident Evaluation P.4-44
P.4.6.7.4 Fuel Cladding and Basket Materials P.4-45
P.4.6.7.5 Maximum Internal Pressures P.4-45
P.4.6.7.6 Evaluation of the 24PTH DSC Performance During Accident Conditions P.4-46
P.4.7 Thermal Evaluation for Loading/Unloading Conditions P.4-47
P.4.7.1 Maximum Fuel Cladding Temperatures During Vacuum Drying P.4-47
P.4.7.2 Evaluation of Thermal Cycling of Fuel Cladding During Vacuum Drying, Helium Backfilling and Transfer Operations P.4-48
P.4.7.3 Reflooding Evaluation P.4-49
P.4.8 Determination of Effective Thermal Properties of the Fuel, Basket and Air Within the HSM-H Closed Cavity P.4-51
P.4.8.1 Determination of Bounding Effective Fuel Thermal Conductivity P.4-51
P.4.8.1.1 Fuel Assemblies Evaluated P.4-51
P.4.8.1.2 Summary of Thermal Properties of Materials P.4-51
P.4.8.1.3 Calculation of Fuel Axial Effective Thermal Conductivity P.4-51
P.4.8.1.4 Calculation of Fuel Transverse Effective Thermal Conductivity P.4-51
P.4.8.1.5 Results P.4-53
P.4.8.2 Calculation of Fuel Effective Specific Heat and Density P.4-54
P.4.8.3 24PTH DSC Basket Effective Thermal Properties P.4-55
P.4.8.4 Effective Air Conductivity in the HSM-H Closed Cavity P.4-55

P.4.9 Determination of Convection Heat Transfer Coefficients for the HSM-H Surfaces and Components P.4-58
P.4.9.1 Convection Coefficient for the HSM-H Side Heat Shield P.4-58
P.4.9.2 Convection Coefficient for the HSM-H Top Heat Shield P.4-63
P.4.9.3 Combination of Heat Transfer Coefficients for the HSM-H Roof and Front Wall P.4-63
P.4.10 Confirmatory Thermal-Hydraulic Analysis Of The HSM-H P.4-65
P.4.11 References P.4-68

P.5 Shielding Evaluation P.5-1
P.5.1 Discussion and Results P.5-5
P.5.2 Source Specification P.5-6
P.5.2.1 Gamma Source Term for MCNP P.5-9
P.5.2.1.1 Design Basis Gamma Fuel Assembly Source Terms P.5-9
P.5.2.1.2 Design Basis CC Source Terms P.5-9
P.5.2.1.3 Uncertainty in Gamma Source Terms P.5-10
P.5.2.2 Neutron Source Term for MCNP P.5-10
P.5.2.3 Axial Peaking P.5-11
P.5.2.4 ANISN Evaluation for Bounding Source Terms P.5-12
P.5.2.5 Reconstituted Fuel P.5-14
P.5.3 Material Densities P.5-16
P.5.4 Shielding Evaluation P.5-17
P.5.4.1 Computer Program P.5-17
P.5.4.2 Spatial Source Distribution P.5-17
P.5.4.3 Cross Section Data P.5-18
P.5.4.4 Flux-to-Dose-Rate Conversion P.5-18
P.5.4.5 Methodology P.5-18
P.5.4.6 Assumptions P.5-18
P.5.4.6.1 Source Term Assumptions P.5-19
P.5.4.6.2 HSM-H Dose Rate Analysis Assumptions P.5-19
P.5.4.6.3 HSM-Model 102 Dose Rate Analysis Assumptions P.5-19
P.5.4.6.4 OS197FC TC and Standardized TC Dose Rate Analysis Assumptions P.5-20
P.5.4.7 Normal Condition Models P.5-20
P.5.4.7.1 24PTH-L DSC in HSM-H P.5-20
P.5.4.7.2 24PTH-S-LC DSC in HSM-Model 102 ..... P.5-21
P.5.4.7.3 24PTH-L DSC in OS197FC TC P.5-23
P.5.4.7.4 24PTH-S-LC in Standardized TC P.5-24
P.5.4.8 Accident Models P.5-24
P.5.4.9 OS197FC TC Models During Fuel Loading Operations P.5-24
P.5.5 Appendix P.5-26
P.5.5.1 Sample SAS2H/ORIGEN-S Input File P.5-26
P.5.5.2 Sample HSM-H MCNP4C2 Model P.5-27
P.5.5.3 Sample OS197FC TC MCNP4C2 Model P.5-43

P.5.5.4 Sample ANISN Model (TC –Group 23) P.5-58
P.5.6 References P.5-63

P.6 Criticality Evaluation P.6-1
P.6.1 Discussion and Results P.6-2
P.6.2 Package Fuel Loading P.6-4
P.6.3 Model Specification P.6-6
P.6.3.1 Description of Calculational Model P.6-6
P.6.3.2 Package Regional Densities P.6-7
P.6.4 Criticality Calculations P.6-9
P.6.4.1 Calculational Method P.6-9
P.6.4.1.1 Computer Codes P.6-9
P.6.4.1.2 Physical and Nuclear Data P.6-10
P.6.4.1.3 Bases and Assumptions P.6-10
P.6.4.1.4 Determination of k_{eff} P.6-12
P.6.4.2 Fuel Loading Optimization P.6-12
P.6.4.3 Criticality Results P.6-25
P.6.5 Critical Benchmark Experiments P.6-26
P.6.5.1 Benchmark Experiments and Applicability P.6-26
P.6.5.2 Results of the Benchmark Calculations P.6-27
P.6.6 Appendix P.6-28
P.6.6.1 References P.6-28
P.6.6.2 Sample CSAS25 Input Files P.6-29
P.6.6.3 Design Basis Case CSAS25 Input Deck P.6-68

P.7 Confinement P.7-1
P.7.1 Confinement Boundary P.7-2
P.7.1.1 Confinement Vessel P.7-2
P.7.1.2 Confinement Penetrations P.7-2
P.7.1.3 Seals and Welds P.7-3
P.7.1.4 Closure P.7-3
P.7.2 Requirements for Normal Conditions of Storage P.7-4
P.7.2.1 Release of Radioactive Material P.7-4
P.7.2.2 Pressurization of Confinement Vessel P.7-4
P.7.3 Confinement Requirements for Hypothetical Accident Conditions P.7-5
P.7.3.1 Fission Gas Products P.7-5
P.7.3.2 Release of Contents P.7-5
P.7.4 References P.7-6

P.8 Operating Systems P.8-1
P.8.1 Procedures for Loading the Cask P.8-2
P.8.1.1 Preparation of the TC and DSC P.8-2
P.8.1.2 DSC Fuel Loading P.8-3
P.8.1.3 DSC Drying and Backfilling P.8-5
P.8.1.4 DSC Sealing Operations P.8-8
P.8.1.5 TC Downending and Transfer to ISFSI P.8-9

P.8.1.6 DSC Transfer to the HSM P.8-9
P.8.1.7 Monitoring Operations P.8-11
P.8.2 Procedures for Unloading the Cask P.8-15
P.8.2.1 DSC Retrieval from the HSM P.8-15
P.8.2.2 Removal of Fuel from the DSC P.8-15
P.8.3 Identification of Subjects for Safety Analysis P.8-24
P.8.4 Fuel Handling Systems P.8-24
P.8.5 Other Operating Systems P.8-24
P.8.6 Operation Support System P.8-24
P.8.7 Control Room and/or Control Areas P.8-24
P.8.8 Analytical Sampling P.8-24
P.8.9 References P.8-25

P.9 Acceptance Tests and Maintenance Program P.9-1
P.9.1 Acceptance Tests P.9-1
P.9.1.1 Visual Inspection P.9-1
P.9.1.2 Structural Tests P.9-1
P.9.1.3 Leak Tests P.9-1
P.9.1.4 Component Tests P.9-2
P.9.1.5 Shielding Integrity Tests P.9-2
P.9.1.6 Thermal Acceptance Tests P.9-2
P.9.1.7 Poison Plate Acceptance Tests P.9-2
P.9.1.7.1 Thermal Conductivity Testing of Poison Plates P.9-2
P.9.1.7.2 B10 Areal Density Testing of Poison Plates P.9-2
P.9.2 Maintenance Program P.9-9
P.9.3 References P.9.10

P.10 Radiation Protection P.10-1
P.10.1 Occupational Exposure P.10-2
P.10.2 Off-Site Dose Calculations P.10-3
P.10.2.1 Activity Calculations P.10-5
P.10.2.2 Dose Rates P.10-6
P.10.3 References P.10-8

P.11 Accident Analyses P.11-1
P.11.1 Off-Normal Operations P.11-2
P.11.1.1 Off-Normal Transfer Loads P.11-2
P.11.1.1.1 Postulated Cause of Event P.11-2
P.11.1.1.2 Detection of Event P.11-2
P.11.1.1.3 Analysis of Effects and Consequences P.11-2
P.11.1.1.4 Corrective Actions P.11-2
P.11.1.2 Extreme Temperatures P.11-3
P.11.1.2.1 Postulated Cause of Event P.11-3
P.11.1.2.2 Detection of Event P.11-3
P.11.1.2.3 Analysis of Effects and Consequences P.11-3

P.11.1.2.4 Corrective Actions P.11-3
P.11.1.3 Off-Normal Releases of Radionuclides P.11-3
P.11.1.3.1 Postulated Cause of Event P.11-4
P.11.1.3.2 Detection of Event P.11-4
P.11.1.3.3 Analysis of Effects and Consequences P.11-4
P.11.1.3.4 Corrective Actions P.11-4
P.11.1.4 Radiological Impact from Off-Normal Operations P.11-4
P.11.2 Postulated Accidents P.11-5
P.11.2.1 Reduced HSM Air Inlet and Outlet Shielding P.11-5
P.11.2.1.1 Cause of Accident P.11-5
P.11.2.1.2 Accident Analysis P.11-5
P.11.2.1.3 Accident Dose Calculations P.11-5
P.11.2.1.4 Corrective Actions P.11-5
P.11.2.2 Earthquake P.11-6
P.11.2.2.1 Cause of Accident P.11-6
P.11.2.2.2 Accident Analysis P.11-6
P.11.2.2.3 Accident Dose Calculations P.11-6
P.11.2.2.4 Corrective Actions P.11-6
P.11.2.3 Extreme Winds and Tornado Missiles P.11-6
P.11.2.3.1 Cause of Accident P.11-6
P.11.2.3.2 Accident Analysis P.11-6
P.11.2.3.3 Accident Dose Calculations P.11-13
P.11.2.3.4 Corrective Actions P.11-13
P.11.2.4 Flood P.11-13
P.11.2.4.1 Cause of Accident P.11-13
P.11.2.4.2 Accident Analysis P.11-13
P.11.2.4.3 Accident Dose Calculations P.11-13
P.11.2.4.4 Corrective Actions P.11-14
P.11.2.5 Accidental TC Drop P.11-14
P.11.2.5.1 Cause of Accident P.11-14
P.11.2.5.2 Accident Analysis P.11-14
P.11.2.5.3 Accident Dose Calculations for Loss of Neutron Shield P.11-14
P.11.2.5.4 Corrective Action P.11-15
P.11.2.6 Lightning P.11-15
P.11.2.7 Blockage of Air Inlet and Outlet Openings P.11-15
P.11.2.7.1 Cause of Accident P.11-15
P.11.2.7.2 Accident Analysis P.11-15
P.11.2.7.3 Accident Dose Calculations P.11-15
P.11.2.7.4 Corrective Action P.11-16
P.11.2.8 DSC Leakage P.11-16
P.11.2.9 Accident Pressurization of DSC P.11-16
P.11.2.9.1 Cause of Accident P.11-16
P.11.2.9.2 Accident Analysis P.11-16
P.11.2.9.3 Accident Dose Calculations P.11-16
P.11.2.9.4 Corrective Actions P.11-16

P.11.2.10 Fire and Explosion P.11-17
P.11.2.10.1 ..... Cause of the Accident P.11-17
P.11.2.10.2 ..... Accident Analysis P.11-17
P.11.2.10.3 ..... Accident Dose Calculations P.11-17
P.11.2.10.4 ..... Corrective Actions P.11-17
P.11.3 References P.11-18

P.12 Conditions for Cask Use - Operating Controls and Limits or Technical Specifications P.12-1

P.13 Quality Assurance P.13-1

P.14 Decommissioning P.14-1

LIST OF TABLES

		Page
Table P.1-1	Key Design Parameters of the NUHOMS®-24PTH System(2)	P.1-13
Table P.2-1	PWR Fuel Specification for the Fuel to be Stored in the NUHOMS®-24PTH DSC	P.2-19
Table P.2-2	Thermal and Radiological Characteristics for Control Components Stored in the NUHOMS® -24PTH DSC	P.2-21
Table P.2-3	PWR Fuel Assembly Design Characteristics for the NUHOMS®-24PTH DSC	P.2-22
Table P.2-4	Maximum Assembly Average Initial Enrichment v/s Neutron Poison Requirements for 24PTH DSC (Intact Fuel)	P.2-23
Table P.2-5	Maximum Assembly Average Initial Enrichment v/s Neutron Poison Requirements for 24PTH DSC (Damaged Fuel)	P.2-25
Table P.2-6	PWR Fuel Qualification Table for Zone 1 Fuel with 1.7 kW per Assembly for the NUHOMS®-24PTH DSC (Fuel w/o CCs)	P.2-26
Table P.2-7	PWR Fuel Qualification Table for Zone 2 Fuel with 2.0 kW per Assembly for the NUHOMS®-24PTH DSC (Fuel w/o CCs)	P.2-27
Table P.2-8	PWR Fuel Qualification Table for Zone 3 Fuel with 1.5 kW per Assembly for the NUHOMS®-24PTH DSC (Fuel w/o CCs)	P.2-28
Table P.2-9	PWR Fuel Qualification Table for Zone 4 Fuel with 1.3 kW per Assembly for the NUHOMS®-24PTH DSC (Fuel w/o CCs)	P.2-29
Table P.2-10	PWR Fuel Qualification Table for Zone 1 Fuel with 1.7 kW per Assembly for the NUHOMS®-24PTH DSC (Fuel w/ CCs)	P.2-30
Table P.2-11	PWR Fuel Qualification Table for Zone 2 Fuel with 2.0 kW per Assembly for the NUHOMS®-24PTH DSC (Fuel w/ CCs)	P.2-31
Table P.2-12	PWR Fuel Qualification Table for Zone 3 Fuel with 1.5 kW per Assembly for the NUHOMS®-24PTH DSC (Fuel w/ CCs)	P.2-32
Table P.2-13	PWR Fuel Qualification Table for Zone 4 Fuel with 1.3 kW per Assembly for the NUHOMS®-24PTH DSC (Fuel w/ CCs)	P.2-33
Table P.2-14	Summary of 24PTH-DSC Load Combinations	P.2-35
Table P.2-15	Summary of Stress Criteria for Subsection NB Pressure Boundary Components	P.2-39
Table P.2-16	Summary of Stress Criteria for Subsection NG Components	P.2-40
Table P.2-17	Classification of NUHOMS®-24PTH DSC Components	P.2-41
Table P.2-18	Summary of NUHOMS®-24PTH DSC and HSM-H Component Design Loadings(1)	P.2-42
Table P.2-19	Design Pressures for Tornado Wind Loading	P.2-45
Table P.2-20	B10 Specification for the NUHOMS®-24PTH Poison Plates	P.2-45
Table P.2-21	Maximum Allowable Heat Load for the NUHOMS®-24PTH DSC	P.2-45
Table P.3.1-1	Alternatives to the ASME Code for the NUHOMS®-24PTH DSC Confinement Boundary	P.3.1-8
Table P.3.1-2	Alternatives to the ASME Code for the NUHOMS®-24PTH DSC Basket Assembly	P.3.1-10
Table P.3.2-1	Summary of the NUHOMS®-24PTH System Component Nominal Weights	P.3.2-2
Table P.3.3-1	ASME Code Materials Data For SA-240 Type 304 and SA-182 Type F304 Stainless Steel	P.3.3-3

Table P.3.3-2 Materials Data For ASTM A36 Steel P.3.3-4
Table P.3.3-3 Static Mechanical Properties for ASTM B29 Lead P.3.3-5
Table P.3.3-4 ASME Code Properties for 6061 Aluminum P.3.3-6
Table P.3.3-5 Analysis Properties for Aluminum Transition Rails P.3.3-7
Table P.3.3-6 Additional Material Properties P.3.3-8
Table P.3.3-7 Concrete Properties P.3.3-9
Table P.3.3-8 Reinforcing Steel Material Properties at Temperature P.3.3-10
Table P.3.3-9 Materials Data for ASTM A992 Steel P.3.3-11
Table P.3.4-1 Summary of Thermal Stress Results - 24PTH Basket P.3.4-12
Table P.3.4-2 Summary of Thermal Forces and Moments in the HSM-H Concrete Components P.3.4-12
Table P.3.6-1 NUHOMS® 24PTH System Normal Operating Loading Identification P.3.6-19
Table P.3.6-2 Maximum NUHOMS®-24PTH-S / 24PTH-L DSC Shell Assembly Stresses for Normal and Off-Normal Loads P.3.6-20
Table P.3.6-3 Maximum NUHOMS®-24PTH-S-LC DSC Shell Assembly Stresses for Normal and Off-Normal Loads P.3.6-21
Table P.3.6-4 NUHOMS® -24PTH Basket Model Components, Element Types and Materials P.3.6-22
Table P.3.6-5 Material Properties Used in Normal Condition 24PTH Basket Analyses P.3.6-23
Table P.3.6-6 Normal Condition Stress Summary for 24PTH Basket Components – Vertical DW/Handling Loads P.3.6-24
Table P.3.6-7 Normal Condition Stress Summary for 24PTH Basket Components Horizontal DW/Handling P.3.6-25
Table P.3.6-8 Normal Condition Fuel Compartment Tubes-to-Steel Insert Plates (Straps) Weld Loads for 24PTH Basket P.3.6-26
Table P.3.6-9 NUHOMS® Off-Normal Operating Loading Identification P.3.6-27
Table P.3.6-10 Maximum NUHOMS® HSM-H Concrete Component Forces and Moment for Normal and Off-Normal Loads P.3.6-28
Table P.3.6-11 Comparison of ANSYS Results at TC Top Lid Center P.3.6-29
Table P.3.6-12 TC Enveloping Thermal Stresses for Load Combinations P.3.6-30
Table P.3.6-13 OS197/OS197H/OS197FC TC Combined Stresses For Normal Condition Loads(1)(2) P.3.6-31
Table P.3.6-14 OS197/OS197H/OS197FC TC Structural Shell Stresses at TC Trunnions P.3.6-32
Table P.3.6-15 Parameters of PWR Fuel Assemblies P.3.6-33
Table P.3.6-16 Fuel Cladding Computed Stresses and Ratios to Yield Stress P.3.6-34
Table P.3.6-17 Stress Intensities of Fuel Tubes for One Foot Side Drop Load P.3.6-35
Table P.3.7-1 Maximum NUHOMS®-24PTH-S/24PTH-L DSC Stresses for Drop Accident Loads P.3.7-25
Table P.3.7-2 Maximum NUHOMS®-24PT-S-LC DSC Stresses for Drop Accident Loads P.3.7-26
Table P.3.7-3 List of Drop Condition LS-DYNA Stress Analyses of the 24PTH Basket Assembly P.3.7-27
Table P.3.7-4 Summary of Material Properties for Drop Accident Analyses of the 24PTH Basket Assembly (1) (2) P.3.7-28

Table P.3.7-5 24PTH Basket, Enveloping Stress Results - 75g Side Drops P.3.7-29
Table P.3.7-6 24PTH Basket, Enveloping Stress Results - 60g End Drop P.3.7-30
Table P.3.7-7 Drop Condition ANSYS Stability Analyses for the 24PTH Basket Assembly P.3.7-31
Table P.3.7-8 NUHOMS®-24PTH-S/24PTH-L DSC Enveloping Load Combination Results for Normal and Off-Normal Loads P.3.7-32
Table P.3.7-9 NUHOMS®-24PTH-S-LC DSC Enveloping Load Combination Results for Normal and Off-Normal Loads P.3.7-33
Table P.3.7-10 NUHOMS®-24PTH-S/24PTH-L DSC Enveloping Load Combination Results for Accident Loads P.3.7-34
Table P.3.7-11 NUHOMS®-24PT-S-LC DSC Enveloping Load Combination Results for Accident Loads P.3.7-35
Table P.3.7-12 NUHOMS®-24PTH-S/24PTH-L DSC Enveloping Load Combination Results for Accident Loads P.3.7-36
Table P.3.7-13 NUHOMS®-24PTH-S-LC DSC Enveloping Load Combination Results for Accident Loads P.3.7-37
Table P.3.7-14 DSC Enveloping Load Combination (Notes to Table P.3.7-8 through Table P.3.7-13 ..... P.3.7-38
Table P.3.7-15 Summary of OS197/OS197H/OS197FC TC Stresses(1)(2)(3) P.3.7-39
Table P.3.7-16 HSM-H Concrete Load Combinations P.3.7-40
Table P.3.7-17 HSM-H Support Steel Structure Load Combinations P.3.7-41
Table P.3.7-18 Ultimate Capacities of Concrete Components P.3.7-42
Table P.3.7-19 Maximum NUHOMS® HSM-H Concrete Component Forces and Moments for Accident Loads P.3.7-43
Table P.3.7-20 Comparison of Highest Combined Shear Forces/Moments with the Capacities P.3.7-44
Table P.3.7-21 Maximum/Minimum Forces/Moments in the Rail Components in the Local System P.3.7-45
Table P.3.7-22 Maximum/Minimum Forces/Moments in the Rail Extension Plates in the Local System P.3.7-46
Table P.3.7-23 Maximum/Minimum Axial Forces in the Cross Member Components P.3.7-47
Table P.3.7-24 Rail Component Results P.3.7-48
Table P.3.7-25 Extension Plates and Cross Members Results P.3.7-49
Table P.4-1 Bulk Air Temperatures at Specified HSM-H Regions for the Various Cases(2) P.4-71
Table P.4-2 HSM-H Components Normal and Off-Normal Maximum Temperatures, 40.8 kW Heat Load P.4-72
Table P.4-3 HSM-H Components Normal and Off-Normal Maximum Temperatures, 31.2 kW Heat Load P.4-73
Table P.4-4 HSM-H Components Normal and Off-Normal Maximum Temperatures, 24 kW Heat Load P.4-74
Table P.4-5 HSM-H Components Maximum Temperatures (°F), 40.8 kW Decay Heat Load, 117°F Ambient, Blocked Vent Accident (Case 9) P.4-75
Table P.4-6 Single HSM-H Components Maximum Temperatures, 40.8 kW Heat Load, -40°F Ambient, Blocked Vent Accident (Case 10) P.4-76
Table P.4-7 Summary of OS197FC Cases P.4-77

Table P.4-8 Cask DSC Gap Hydraulic Characteristics as Function of Circumferential Position P.4-78
Table P.4-9 OS197FC TC Components and DSC Shell Temperatures with 40.8 kW Decay Heat Load under Normal and Off-Normal Conditions P.4-79
Table P.4-10 OS197FC TC Components and DSC Shell Temperatures with 31.2 kW Decay Heat Load, without Aluminum Inserts under Normal and Off-Normal Conditions P.4-80
Table P.4-11 OS197FC TC Components and DSC Shell Temperatures with 31.2 kW Decay Heat Load, with Aluminum Inserts under Normal and Off-Normal Conditions P.4-81
Table P.4-12 Steady-State Temperatures for a Loss of Neutron Shield P.4-82
Table P.4-13 Fire Accident Temperatures with 40.8 kW Decay Heat Load P.4-83
Table P.4-14 Fuel Cladding Normal Condition Maximum Temperatures P.4-84
Table P.4-15 DSC Basket Assembly Maximum Normal Operating Component Temperatures; HLZC 1 (40.8 kW) P.4-85
Table P.4-16 DSC Basket Assembly Maximum Normal Operating Component Temperatures; HLZC 4 (31.2 kW) P.4-86
Table P.4-17 DSC Basket Assembly Maximum Normal Operating Component Temperatures; HLZC 5 (24 kW) P.4-87
Table P.4-18 24PTH DSC Initial Helium Fill Gas Molar Quantities P.4-88
Table P.4-19 24PTH DSC Maximum Normal Operating Condition Pressures P.4-89
Table P.4-20 Fuel Cladding Off-Normal Condition Maximum Temperatures P.4-90
Table P.4-21 DSC Basket Assembly Maximum Off-Normal Operating Component Temperatures, HLZC 1[(4)] (40.8 kW) P.4-91
Table P.4-22 DSC Basket Assembly Maximum Off-Normal Operating Component Temperatures, HLZC 4 (31.2 kW) P.4-92
Table P.4-23 DSC Basket Assembly Maximum Off-Normal Operating Component Temperatures, HLZC 5 (24 kW) P.4-93
Table P.4-24 24PTH DSC Maximum Off-Normal Operating Condition Pressures P.4-94
Table P.4-25 Fuel Cladding Accident Condition Maximum Temperatures P.4-95
Table P.4-26 DSC Basket Assembly Accident Maximum Component Temperatures; HLZC 1 (40.8 kW) P.4-96
Table P.4-27 DSC Basket Assembly Accident Maximum Component Temperatures; HLZC 4 (31.2 kW) P.4-97
Table P.4-28 DSC Basket Assembly Accident Maximum Component Temperatures; HLZC 5 (24 kW) P.4-98
Table P.4-29 24PTH DSC Maximum Accident Condition Pressures P.4-99
Table P.4-30 Vacuum Drying Fuel Cladding Maximum Temperatures (°F) P.4-100
Table P.4-31 DSC Basket Assembly Maximum Component Temperatures during Vacuum Drying, HLZC 1 (40.8 kW) P.4-101
Table P.4-32 DSC Basket Assembly Maximum Component Temperatures during Vacuum Drying, HLZC 4 (31.2 kW) P.4-102
Table P.4-33 DSC Basket Assembly Maximum Component Temperatures during Vacuum Drying, HLZC 5 (24 kW) P.4-103
Table P.4-34 24PTH-S-LC DSC Shell Temperatures for Storage in HSM Model 102 ..... P.4-104
Table P.4-35 NUHOMS®-24PTH DSC Cavity Free Volumes P.4-105

Table P.4-36 Fuel Rod Helium Fill Gas Released per DSC P.4-106
Table P.4-37 Fission Gas Released per DSC P.4-107
Table P.4-38 CC Gas Released per DSC P.4-108
Table P.4-39 24PTH-S-LC DSC Shell Maximum Temperatures during Transfer in Standardized TC with 24 kW Heat Load P.4-109
Table P.4-40 Comparison Of Peak Component Temperatures For 117°F Ambient With 40.8 kW Decay Heat Load P.4-110
Table P.4-41 Maximum Normal and Off-Normal OS197 TC Component Temperatures with 40.8 kW Decay Heat Load (with Air Circulation) P.4-111
Table P.4-42 Maximum Normal and Off-Normal OS197 TC Component Temperatures with 31.2 kW Decay Heat Load (with Air Circulation) P.4-112
Table P.4-43 HSM-H Concrete and DSC Shell temperatures with and without Side Heat Shield Fins P.4-113
Table P.5-1 Summary of NUHOMS®-24PTH-L DSC in HSM-H, Maximum and Average Dose Rates, Configuration 2 (2) P.5-65
Table P.5-2 Summary of NUHOMS®-24PTH-S-LC DSC in HSM-Model 102, Maximum and Average Dose Rates, Configuration 5 ..... P.5-66
Table P.5-3 Summary of NUHOMS®-24PTH-L DSC, OS197FC TC Maximum Dose Rates During Transfer Operations, Configuration 2 ..... P.5-67
Table P.5-4 Summary of NUHOMS®-24PTH-L DSC, OS197FC TC Maximum Dose Rates During Decontamination and Welding Operations, Configuration 2 ..... P.5-68
Table P.5-5 Summary of NUHOMS®-24PTH-S-LC DSC, Standardized TC Maximum Dose Rates During Transfer Operations, Configuration 5 ..... P.5-69
Table P.5-6 PWR Fuel Assembly Material Mass P.5-70
Table P.5-7 Elemental Composition of LWR Fuel-Assembly Structural Materials P.5-71
Table P.5-8 Flux Scaling Factors By Fuel Assembly Region P.5-72
Table P.5-9 Gamma and Neutron Source Term for 2.0 kW Fuel in TC (62 GWd/MTU, 3.4 wt. % U-235 and 5.6-Year Cooled Fuel) P.5-73
Table P.5-10 Gamma and Neutron Source Term for 2.0 kW Fuel in HSM-H (41 GWd/MTU, 3.3 wt. % U-235 and 3.0-Year Cooled Fuel) P.5-74
Table P.5-11 Gamma and Neutron Source Term for 1.5 kW Fuel in TC or HSM (32 GWd/MTU, 2.6 wt. % U-235 and 3.0-Year Cooled Fuel) P.5-75
Table P.5-12 Design-Basis CC Source Terms P.5-76
Table P.5-13 Source Term Peaking Factor Summary P.5-77
Table P.5-14 Shielding Material Densities P.5-78
Table P.5-15 Material Densities for Fuel/Basket Region Used in ANISN Models P.5-79
Table P.5-16 Neutron Source for ANISN Calculation P.5-80
Table P.5-17 ANISN Response Function for the OS197FC TC P.5-81
Table P.5-18 ANISN Response Function for the HSM-H P.5-82
Table P.5-19 Flux to Dose Rate Conversion Factors P.5-83
Table P.5-20 Gamma and Neutron Macroscopic Cross Sections P.5-84
Table P.5-21 Surface Average Dose Rates on HSM-Model 102 with 24PTH-S-LC DSC P.5-85
Table P.5-22 Maximum Dose Rates on HSM-Model 102 with 24PTH-S-LC DSC P.5-86
Table P.5-23 OS917FC TC Total Dose Rates (mrem/hr) at Cask Centerline for 2.0 kW Case(1) P.5-87

Table P.5-24 HSM-H Total Dose Rates (mrem/hr) at Roof for 2.0 kW Case[1] P.5-88
Table P.5-25 OS197FC TC Total Dose Rates (mrem/hr) at Cask Centerline for 1.5 kW Case[1] P.5-89
Table P.5-26 HSM-H Total Dose Rates (mrem/hr) at Roof for 1.5 kW Case[1] P.5-90
Table P.6-1 Minimum B10 Content in the Neutron Poison Plates P.6-88
Table P.6-2 Authorized Contents for NUHOMS®-24PTH System P.6-89
Table P.6-3 Maximum Assembly Average Initial Enrichment for Each Configuration (Intact Fuel) P.6-90
Table P.6-4 Maximum Assembly Average Initial Enrichment for Each Configuration (Damaged Fuel) P.6-92
Table P.6-5 Parameters For PWR Assemblies P.6-93
Table P.6-6 NUHOMS®-24PTH Basket Dimensions P.6-95
Table P.6-7 Description of the Basic KENO Model Units for Intact Fuel P.6-96
Table P.6-8 Material Property Data P.6-97
Table P.6-9 Most Reactive Fuel Type Evaluation Results P.6-98
Table P.6-10 Transition Rail Material Evaluation Results P.6-100
Table P.6-11 Fuel Clad OD Thickness Evaluation Results P.6-101
Table P.6-12 Poison Plate Thickness Evaluation Results P.6-102
Table P.6-13 Fuel compartment tube Width Evaluation Results P.6-103
Table P.6-14 Fuel compartment tube Thickness Evaluation Results P.6-104
Table P.6-15 B&W 15x15 Class Assembly without CCs Final Results P.6-105
Table P.6-16 B&W 15x15 Class Assembly with CCs Final Results P.6-112
Table P.6-17 B&W 15x15 Class Assembly BORAL® Poison Results P.6-115
Table P.6-18 CE 14x14 Class Assembly without CCs Final Results P.6-116
Table P.6-19 CE 14x14 Class Assembly With CCs Final Results P.6-118
Table P.6-20 CE 15x15 Class Assembly without CCs Final Results P.6-119
Table P.6-21 CE 16x16 Class Assembly without CCs Final Results P.6-125
Table P.6-22 WE 14x14 Class Assembly without CCs Final Results P.6-127
Table P.6-23 WE 15x15 Class Assembly without CCs Final Results P.6-128
Table P.6-24 WE 15x15 Class Assembly with CCs Final Results P.6-134
Table P.6-25 WE 17x17 Class Assembly without CCs Final Results P.6-137
Table P.6-26 WE 17x17 Class Assembly with CCs Final Results P.6-144
Table P.6-27 Summary of Maximum k_{eff} for Each Fuel Assembly Class Final Results P.6-147
Table P.6-28 Key Parameters Utilized in the Damaged Assembly Calculations P.6-148
Table P.6-29 Rod Pitch Study Results P.6-149
Table P.6-30 Optimum Rod Pitch with Addition and Deletion of Rods P.6-155
Table P.6-31 Single Ended Shear Evaluation Results P.6-159
Table P.6-32 Double Ended Shear Break Evaluation Results P.6-163
Table P.6-33 Evaluation of Shifting of Fuel Rods beyond Poison P.6-165
Table P.6-34 Comparison of Various Damaged Assembly Configurations P.6-166
Table P.6-35 Dancoff Factor Calculation Results P.6-167
Table P.6-36 Damaged Assembly/Intact Assembly Final Results P.6-170
Table P.6-37 Criticality Results for Intact Fuel Assemblies with 23.145" "Egg-Crate" P.6-174
Table P.6-38 Criticality Results for Damaged Fuel Assemblies with with 23.145" "Egg-Crate" P.6-175

Table P.6-39 Summary of Criticality Results for Intact Fuel Assemblies P.6-176
Table P.6-40 Summary of Criticality Results for Damaged Fuel Assemblies P.6-177
Table P.6-41 Benchmarking Results P.6-178
Table P.6-42 USL-1 Results P.6-182
Table P.6-43 USL Determination for Criticality Analysis P.6-183
Table P.9-1 B10 Specification for the NUHOMS®-24PTH Poison Plates P.9.11
Table P.9-2 Specified Boron Content Borated Aluminum (90% B10 Credit) P.9.11
Table P.9-3 Specified B4C Content for Metal Matrix Composites (90% B10 Credit) P.9.11
Table P.10-1 Occupational Exposure Summary, 24PTH System P.10-9
Table P.10-2 Total Annual Exposure, 24PTH-L Within HSM-H P.10-10
Table P.10-3 Total Annual Exposure, 24PTH-S-LC Within HSM-Model 102 ..... P.10-11
Table P.10-4 HSM-H/HSM-Model 102 Gamma-Ray Spectrum Calculation Results P.10-12
Table P.10-5 HSM-H/HSM-Model 102 Neutron Spectrum Calculation Results P.10-13
Table P.10-6 Summary of ISFSI Surface Activities, 24PTH-L DSC Within HSM-H P.10-14
Table P.10-7 Summary of ISFSI Surface Activities, 24PTH-S-LC DSC Within HSM-Model 102 ..... P.10-15
Table P.10-8 MCNP Front Detector Dose Rates for 2x10 Array, 24PTH-L DSC Within HSM-H P.10-16
Table P.10-9 MCNP Back Detector Dose Rates for the Two 1x10 Arrays, 24PTH-L DSC Within HSM-H P.10-17
Table P.10-10 MCNP Side Detector Dose Rates, 24PTH-L DSC Within HSM-H P.10-18
Table P.10-11 MCNP Front Detector Dose Rates for 2x10 Array, 24PTH-S-LC DSC Within HSM-Model 102 ..... P.10-19
Table P.10-12 MCNP Back Detector Dose Rates for the Two 1x10 Arrays, 24PTH-S-LC DSC Within HSM-Model 102 ..... P.10.20
Table P.10-13 MCNP Side Detector Dose Rates, 24PTH-S-LC DSC Within HSM-Model 102 ..... P.10.21
Table P.11-1 Comparison of Total Dose Rates for HSM-H Loaded with 24PTH-S-LC, with and without Adjacent HSM Shielding Effects P.11-19
Table P.11-2 Calculated Accident Dose Rates on the Side of the OS197FC TC and Standardized TC P.11-20

LIST OF FIGURES

		Page
Figure P.1-1	NUHOMS®-24PTH DSC Components	P.1-14
Figure P.1-2	Disassembled View of the NUHOMS® 24PTH DSC Basket	P.1-15
Figure P.1-3	NUHOMS® HSM-H Schematic	P.1-16
Figure P.1-4	Schematic View of the HSM-H—Support Structure	P.1-17
Figure P.1-5	NUHOMS® OS197FC TC Top Lid (Bottom View)	P.1-18
Figure P.1-6	NUHOMS® Cask Support Skid for OS197FC TC	P.1-19
Figure P.2-1	Heat Load Zoning Configuration No. 1 for 24PTH-S and 24PTH-L DSCs (with or without Control Components)	P.2-46
Figure P.2-2	Heat Load Zoning Configuration No. 2 for 24PTH-S and 24PTH-L DSCs (with or without Control Components)	P.2-47
Figure P.2-3	Heat Load Zoning Configuration No. 3 for 24PTH-S and 24PTH-L DSCs (with or without Control Components)	P.2-48
Figure P.2-4	Heat Load Zoning Configuration No. 4 for 24PTH-S and 24PTH-L DSCs (with or without Control Components)	P.2-49
Figure P.2-5	Heat Load Zoning Configuration No. 5 for 24PTH-S-LC DSC (with or without Control Components)	P.2-50
Figure P.2-6	Location of Damaged Fuel Inside 24PTH DSC	P.2-51
Figure P.2-7	24PTH-S and 24PTH-L DSC Pressure Boundary	P.2-52
Figure P.2-8	24PTH-S–LC DSC Pressure Boundary	P.2-53
Figure P.3.1-1	24PTH-S and 24PTH-L DSC Pressure Boundary	P.3.1-12
Figure P.3.1-2	24PTH-S-LC DSC Pressure Boundary	P.3.1-13
Figure P.3.3-1	Stress-Strain Relationship for SA-240 Type 304 / SA-182 Type F304 Material Used in the Elastic-Plastic Analysis	P.3.3-12
Figure P.3.4-1	Potential Versus pH Diagram for Aluminum-Water System	P.3.4-13
Figure P.3.4-2	Applied Bounding Temperatures for Thermal Stress Analysis of 24PTH DSC	P.3.4-14
Figure P.3.6-1	24PTH-S / 24PTH-L DSC Shell Assembly Top End 90° Analytical Model	P.3.6-36
Figure P.3.6-2	24PTH-S / 24PTH-L DSC Shell Assembly Bottom End 90° Analytical Model	P.3.6-37
Figure P.3.6-3	Partial View of 24PTH-S / 24PTH-L DSC Shell Assembly Bottom End 180° Analytical Model Showing End Plates and Grapple Assembly	P.3.6-38
Figure P.3.6-4	24PTH-S-LC DSC Shell Assembly Axisymmetric Analysis ANSYS Model	P.3.6-39
Figure P.3.6-5	24PTH-S-LC DSC Shell Assembly Top and Bottom End 3D ANSYS Models	P.3.6-40
Figure P.3.6-6	24PTH Basket LS-DYNA Stress Analysis Model	P.3.6-41
Figure P.3.6-7	24PTH Basket LS-DYNA Finite Element Stress Analysis Model	P.3.6-42
Figure P.3.6-8	24PTH Basket Model Showing Fuel Compartment Tubes, Steel Insert Plates (Straps), and Beam Elements Modeling Connection Welds	P.3.6-43
Figure P.3.6-9	24PTH Basket LS-DYNA Model Analyses Results – Deadweight Stresses	P.3.6-44

Figure P.3.6-10 24PTH Basket LS DYNA Model Analysis Results – Thermal Stresses P.3.6-45
Figure P.3.6-11 OS197FC TC Top Lid (1/32 Segment) ANSYS Models with (Top View) and without (Bottom View) Vent Cutouts P.3.6-46
Figure P.3.6-12 Detailed View of TC Lid Model without (Top View) and with (Bottom View) Vent Cutouts P.3.6-47
Figure P.3.6-13 OS197FC TC Temperature Distribution for 40.8 kW with Air Circulation P.3.6-48
Figure P.3.6-14 OS197FC TC Temperature Distribution for 31.2 kW without Air Circulation P.3.6-49
Figure P.3.6-15 OS197FC TC Thermal Stress Analysis Model P.3.6-50
Figure P.3.6-16 OS197FC TC Thermal Stress Analysis Results for 40.8 kW with Air Circulation P.3.6-51
Figure P.3.6-17 OS197FC TC Thermal Stress Analysis Results for 31.2 kW without Air Circulation P.3.6-52
Figure P.3.6-18 Geometry Model #1: Central Crack in Finite Width Under Tension [3.29] P.3.6-53
Figure P.3.6-19 Geometry Model #2: Through-Wall Circumferential Crack in Cylinder Under Bending [3.30] P.3.6-54
Figure P.3.7-1 DSC Lift-Off Evaluation P.3.7-50
Figure P.3.7-2 0° Side Drop Stresses, 24PTH Basket (TC Support Rails at ±18.5°) P.3.7-51
Figure P.3.7-3 45° Side Drop Stresses, 24PTH Basket (TC Support Rails at ±18.5°) P.3.7-52
Figure P.3.7-4 24PTH Basket LS-DYNA Stability Analysis Model (TC Support Rails at ±18.5°) P.3.7-53
Figure P.3.7-5 0° Drop Stability Analysis- Displaced Shape at 172g P.3.7-54
Figure P.3.7-6 Displacement Time History for 0° Drop Stability Analysis (TC Support Rails at ±18.5°)) P.3.7-55
Figure P.3.7-7 45° Drop Stability Analysis - Resultant Displacements at 158g P.3.7-56
Figure P.3.7-8 Displacement Time History for 45° Drop Stability Analysis P.3.7-57
Figure P.3.7-9 180° Drop Stability Analysis – Displaced Shape at 167g P.3.7-58
Figure P.3.7-10 Displacement Time History for 180° Drop Stability Analysis P.3.7-59
Figure P.3.7-11 ANSYS Model of the HSM-H for Stress Analysis P.3.7-60
Figure P.3.7-12 ANSYS Model of the DSC and the DSC Support Structure P.3.7-61
Figure P.3.7-13 Symbolic Notations of Force and Moment Capacities (Also for Computed Forces and Moments) P.3.7-62
Figure P.3.7-14 Components of HSM-H Support Structure P.3.7-63
Figure P.3.7-15 24PTH-S-LC Plastic Strain Plot – 60g Bottom End Drop + 20 psi Off-Normal Pressure P.3.7-64
Figure P.4-1 HSM-H Air Flow Diagram P.4-114
Figure P.4-2 Convection Regions around 24PTH DSC in the HSM-H P.4-115
Figure P.4-3 24PTH DSC Shell Assembly in HSM-H Finite Element Model P.4-116
Figure P.4-4 Single HSM-H with 24PTH DSC Shell Assembly Finite Element Model P.4-117
Figure P.4-5 HSM-H with 24PTH DSC Finite Element Model for Blocked Vent Analysis P.4-118

Figure P.4-6 Temperature Distribution in HSM-H and 24PTH-S-LC DSC Shell Assembly, 24 kW Heat Load, 117°F Ambient P.4-119
Figure P.4-7 Temperature Distribution in HSM-H and 24PTH-S-LC DSC Shell Assembly, 24 kW Heat Load, -40°F Ambient P.4-120
Figure P.4-8 Temperature Distribution in HSM-H and 24PTH-S or -L DSC Shell Assembly, 31.2 kW Heat Load, 117°F Ambient P.4-121
Figure P.4-9 Temperature Distribution in HSM-H and 24PTH-S or -L DSC Shell Assembly, 31.2 kW Heat Load, -40°F Ambient P.4-122
Figure P.4-10 Temperature Distribution in HSM-H, Heat Shield, Support Rail, and 24PTH-S or –L DSC Shell Assembly, 31.2 kW Heat Load, without Fins on the Side Heat Shield, 117°F Ambient P.4-123
Figure P.4-11 Temperature Distribution in HSM-H, Heat Shield, Support Rail, and 24PTH-S or –L DSC Shell Assembly, 40.8 kW Heat Load, 117°F Ambient P.4-124
Figure P.4-12 Temperature Distribution in HSM-H, Heat Shield, Support Rail, and 24PTH-S or –L DSC Shell Assembly, 40.8 kW Heat Load, 100°F Ambient P.4-125
Figure P.4-13 Temperature Distribution in HSM-H and 24PTH DSC Shell Assembly, 40.8 kW Heat Load, -40°F Ambient P.4-126
Figure P.4-14 Temperature Distribution in HSM-H and 24PTH DSC Shell Assembly, 40.8 kW heat load, at 38.5 (typical) hours of Blocked vent, 117°F ambient P.4-127
Figure P.4-15 Temperature-Time Histories of HSM-H Model Components during Blocked Vents Accident Case, 40.8 kW, 117°F Ambient P.4-128
Figure P.4-16 Temperature Distribution in a Single HSM-H and 24PTH DSC Shell Assembly, 40.8 kW Heat Load, -40°F Ambient, Maximum Temperature Gradients through Concrete Walls P.4-129
Figure P.4-17 Temperature Distribution in a Single HSM-H, 40.8 kW Heat Load, -40°F Ambient, Maximum Temperature Gradients through Concrete Walls. Blocked Vent Transient at 38.5 Hours P.4-130
Figure P.4-18 Plan & Elevation Views of Short and Long Canister Spacers P.4-131
Figure P.4-19 OS197FC TC Lid With Slots For Air Exhaust P.4-132
Figure P.4-20 Perspective View of OS197FC TC Assembly Thermal Model P.4-133
Figure P.4-21 Perspective View of Thermal Model for Closure Lid, TC Cover, Neutron Shield, and TC Spacer P.4-134
Figure P.4-22 Perspective View of Thermal Model For DSC Shell & Ends Used For Steady-State Analyses P.4-135
Figure P.4-23 Perspective View of Thermal Model For DSC Shell, Ends, & Basket Used For Transient Analyses in OS197FC TC P.4-136
Figure P.4-24 Temperature Distribution at 11.5 hours for OS197FC TC during Transfer of 24PTH DSC, 40.8 kW Heat Load and 117°F Ambient P.4-137
Figure P.4-25 Temperature Distribution at 11.5 hours for 24PTH DSC Shell Assembly during Transfer in OS197FC TC, 40.8 kW Heat Load and 117°F Ambient P.4-138
Figure P.4-26 Temperature Distribution at 28.3 hours for OS197FC TC during Transfer of 24PTH DSC, 31.2 kW Heat Load and 117°F Ambient P.4-139

Figure P.4-27 Temperature Distribution at 28.3 hours for 24PTH DSC Shell Assembly during Transfer in OS197FC TC, 31.2 kW Heat Load and 117°F Ambient P.4-140
Figure P.4-28 Transient Temperature Response during Loading of 24PTH DSC with 40.8 kW into OS197FC TC, 100°F without Insolation (Cask Vertical) P.4-141
Figure P.4-29 Transient Temperature Response during Loading of 24PTH DSC with 31.2 kW into OS197FC TC, 100°F without Insolation (Cask Vertical) P.4-142
Figure P.4-30 Transient Temperature Response during Transfer of 24PTH DSC with 40.8 kW into OS197FC TC, 100°F with Insolation (Cask Horizontal) P.4-143
Figure P.4-31 Transient Temperature Response during Transfer of 24PTH DSC with 40.8 kW into OS197FC TC and Loss of Air Circulation Accident (Cask Horizontal) P.4-144
Figure P.4-32 Transient Temperature Response during Transfer of 24PTH DSC with 31.2 kW into OS197FC TC and Loss of Air Circulation Accident (Cask Horizontal) P.4-145
Figure P.4-33 Loss of Neutron Shield and Air Circulation (if used) Accident Transient Temperature Response with 40.8 kW (Cask Horizontal) P.4-146
Figure P.4-34 Loss of Neutron Shield and Air Circulation (if used) Accident Transient Temperature Response with 31.2 kW (Cask Horizontal) P.4-147
Figure P.4-35 24PTH DSC in OS197FC TC Fire Accident Transient Response with 40.8 kW P.4-148
Figure P.4-36 24PTH-S and 24PTH-L DSC, HLZC 1, 40.8 kW Maximum Decay Heat P.4-149
Figure P.4-37 24PTH-S and 24PTH-L DSC HLZC 4, 31.2 kW Maximum Decay Heat P.4-150
Figure P.4-38 24PTH-S-LC DSC HLZC 5, 24 kW Maximum Decay Heat P.4-151
Figure P.4-39 24PTH DSC Thermal ANSYS Model P.4-152
Figure P.4-40 24PTH DSC Thermal ANSYS Model, Basket Components P.4-153
Figure P.4-41 Temperature Distribution in 24PTH DSC for 100°F Transfer Case with HLZC 4 ..... P.4-154
Figure P.4-42 Maximum Fuel Temperatures during Vacuum Drying Transient with Air for HLZCs 1, 4, and 5 ..... P.4-155
Figure P.4-43 Finite Element Model of B&W 15x15 Fuel Assembly P.4-156
Figure P.4-44 Axial Fuel Effective Thermal Conductivity, All Fuels P.4-157
Figure P.4-45 Axial Fuel Effective Thermal Conductivity, B&W 15x15 Fuel Types P.4-158
Figure P.4-46 Fuel Transverse Effective Thermal Conductivity in Helium, All Fuels P.4-159
Figure P.4-47 Fuel Transverse Effective Thermal Conductivity in Vacuum, All Fuels P.4-160
Figure P.4-48 Fuel Transverse Effective Thermal Conductivity in Helium, B&W 15x15 Fuels P.4-161
Figure P.4-49 Fuel Transverse Effective Thermal Conductivity in Vacuum, B&W 15x15 Fuels P.4-162
Figure P.4-50 Gaps Used in the 24PTH DSC ANSYS Model P.4-163

Figure P.4-51 Elevation View Of Model Layout P.4-164
Figure P.4-52 Isometric View Of Model Layout P.4-164
Figure P.4-53 Model View From Underside Of HSM-H P.4-165
Figure P.4-54 DSC Within HSM-H P.4-166
Figure P.4-55 Perspective View Of Meshing At X-Y Plane Of HSM-H P.4-167
Figure P.5-1 ANISN HSM-H Model P.5-91
Figure P.5-2 ANISN OS197FC TC Model P.5-92
Figure P.5-3 24PTH-L DSC Within HSM-H, Side View at Centerline of DSC P.5-93
Figure P.5-4 24PTH-L DSC Within HSM-H, Head-on View at X=0 ..... P.5-94
Figure P.5-5 24PTH-L DSC Within HSM-H, Head-on View Showing Top Vents P.5-95
Figure P.5-6 24PTH-L DSC Within HSM-H, Head-on View at Lid End of DSC (X=225 cm) P.5-96
Figure P.5-7 24PTH-L DSC Within HSM-H, Head-on View at Bottom End of DSC (X=-225 cm) P.5-97
Figure P.5-8 24PTH-L DSC Within OS197FC TC, Axial View of Transfer Model P.5-98
Figure P.5-9 24PTH-L DSC Within OS197FC TC, Top View of Transfer Model Showing Cask Lid with Gap, Top Nozzle, and Plenum P.5-99
Figure P.5-10 24PTH-L DSC Within OS197FC TC, Bottom View of Transfer Model Showing Cask Bottom and Bottom Nozzle P.5-100
Figure P.5-11 24PTH-L DSC Within OS197FC TC, Radial Cut View of Transfer Models Showing Fuel Locations P.5-101
Figure P.5-12 24PTH-S-LC DSC Within Standardized TC, Axial View of Transfer Model P.5-102
Figure P.5-13 24PTH-S-LC DSC Within Standardized TC, Top View of Transfer Model Showing Cask Lid with Gap, Top Nozzle, and Plenum P.5-103
Figure P.5-14 24PTH-S-LC DSC Within Standardized TC, Bottom View of Transfer Model Showing Cask Bottom and Bottom Nozzle P.5-104
Figure P.5-15 24PTH-S-LC DSC Within Standardized TC, Radial Cut Views of Transfer Model Showing Fuel Locations P.5-105
Figure P.5-16 HSM-H with 24PTH-L DSC, Front Door Centerline Dose Rate P.5-106
Figure P.5-17 HSM-H with 24PTH-L DSC, Roof Centerline Dose Rate P.5-107
Figure P.5-18 HSM-H with 24PTH-L DSC, Side Shield Wall Surface at DSC Centerline Dose Rate P.5-108
Figure P.5-19 OS197FC TC with 24PTH-L DSC, Side Surface Dose Rate P.5-109
Figure P.5-20 OS197FC TC with 24PTH-L DSC, Top Surface Dose Rate P.5-110
Figure P.5-21 OS197FC TC with 24PTH-L DSC, Bottom Surface Dose Rate P.5-111
Figure P.5-22 Standardized Transfer Cask with 24PTH-S-LC DSC, Side Surface Dose Rate P.5-112
Figure P.5-23 Standardized Cask with 24PTH-S-LC DSC, Top Surface Dose Rate P.5-113
Figure P.5-24 Standardized Cask with 24PTH-S-LC DSC, Bottom Surface Dose Rate P.5-114
Figure P.6-1 NUHOMS®-24PTH DSC Cross Section P.6-184
Figure P.6-2 Basket Views and Dimensions P.6-185
Figure P.6-3 Basket Model Compartment Wall (View G) P.6-186
Figure P.6-4 Basket Model Compartment Wall (View F) P.6-187
Figure P.6-5 Basket Model Compartment Wall With Fuel Assembly (View G) P.6-188
Figure P.6-6 Basket Model Compartment Wall With Fuel Assembly (View F) P.6-189

Figure P.6-7 Basket Compartment With Fuel Assembly (Section A) P.6-190
Figure P.6-8 Basket Compartment With Fuel Assembly (Section B) P.6-191
Figure P.6-9 Fuel Position and Poison Plate Location in the 24PTH DSC Design P.6-192
Figure P.6-10 Fuel Position and Poison Plate Location in the KENO Model of 24PTH DSC P.6-193
Figure P.6-11 KENO V.a UNits and Radial Cross Sections of the Model of 24PTH DSC P.6-194
Figure P.6-12 Exxon 15x15 Fuel Assembly with Radial Variation in Enrichment P.6-195
Figure P.6-13 B&W 15x15 Class Assembly KENO Model P.6-196
Figure P.6-14 CE 14x14 Class Assembly KENO Model P.6-197
Figure P.6-15 CE 15x15 Class Assembly KENO Model P.6-198
Figure P.6-16 CE 16x16 Class Assembly KENO Model P.6-199
Figure P.6-17 WE 14x14 Class Assembly KENO Model P.6-200
Figure P.6-18 WE 15x15 Class Assembly KENO Model P.6-201
Figure P.6-19 WE 17x17 Class Assembly KENO Model P.6-202
Figure P.6-20 WE 14x14 Class Assembly, Single Shear Study Model P.6-203
Figure P.6-21 CE 16x16 Class Assembly, Double Shear Study Model P.6-204
Figure P.6-22 CE 14x14 Class Assembly, 8 Damaged / 16 Intact Fuel Assemblies P.6-205
Figure P.6-23 WE 15x15 Class Assembly, 12 Damaged / 12 Intact Fuel Assemblies P.6-206
Figure P.6-24 Basket Model Compartment Wall (View G) P.6-207
Figure P.6-25 Basket Model Compartment Wall (View F) P.6-208
Figure P.8-1 NUHOMS® System Loading Operations Flow Chart P.8-12
Figure P.8-2 NUHOMS® System Retrieval Operations Flow Chart P.8-21
Figure P.10-1 Annual Exposure from the ISFSI as a Function of Distance, 24PTH-L DSC Within HSM-H P.10-22
Figure P.10-2 Annual Exposure from the ISFSI as a Function of Distance, 24PTH-S-LC DSC Within HSM-Model 102 ..... P.10-23
Figure P.11-1 HSM-H Dimensions for Missile Impact Stability Analysis P.11-21

P.1 General Discussion

This Appendix to the NUHOMS® Final Safety Analysis Report (FSAR) addresses the Important to Safety aspects of adding the NUHOMS®-24PTH system to the Standardized NUHOMS® system described in the FSAR.

The NUHOMS®-24PTH system is a modular canister based spent fuel storage and transfer system, similar to the Standardized NUHOMS®-24P system described in the FSAR. The NUHOMS®-24PTH system consists of the following new or modified components:

- A new dual purpose (Storage/Transportation) Dry Shielded Canister (DSC), with three alternate configurations, designated as DSC Type NUHOMS®-24PTH-S, -24PTH-L, and -24PTH-S-LC,
- A new 24PTH DSC basket design, which is provided with two alternate options: with aluminum inserts (Type 1) or without aluminum inserts (Type 2) as shown in Figure P.1-1. In addition, depending on the boron content in the basket poison plates, each basket type is designated as Type A (low B10), Type B (moderate B10) or Type C (high B10) which results in six different basket types (Type 1A, 1B, 1C, 2A, 2B, or 2C),
- A modified version of the Standardized Horizontal Storage Module (HSM) Model 102 described in the FSAR, designated as HSM-H, equipped with special design features which provide enhanced shielding and heat rejection capabilities, and
- The OS197/OS197H Transfer Cask (TC) described in the FSAR, is provided with an optional modified top lid to allow air circulation through the TC/DSC annulus during transfer operations at certain heat loads when time limits for transfer operations cannot be satisfied. The OS197 TC with a modified top lid is designated as *the* OS197FC TC. *The OS197H TC with a modified top lid is designated as the OS197HFC TC. Throughout this Appendix, "OS197FC" is a generic designation intended to apply to the OS197FC or OS197HFC TCs unless otherwise explicitly stated.*

The 24PTH DSC is designed to accommodate up to 24 intact (or up to 12 damaged and balance intact) PWR fuel assemblies, with characteristics as described in Chapter P.2. The 24PTH-S and 24PTH-L are the short and long cavity configurations of the 24PTH DSC designed for a maximum heat load of 40.8 kW. They are transferred to the ISFSI for storage in the HSM-H in either the OS197/OS197H or OS197FC TC depending upon the heat load.

The 24PTH-S-LC DSC is a modified version of 24PTH-S DSC, provided with thinner top and bottom lead shield plugs instead of steel, resulting in a longer cavity length. This DSC type is designed for a maximum heat load of 24 kW per DSC and may be stored in either the currently licensed Standardized HSM Model 102, or in the new HSM-H, while the currently licensed Standardized TC (with a solid neutron shield) is used for onsite transfer.

Fuel assemblies with Control Components are to be stored only in 24PTH-L and 24PTH-S-LC DSC Types, due to their longer cavity length.

Figure P.1-4 shows these features in a cross sectional view of the HSM-H. The key design parameters and estimated weights of the HSM-H module are shown in Table P.1-1. The geometry and materials used to fabricate the HSM-H module are shown in the Parts List on Drawings NUH-03-7001-SAR included in Section P.1.5.

P.1.2.1.3 NUHOMS®-OS197FC Transfer Cask

The OS197FC TC is a modified version of the OS 197/OS197H TC described in the FSAR and in the drawings included in Appendix E of the FSAR.

The top lid of the OS197/OS197H TC is scalloped out at sixteen locations on the lid underside (See Figure P.1-5) to provide slots that provide an exit path for air circulation through the TC/DSC annulus. This external air circulation feature is needed during the transfer mode if decay heat is greater than 31.2 kW and basket type used in the DSC is 1A, 1B, or 1C and specific time limits for transfer are not met, *or if the decay heat is greater than 24.0 kW (but not greater than 31.2 kW) and basket type used is 2A, 2B, 2C, and specific time limits for transfer are not met.*

To achieve this air circulation, the NUHOMS® TC support skid is modified by the addition of two motor-driven redundant industrial grade blowers and associated hoses (See Figure P.1-6) which are connected via a cone adapter to the ram access opening. The TC spacer inside the TC cavity also requires minor modifications to ensure distribution of the airflow to the perimeter region of the TC. The air circulation system is sized to provide a minimum capacity of 450 cfm.

The modifications necessary to convert OS197/OS197H TC into a OS197FC TC are shown on Drawings NUH-03-8000-SAR and NUH-03-8006-SAR, included in Section P.1.5.

P.1.2.2 Operational Features

P.1.2.2.1 General Features

The NUHOMS®-24PTH DSC is designed to safely store 24 intact standard PWR fuel assemblies or up to 12 damaged and remaining intact fuel assemblies with or without CCs. The NUHOMS®-24PTH DSC is designed to maintain the fuel cladding temperature below allowable limits during normal storage, short-term accident conditions, short-term off-normal conditions and fuel loading/transfer operations.

The criticality control features of the NUHOMS®-24PTH DSC are designed to maintain the neutron multiplication factor k-effective less than the upper subcritical limit equal to 0.95 minus benchmarking bias and modeling bias under all conditions.

P.1.2.2.2 Sequence of Operations

The sequence of operations to be performed in loading fuel into the NUHOMS®-24PTH DSCs is presented in Chapter P.8.

Table P.1-1
Key Design Parameters of the NUHOMS®-24PTH System[2]

Parameter	24PTH DSC Type		
	24PTH-S	24PTH-L	24PTH-S-LC
DSC Length (in.)	186.55 (Maximum)	192.55 (Maximum)	186.55 (Maximum)
DSC Outside Diameter (in)	67.19	67.19	67.19
DSC Cavity Length (in.)	169.6	175.6	173.28
DSC Shell Thickness (in)	0.5	0.5	0.5
DSC Loaded Weight, Dry[1] (kips)	92.4/89.0	93.7/90.1	89.5
DSC Loaded Weight, Wet[1] (kips)	96.6/93.2	98.4/94.8	95.1
HSM-H Single Module Weight, Empty (kips)	306.1		
HSM-H Single Module Weight, Loaded (kips)	398.5	399.8	395.6
HSM Model 102 Weight, Empty (kips)	NA	NA	263.0
HSM Model 102 Weight, Loaded (kips)	NA	NA	352.5

HSM-H	
Overall Length (without shield walls), in	248
Overall Width (without shield walls), in	116
Overall Height, in	222

Notes: (1) The 24PTH-S and 24PTH-L DSC weights are provided with and without aluminum inserts in the R45 transition rails of the basket. The 24PTH-S-LC DSC does not include aluminum inserts.
(2) *Unless* stated otherwise, nominal values are provided.

Figure Withheld Under 10 CFR 2.390

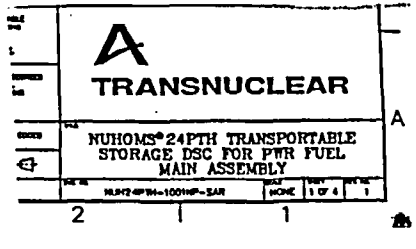

Figure Withheld Under 10 CFR 2.390

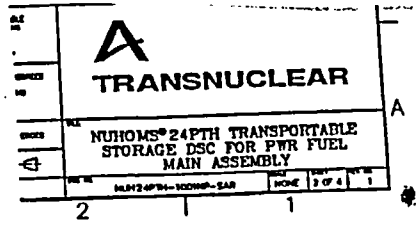

Figure Withheld Under 10 CFR 2.390

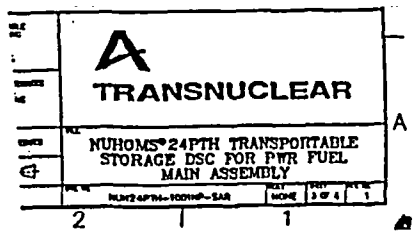

Figure Withheld Under 10 CFR 2.390

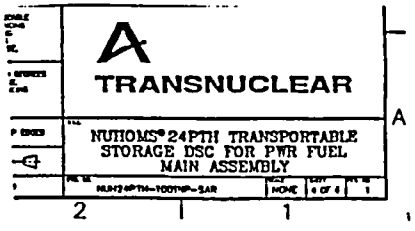

Figure Withheld Under 10 CFR 2.390

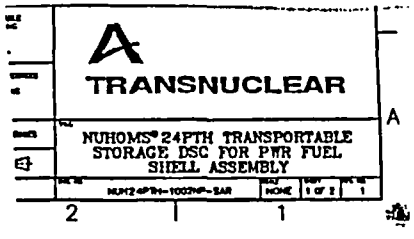

Figure Withheld Under 10 CFR 2.390

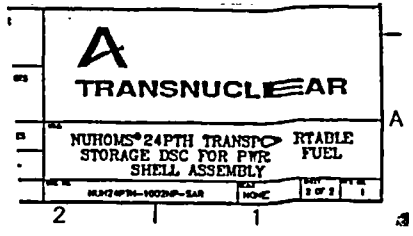

Figure Withheld Under 10 CFR 2.390

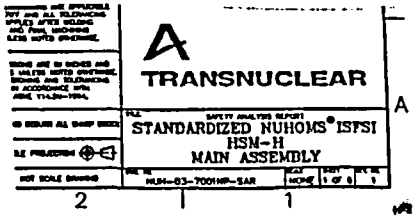

Figure Withheld Under 10 CFR 2.390

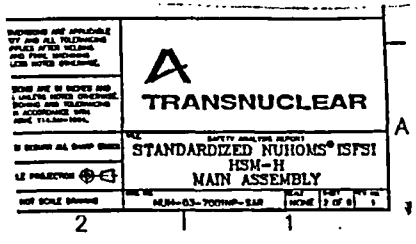

Figure Withheld Under 10 CFR 2.390

TRANSNUCLEAR

SAFETY ANALYSIS REPORT

STANDARDIZED NUHOMS® ISFSI
HSM-H
MAIN ASSEMBLY

NUH-03-7000HP-SAR | NONE | 3 OF 6 | 1

2 1 1 A

Figure Withheld Under 10 CFR 2.390

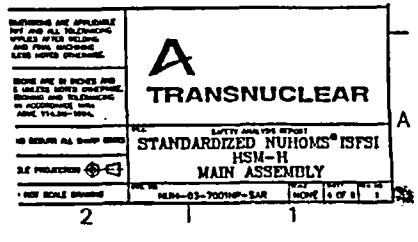

Figure Withheld Under 10 CFR 2.390

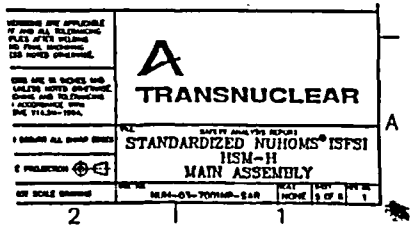

Figure Withheld Under 10 CFR 2.390

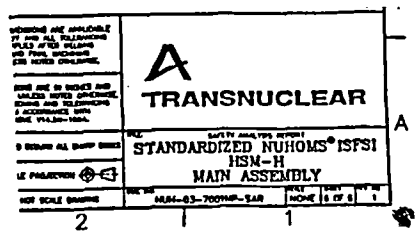

P.2.5 Summary of NUHOMS®-24PTH DSC and HSM-H Design Criteria

P.2.5.1 24PTH DSC Design Criteria

The principal design criteria for the NUHOMS®-24PTH DSC are presented in *Table P.2-18*. The NUHOMS®-24PTH DSC is designed to store intact and/or damaged PWR fuel assemblies with or without Control Components with assembly average burnup, initial enrichment and cooling time as described in Table P.2-1 and Table P.2-3. The maximum total heat generation rate of the stored fuel is limited to 2.0 kW per fuel assembly (1.5 kW for 24PTH-S-LC DSC) and 40.8 kW per canister (24.0 kW for 24PTH-S-LC DSC) in order to keep the maximum fuel cladding temperature below the limit [2.5] necessary to ensure cladding integrity. The fuel cladding integrity is assured by the NUHOMS®-24PTH DSC and basket design which limits fuel cladding temperature and maintains a nonoxidizing environment in the DSC cavity as described in Section P.4.

The NUHOMS®-24PTH DSC (shell and closure) is designed and fabricated as a Class 1 component in accordance with the rules of the ASME Boiler and Pressure Vessel Code, Section III, Subsection NB [2.2], and the alternative provisions to the ASME Code as described in Table P.3.1-1.

The NUHOMS®-24PTH DSC is designed to maintain a subcritical configuration during loading, handling, storage and accident conditions. A combination of fixed neutron absorbers, soluble boron in the pool and favorable geometry are employed to maintain the upper subcritical limit of 0.9411. The fixed neutron absorbers are in the form of borated aluminum metallic plates or Boral®. The basket is designed and fabricated in accordance with the rules of the ASME Boiler and Pressure Vessel Code, Section III, Subsection NG, Article NG-3200 [2.2] and the alternative provisions to the ASME Code as described in Table P.3.1-1.

The NUHOMS®-24PTH DSC design, fabrication and testing are covered by Transnuclear's Quality Assurance Program, which conforms to the criteria in Subpart G of 10CFR72.

The NUHOMS®-24PTH DSC is designed to withstand the effects of severe environmental conditions and natural phenomena such as earthquakes, tornadoes, lightning and floods. Section P.11 describes the NUHOMS®-24PTH DSC behavior under these accident conditions.

P.2.5.2 HSM-H Design Criteria

The principal design criteria for the NUHOMS® HSM-H module and steel support structure are presented in Table P.2-18. The load combination and design criteria for concrete and support structure components are the same as those described in Section 3.2.5.1. These criteria, provided in Tables 3.2-4, 3.2-5, 3.2-8 and 3.2-10 are also applicable to the HSM-H design.

Table P.2-14
Summary of 24PTH-DSC Load Combinations

Load Case	Horizontal DW		Vertical DW		Internal Pressure	External Pressure	Thermal Condition	Lifting Loads	Other Loads	Service Level
	DSC	Fuel	DSC	Fuel						
Non-Operational Load Cases										
NO-1 Fab. Leak Testing	–	–	–	–	–	14.7 psi	70°F	–	155 kip axial	Test
NO-2 Fab. Leak Testing	–	–	–	–	18 psi				155 kip axial	Test
NO-3 DSC Uprighting	x	–	–	–	–	–	70°F	x	–	*B*
NO-4 DSC Vertical Lift	–	–	x	–	–	–	70°F	x	–	*B*
Fuel Loading Load Cases										
FL-1 DSC/Cask Filling	–	–	Cask	–	–	Hydrostatic	100°F Cask	x	x	A
FL-2 DSC/Cask Filling	–	–	Cask	–	Hydrostatic	Hydrostatic	100°F Cask	x	x	A
FL-3 DSC/Cask Xfer	–	–	Cask	–	Hydrostatic	Hydrostatic	100°F Cask	–	–	A
FL-4 Fuel Loading	–	–	Cask	x	Hydrostatic	Hydrostatic	100°F Cask	–	–	A
FL-5 Xfer to Decon	–	–	Cask	x	Hydrostatic	Hydrostatic	100°F Cask	–	–	A
FL-6 Inner Cover plate Welding	–	–	Cask	x	Hydrostatic	Hydrostatic	100°F Cask	–	–	A
FL-7 Fuel Deck Seismic Loading	–	–	Cask	X	Hydrostatic	Hydrostatic	100°F Cask	–	Note 10	D
Draining/Drying Load Cases										
DD-1 DSC Blowdown	–	–	Cask	X	Hydrostatic+ 20 psi	Hydrostatic	100°F Cask	–	–	B
DD-2 Vacuum Drying	–	–	Cask	X	0 psia	Hydrostatic+ 14.7psi	100°F Cask	–	–	B
DD-3 Helium Backfill	–	–	Cask	X	18 psi	Hydrostatic	100°F Cask	–	–	B
DD-4 Final Helium Backfill	–	–	Cask	X	3.5 psi	Hydrostatic	100°F Cask	–	–	B
DD-5 Outer Cover Plate Weld	–	–	Cask	X	3.5 psi	Hydrostatic	100°F Cask	–	–	B
Transfer Trailer Loading										
TL-1 Vertical Xfer to Trailer	–	–	Cask	x	15 psi	–	0°F Cask	–	–	A
TL-2 Vertical Xfer to Trailer	–	–	Cask	x	15 psi	–	100°F Cask	–	–	A
TL-3 Laydown	Cask	X	–	–	15 psi	–	0°F Cask	–	–	A
TL-4 Laydown	Cask	X	–	–	15 psi	–	100°F Cask	–	–	A

Table P.2-18
Summary of NUHOMS®-24PTH DSC and HSM-H Component Design Loadings[1]
(continued)

Component	Design Load Type	SAR Section Reference	Design Parameters	Applicable Codes
HSM-H Module	---	---	---	ACI 349-97, ACI 318-*95* (for *construction* only)
	Flood	P.2.2.5.2.3(C)	Maximum water height: 50 ft. Maximum velocity of water 15'/sec.	10CFR72.122(b)
	Seismic	P.2.2.5.2.3(D)	Horizontal ground acc: 0.30g Vertical ground acc.: 0.20g	NRC Reg. Guides 1.60 & 1.61 [2.11] and [2.12]
	Dead Load	P.2.2.5.2.1(A)	150 pcf concrete structure and weight of support steel structure	ANSI 57.9-1984 [2.9]
	Normal and Off-Normal Operating Temperature	P.2.2.5.2.1(C) P.2.2.5.2.2(A)	Normal: Ambient air temperature 0°F -100°F Off Normal: Ambient air temperature -40°F to 117°F	ANSI 57.9-1984 [2.9]
	Normal Handling Loads	P.2.2.5.2.1(D)	1. Hydraulic ram load of 80,000 lb.(DSC HSM insertion) 60,000 lb (DSC HSM extraction) on the rails	ANSI 57.9-1984 [2.9]
	Off-Normal Handling Loads	P.2.2.5.2.2(B)	Hydraulic ram load of: 80,000 lb (DSC insertion) 80,000 lb (DSC extraction) on both rails	ANSI-57.9-1984 [2.9]
	Design Basis Wind Load	P.2.2.5.2.1(E)	Conservatively assumed to be same as tornado generated wind load.	ASCE 7-95 [2.8]
	Live Load	P.2.2.5.2.1(B)	200 psf (including snow and ice load) on the roof DSC weight (110 kips)	ANSI-57.9-1984 [2.9] ASCE 7-95 [2.8]
	Accident Temperature	P.2.2.5.2.3(A)	Ambient air temperature of –40°F and 117°F with inlet and outlet vents blocked number for condition depending upon heat load	10CFR72.122(n)
	Tornado Wind Load	P.2.2.5.2.3(B)	Maximum wind speed of 360 mph and a pressure drop of 3 psi	ASCE 7-95 [2.8] NRC Regulatory Guide 1.76 [2.6]
	Tornado Missile Load	P.2.2.5.2.3(B)	See Section P.2.2.1.3 for missiles considered.	NUREG-0800 Section 3.5.1.4 [2.7]

Note:
(1) The design criteria for the TC remain unchanged from the FSAR (FSAR Table 3.2-1).

Table P.2-19
Design Pressures for Tornado Wind Loading

HSM-H Wall Orientation(1)	Velocity Pressure (psf)	Pressure Coefficient(2)	Max/Min Design Pressure (psf)
Front	344	+0.68	234
Left	344	-0.60	-207
Rear	344	-0.43	-148
Right	344	-0.60	-207
Roof	344	-0.60	-207

Notes:
(1) Wind direction assumed to be from front. Wind loads from other directions may be found by rotating table values to desired wind direction.
(2) Pressure coefficient (used) = Gust factor (0.85)* Max/Min pressure coefficient.

Table P.2-20
B10 Specification for the NUHOMS®-24PTH Poison Plates

NUHOMS ®-24PTH DSC Basket Type (1)	Minimum B10 Aerial Density, gm/cm²	
	Natural or Enriched Boron aluminum Alloy / Metal Matric Composite (MMC)	Boral®
1A or 2A	.007	.009
1B or 2B	.015	.019
1C or 2C	.032	.040

Notes:
(1) Basket Type 1 contains aluminum inserts in the R45 transition rails; Type 2 does not contain aluminum inserts.

Table P.2-21
Maximum Allowable Heat Load for the NUHOMS®-24PTH DSC

24PTH DSC Type	*Basket Type (2)(3)*	*Transfer Cask*	*Max. Heat Load (kW) per DSC*
24PTH-S or 24PTH-L(1)	*1A, 1B, or 1C*	*OS197FC*	*40.8*
		OS197/OS197H	*31.2*
24PTH-S or 24PTH-L(1)	*2A, 2B, or 2C*	*OS197FC*	*31.2*
24PTH-S-LC(1)	*2A, 2B, or 2C*	*Standardized TC (solid neutron shield)*	*24.0*

Notes:
(1) Allows storage of control components.
(2) Basket Type 1 (1A, 1B, 1C) has heat conductive aluminum inserts in the R45 basket transition rails.
(3) Basket Type 2 (2A, 2B, 2C) does not have heat conductive aluminum inserts in the R45 basket transition rails.

The 24PTH-DSC is supported inside the base unit on two carbon steel rails. The rail assembly spans between the front and the rear wall of the base unit and acts as a sliding surface during 24PTH-DSC insertion and retrieval.

The air inlet vents are located at the bottom of the side walls of the base unit. The air outlet vents are formed along the sides of the roof. A roof vent shield cap above the outlet vent provides additional shielding. Steel liner plates are used at the inlet and outlet vents to provide additional shielding and reduce dose rates.

For thermal protection of the HSM-H concrete, stainless steel heat shields with anodized aluminum backing plates and fins are installed on the sidewalls of the base unit. Heat shields with stainless steel mounting bars and aluminum louvers are also installed under the roof. The heat shields guide cooling airflow through the HSM-H.

The HSM-H front *standard* door is a composite door, which consists of a rectangular steel *face* plate at the front attached to a circular thick steel plate and a circular reinforced concrete block at the rear. *The rectangular steel face plate of the door is attached to the front wall concrete using four bolts anchored through four embedments. The alternate circular door is similar to the standard door except that the front face plate is a circular steel plate. The circular steel plate of the door is attached to the front wall concrete by four clamps which are located at the 45° line in each quadrant of the door. The clamps consist of four "L" shaped clips which are bolted to the front wall concrete through four embedments.* The door provides missile protection and shielding for the 24PTH-DSC.

During 24PTH-DSC insertion/retrieval operations, the TC is docked with the HSM-H docking surface and mechanically secured to the HSM-H cask restraint embedments provided in the front of the HSM-H base unit. These embedments are equally spaced on either side of the HSM-H access opening and serve to restrain the transfer cask during insertion/retrieval of the 24PTH-DSC.

P.3.1.1.3 General Description of the HSM Model 102

The 24PTH-S-LC DSC, which has a maximum heat load of 24 kW, is stored in either HSM-H or HSM Model 102. The description of HSM Model 102 is included in Appendix E drawings for the standardized HSM. There is no change to the design of HSM Model 102 to accommodate the 24PTH-S-LC DSC.

P.3.1.1.4 General Description of the OS197FC TC

The OS197FC TC is identical to the OS197/OS197H TCs described in the FSAR and in the drawings included in Appendix E of the FSAR, with the exception of the TC top lid, which is modified to improve the TC thermal performance. The modification consists of adding vent passages around the periphery of the TC, in between the bolt holes. The vents are added to permit airflow through the TC. Ambient air is circulated at the bottom of the TC through the ram access opening and distributed to the annular space between the DSC and the TC. The cooling air travels through the TC length and exists through the vent passages in the TC top lid. Figure P.1.1-5 shows an isometric view of the modified TC top lid. Drawing NUH-03-8000-SAR describes the OS197FC TC and Drawing NUH-03-8006-SAR shows the TC top lid modification as implemented in the OS197FC TC. These drawings are provided in Section P.1.5.

Table P.3.1-2
Alternatives to the ASME Code for the NUHOMS®-24PTH DSC Basket Assembly
(Concluded)

Reference ASME Code Section/Article	Code Requirement	Alternatives, Exception, Justification & Compensatory Measures
NG-3352	Table NG 3352-1 lists the permissible welded joints	The fusion (spot) type welds between the stainless steel insert plates (straps) and the stainless steel fuel compartment tube are not permissible welds per Table NG-3352-1. These welds are qualified by testing. The required minimum tested capacity of the welded connection (at each side of the tube) shall be 36 Kips (at room temperature). This value is based on a margin of safety (test-to-design) of 1.6, which is larger than the Code-implied margin of safety for Level D loads. The minimum capacity shall be determined by shear tests of individual specimens made from production material. The tests shall be corrected for temperature differences (test-to-design) and for material properties (actual-to-ASME Code minimum values) to demonstrate that the capacity of the welded connection with ASME minimum properties, tested at design temperatures, will meet the 36 Kips test requirement. The capacity of the welded connection is determined from the *test of the weld pattern of a typical insert plate to the tube connection.*

For the stress analyses of the 24PTH *DSC*, material properties for the Type 304 steel materials are taken from Table P.3.3-1. For elastic-plastic analyses, the plastic slope is taken as 0.05E (5% of the elastic modulus at temperature). Figure P.3.3-1 *shows the stress-strain relationship used for the elastic-plastic analysis.* Properties for the aluminum rails are taken directly from Table P.3.3-5 [3.3]. For elastic-plastic analyses, the plastic slope of the aluminum is taken as 0.01E. This approximates elastic-perfectly plastic properties while providing a small stiffness to enhance analytical stability.

Table P.3.3-6 provides additional material properties.

P.3.3.2 HSM-H Material Properties

The temperature dependent material properties for concrete and reinforcing steel are taken from [3.26] and are provided in Table P.3.3-7 and Table P.3.3-8 respectively.

The material properties of the ASTM A992 steel used for fabrication of the rails of the support structure are listed in Table P.3.3-9. The material properties used for the Type 304 stainless steel used for the heat shield support plate and the A36 steel used for the rail assembly extension plates are provided in Table 8.1-3. The heat shield fins, the aluminum backing sheet, and the louvered heat shield are made of commercial grade aluminum.

P.3.3.3 Materials Durability

The materials used in the fabrication of the NUHOMS®-24PTH system are shown in Table P.3.3-1 through Table P.3.3-9. Essentially all of the materials meet the appropriate requirements of the ASME Code, ACI Code, and appropriate ASTM Standards. The durability of the DSC shell assembly and basket assembly stainless steel components and the HSM-H steel components is well beyond the design life of the applicable components. The aluminum material used in the basket is only relied upon for its thermal conductivity and bearing strength properties. The poison material selected for criticality control of the NUHOMS®-24PTH system has been tested and is currently in use for similar applications. Additionally, the NUHOMS®-24PTH basket assembly resides in an inert helium gas environment for the majority of the design life. The specifications controlling the mix of concrete, specified minimum concrete strength requirements, and fabrication control ensure durability of the materials for this application. Therefore, the materials used in the NUHOMS®-24PTH system will maintain the required properties for the design life of the system.

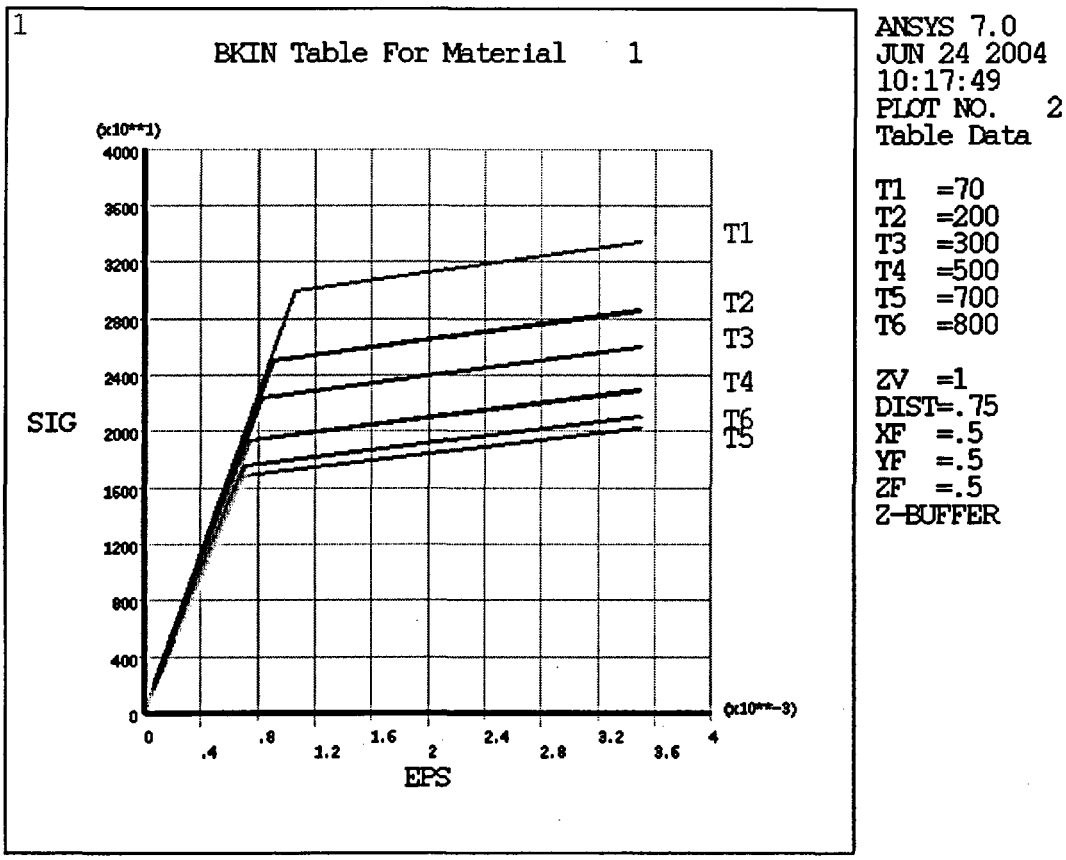

Figure P.3.3-1
Stress-Strain Relationship for SA-240 Type 304 / SA-182 Type F304 Material Used in the Elastic-Plastic Analysis

The hand calculations performed to evaluate the effects of differential thermal expansion are based on temperatures for the vacuum drying case. This case is selected because it maximizes the temperature differential between the DSC shell and the internal basket assembly components.

Radial Expansion

In the radial direction, the thermal expansion of the neutron absorbing/ aluminum heat transfer materials are evaluated to ensure no interferences with the R90 transition rails *(see sketch below)*.

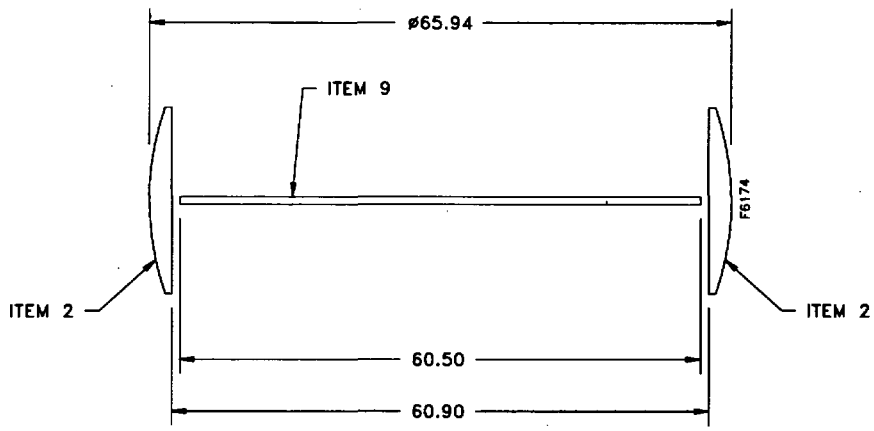

This evaluation is done using the average temperatures of the aluminum/neutron absorbing plates along its radial length, as follows:

$$\begin{aligned}\Delta L_{al/Neu} &= \alpha_{al} L_{plate} \Delta T \\ &= \left(1.38\, x\, 10^{-5} {}^{\circ}F^{-1}\right)\left(60.5\, in\right)\left(445^{\circ}F - 70^{\circ}F\right) \\ &= 0.313\, in\end{aligned}$$

The required clearance is 0.313 inch. This is conservatively compared with the cold gap of 0.40 inch provided in the design *(69.90 inch - 60.40 inch from above sketch)* and is therefore adequate.

Adequate gap for thermal expansion of the basket in the radial direction can be demonstrated by considering the thermal expansion of the insert plate/fuel compartment tubes assembly as shown in the sketch below (item numbers are in reference to SAR drawing NUH24PTH-1003-SAR, except as noted). Assuming the average temperature for the insert plate/fuel compartment tubes assembly and the R90 rails to be the same as for the aluminum plates (item 9 in the sketch above), the radial expansion of the basket is approximately calculated as:

$$\begin{aligned}\Delta L_{insert\ plate/tube} &= \alpha_{steel} L_{insert\ plate/tube} \Delta T_{insert\ plate/tube} + \alpha_{R90\ rails} L_{R90\ rails} \Delta T_{R90\ rails} \\ &= \left(9.5E10^{-6} {}^{\circ}F^{-1}\right)\left(60.9\ in\right)\left(445^{\circ}F - 70^{\circ}F\right) + \left(1.38E10^{-5} {}^{\circ}F^{-1}\right)\left(65.94\ in - 60.90\ in\right)\left(445^{\circ}F - 70^{\circ}F\right) \\ &= 0.24\ in\end{aligned}$$

The radial expansion of the shell is:

$$\begin{aligned}\Delta L_{shell} &= \alpha_{steel} D_{shell} \Delta T_{shell} \\ &= \left(8.9E10^{-6} {}^{\circ}F^{-1}\right)\left(66.19\ in\right)\left(215^{\circ}F - 70^{\circ}F\right) \\ &= 0.085\ in\end{aligned}$$

The remaining gap after thermal expansion is 0.25 + 0.085 -0.24 =0.09 in. Therefore, the radial gap for the basket assembly is adequate.

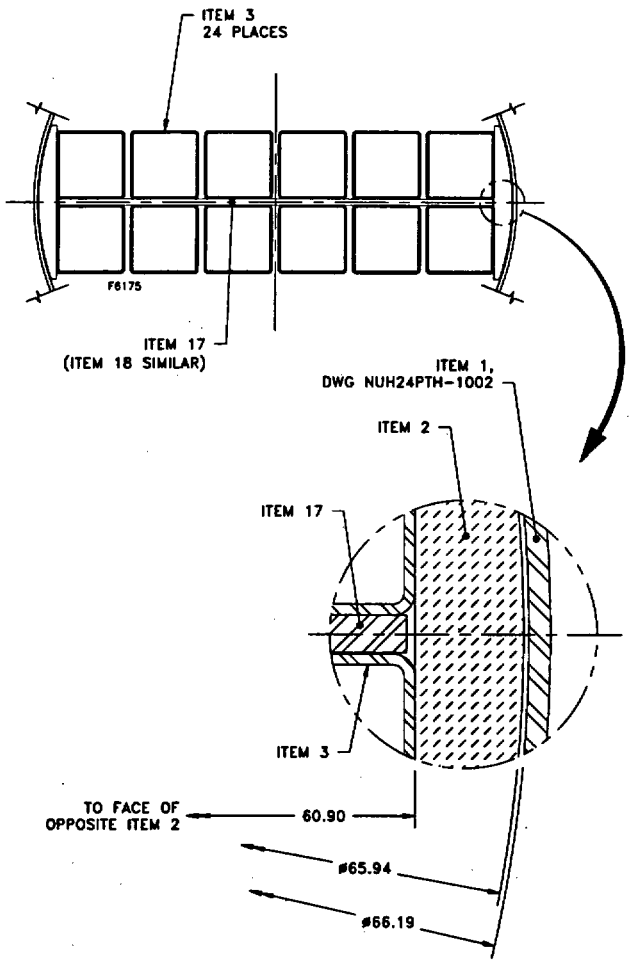

Axial Expansion

For the vacuum drying condition, axial thermal expansion of the basket components is calculated below.

24PTH Axial Thermal Expansion, Vacuum Drying

Component	T_{max} (°F)	α_{avg} (°F^{-1})	L (in)	ΔL (in)
Tube (24PTH-S/-L)	580	9.8E-06	174.6	0.873
Tube (24PTH-S-LC)	573	9.8E-06	172.3	0.849
Aluminum/ Poison Plates (24PTH-S/-L)	572	1.41E-05	20.8	0.147
Aluminum/ Poison Plates (24PTH-S-LC)	567	1.41E-05	21.3	0.149
R45 Type 304 T. Rails (24PTH-S/-L)	580	9.8E-06	174.6	0.873
R45 Type 304 T. Rails (24PTH-S-LC)	573	9.8E-06	172.3	0.849
R90 6061 (Al.) T. Rails (24PTH-S/-L)	572	1.41E-05	173.6	1.229
R90 6061 (Al.) T. Rails (24PTH-S-LC)	567	1.41E-05	171.3	1.200
DSC Cavity (24PTH-S/-L)	215	9.0E-06	175.6	0.228
DSC Cavity (24PTH-S-LC)	215	9.0E-06	173.3	0.225

Relative expansion is determined by comparing values calculated above. For example, the "worst case" required clearances between the end of the DSC cavity and the structural parts of the basket assembly can be determined by comparing the cavity expansion to the expansion of the basket assembly calculated using the maximum component temperatures:

Table P.3.4-1
Summary of Thermal Stress Results - 24PTH Basket

Basket Component	Maximum Stress Intensities (ksi)
Tube Structure	7.85
R45 Transition Rail	8.72
R90 Transition Rail	1.44

Table P.3.4-2
Summary of Thermal Forces and Moments in the HSM-H Concrete Components

Thermal Case	Concrete Component	Forces/Moments			
		Shear, V_{o1} (1) (kips/ft)	Shear, V_{o2} (1) (kips/ft)	Moment, M_1 (2) (kip-in/ft)	Moment, M_2 (2) (kip-in/ft)
Normal Thermal (TN)	Rear Wall	4	6	47	60
	Side Wall	7	6	46	32
	Front Wall	16	23	1318	596
	Roof	3	5	111	234
Off-Normal Thermal (TO)	Rear Wall	4	5	51	39
	Side Wall	6	6	45	29
	Front Wall	16	23	1315	506
	Roof	3	5	93	233
Accident Thermal (TA)	Rear Wall	*9*	*19*	*140*	*229*
	Side Wall	92	32	184	340
	Front Wall	*41*	*38*	*1772*	*3325*
	Roof	11	20	349	830

Notes:

(1) V_{o1} and V_{o2} are out of plane shears.

(2) M_1 and M_2 are out of plane moments.

which is also modeled with fully integrated shell elements. The steel insert plates-to-tube welds are modeled with beam elements. Symmetry boundary conditions are applied at the ±Z faces of the model. At the –Z face the model is unrestrained to permit axial thermal expansion.

The TC shell and TC rails, which are extremely rigid relative to the other parts of the structure, are included as rigid bodies and are fixed. Therefore, the TC shell is modeled with only one through-thickness element. Table P.3.6-4 lists the structural parts included in the model.

The finite element model showing the geometry of the basket model is shown in Figure P.3.6-7. Figure P.3.6-8 *(top)* shows the fuel compartment tubes *and the insert plates (only those around the perimeter can be seen in this view).* Figure P.3.6-8 *(bottom) shows the basket insert plates and the beam elements used to model the welds (the fuel compartment tubes and some transition rails are excluded for clarity).*

Contact is specified between all adjacent surfaces throughout the model. Contact elements are included between the following interfacing components:

- Fuel compartment tubes to adjacent tubes
- Fuel compartment tubes to basket straps
- Fuel compartment tubes to transition rails,
- Transition rails to DSC shell ID, and
- DSC shell OD to TC ID and TC rails.

The heat conducting aluminum and neutron absorbing poison plates are not explicitly modeled (their weight is accounted for by adjusting the density of the materials used for the fuel compartment tubes and R45 transition rails). The thicknesses of the shell elements for the fuel compartment tubes and the R45 transition rails are adjusted to properly account for the contact that exists between these adjacent surfaces. Generally, contact is modeled using the LS-DYNA surface-to-surface contact algorithm, except for the contact between the edges of the R45 transition rail plates that interface with the DSC shell (including the stiffener plates), which is modeled using the nodes-to-surface contact algorithm.

Inertial loads are applied to the structure by including the appropriate weight density of the materials and applying accelerations. Because the aluminum/neutron absorbing plates (captured in between the fuel compartment tubes), and the heat conductive aluminum inserts (captured in between the stiffener plates in the R45 transition rails), are not explicitly modeled, equivalent densities are determined for these components to provide the analysis with the appropriate mass of the system. Fuel loads are applied using pressure loads on the fuel compartment tube elements. Thermal effects are included by applying temperatures corresponding to the bounding temperature profile shown in Figure P.3.4-2.

For the normal condition stress analyses, 1g loads are applied and deadweight stresses determined. These deadweight stresses are classified as primary membrane and membrane plus bending stresses. Separate analyses were performed to determine thermal stress, as discussed in Section P.3.4.4.3. The thermal plus deadweight stresses are classified as primary plus secondary. Tables of the temperature-dependent material properties (e.g., S_y versus temperature) are

included in the LS-DYNA model, such that the appropriate properties are applied at each point in the structure. *Material Type 4 (*mat-elastic-plastic-thermal) is used to prescribe temperature dependent material properties in the LS-DYNA analysis.*

Stress intensities are calculated for all the elements in the model. Maximum stress intensities are compared with the appropriate allowable stress values and are reported in this section.

(B) Material Properties

The material properties used in the LS-DYNA stress analyses are summarized in Table P.3.6-5. With the exception of the solid aluminum transition rails, properties for all materials are directly from the ASME Code. Properties for the aluminum rails are described in Section P.3.3.1.

P.3.6.1.3.2 Normal Condition Loading

Postulated loads on the 24PTH basket structure for non-accident conditions are described in the following sections. The loads and load combinations for the 24PTH basket structure are simplified by consideration that the basket is unaffected by either pressure loads or HSM Model 102/HSM-H insertion/retrieval loads.

(A) Thermal

The analysis of the 24PTH basket for thermal loads is described in P.3.4.4. As shown in Section P.3.4.4.3.1, thermal stresses are small.

(B) Deadweight

Deadweight load conditions include: (1) vertical deadweight during fuel loading operations, (2) horizontal deadweight in the TC with support through the cask rails at ±18.5°, and (3) horizontal deadweight in the HSM Model 102/HSM-H with support through the HSM Model 102/HSM-H rails at ±30°.

Under axial loads, the fuel assemblies and fuel compartment tubes are supported by the bottom of the TC. Thus, the fuel assemblies react directly against the bottom of the DSC/TC and do not load the basket structure. Stresses under axial loading are from self weight of the basket structure. Maximum axial compressive stresses occur at the supported end of the basket.

Vertical deadweight was evaluated using hand calculations and by comparing the calculated axial compression stresses to stability allowables developed considering both stability criteria and the general membrane criteria (P_m) from Subsection NG (see P.2.2.5.1). The calculated stresses for the vertical deadweight condition are also applied to the vacuum drying case.

Calculated stresses are listed in Table P.3.6-6 along with the appropriate compressive allowables. The results from this table show that the stresses for this load condition are small.

Horizontal deadweight cases were evaluated using the LS-DYNA model described in P.3.6.1.3.1. As appropriate the elements representing the support rails were located at either ±18.5° or ±30° from bottom center for support by the TC or HSM Model 102/HSM-H, respectively. Thus, the following analysis cases were evaluated:

1. 24PTH DSC supported at ±18.5° (TC Condition)

2. 24PTH DSC supported at ±30° (HSM Model 102/HSM-H Condition)

Primary plus secondary stresses were evaluated by combining deadweight stresses with the thermal stresses resulting from the bounding temperature distribution. Conservatively, the maximum deadweight stress intensities are combined with the maximum thermal stress intensities by absolute summation. Maximum stresses for basket steel components and R90 aluminum transition rails are summarized in Table P.3.6-7 along with a comparison to Level A allowables from Subsection NG.

(C) Vacuum Drying

As described above, the axial compression stresses under the vacuum drying condition are equal to the axial compression stresses under vertical deadweight.

As described in P.3.4.4.3.1, maximum stresses from the vacuum drying temperature distribution are bounded by the temperature distribution used in the structural evaluations and the results are listed in Table P.3.4-1. These thermal stresses are classified as secondary by the Code and, as shown by the table, these stresses are small.

(D) Handling/On-Site Transfer Loads

These cases include the loads associated with loading (and unloading) the 24PTH DSC into HSM Model 102/HSM-H and the inertial loads associated with on-site handling. The insertion/retrieval loads do not directly impact the 24PTH basket assembly and do not require additional consideration. The inertia loads to be considered are:

- DW + 1g Axial
- DW + 1g Transverse.
- DW + 1g Vertical
- DW + 0.5g Axial + 0.5 Transverse + 0.5 Vertical

These loads are enveloped by a 2g resultant acceleration applied in the most critical orientation.

The 2.0g resultant axial load is evaluated using hand calculations and the same methodology used for the vertical deadweight analyses. Maximum compressive stresses resulting from this load case are listed in Table P.3.6-6 along with a comparison to the axial stability criteria described in P.2.2.5.1.2.

Loads transverse to the axis of the DSC are evaluated using the LS-DYNA models described in P.3.6.1.3.1. Primary *handling* stresses are based on twice the horizontal deadweight stresses. Conservatively, in the evaluation of primary plus secondary stresses, the maximum handling stress intensities are combined with the maximum thermal stress intensities by absolute

summation. Enveloping 24PTH basket stresses are summarized in Table P.3.6-7 along with a comparison to Service Level A allowables.

(E) Evaluation of Results

Normal and off-normal conditions stresses are summarized in Table P.3.6-6 and Table P.3.6-7 for basket stainless steel and aluminum components. LS-DYNA plots showing typical analysis results for the 24PTH basket are provided in Figure P.3.6-9 and Figure P.3.6-10 for deadweight and thermal stresses, respectively. The results summarized in Table P.3.6-6 and Table P.3.6-7, show that the basket stress criteria is met.

Loads on the welds connecting the steel insert plates (straps) and the fuel compartment tubes are evaluated using the beam element forces obtained from the LS-DYNA analysis. On each face of the fuel tubes, two welds (beams) were modeled between the tube and the adjacent basket straps(s). The Resultant loads on the face of each fuel compartment tube are determined as follows:

$$F_{\text{Resultant}} = \sqrt{\left(F_{Ax}^{1} + F_{Ax}^{2}\right)^2 + \left(F_{V1}^{1} + F_{V1}^{2}\right)^2 + \left(F_{V2}^{1} + F_{V2}^{2}\right)^2}$$

Where: F_{Ax}^{i} = Axial force at weld element 'i'. Compressive forces are set to zero (0 lb) since compression loads will be transmitted by bearing through the parts and will not stress the welds.

F_{V1}^{i} = Shear force (Direction 1) at weld element 'i'.

F_{V2}^{i} = Shear force (Direction 2) at weld element 'i'.

For each of the stress analyses, maximum weld loads are determined for each side of each tube. The maximum normal condition loads are listed in Table P.3.6-8.

Within the basket fuel compartment tube structure are plates of Type 1100 aluminum and neutron absorbing materials, which perform heat transfer and criticality functions. As shown in Section P.4, the maximum short-term basket temperature for normal and off-normal conditions is 683°F, which is well below the melting point of the aluminum plates (approximately 1200°F). As discussed in Section P.3.4, adequate clearance is provided for thermal expansion so that thermal stresses in the aluminum plates are negligible. These plates are supported by the steel insert plates (straps) and are sandwiched between the steel fuel compartment tubes. This ensures that the aluminum and neutron absorbing plates remain in position to perform their heat transfer and criticality functions.

P.3.6.1.4 NUHOMS® HSM-H Structural Analysis

The reinforced concrete and the support steel structure of the HSM-H are analyzed for the normal, off-normal, and postulated accident conditions using finite element models described in Section P.3.7.11.6. These models are used to evaluate concrete and support structure forces and

TC Cask Component	Maximum Temperature (°F)
Top Forging Inner Liner	297 384
Bottom Forging Structural Shell	259 329
NS-3 Cover Plate Ram Access Forging	217 201
Bottom End Cover Plate Top Lid	227 273
Lead (Shielding)	379

Table P.3.6-12 summarizes the enveloping thermal stresses for each TC component. These thermal stresses are combined with existing mechanical load stresses, based on the bounding stresses for the OS197H TC and are summarized in Table P.3.6-13. In Table P.3.6-13 the maximum primary plus secondary stresses are added by absolute sum, irrespective of location of the maximum stress, for each TC component. The combined stresses are compared to the allowable stress at temperature (400°F). The stresses listed in Table P.3.6-13 are applicable to regions away from the trunnions. Table P.3.6-14 summarizes the stresses at/or in the vicinity of the TC trunnions.

Payload Lift Evaluation

The evaluations for the OS197 and OS197H TCs are based on *DSC maximum allowable wet payload weight of 102,410 lbs and 126,000 lbs, and maximum allowable DSC* dry payload *weights* of *97,250* lbs and 116,000 lbs, respectively. The maximum total cask payload with a dry-loaded NUHOMS®-24PTH DSC is approximately 94,000 lbs *and wet-loaded 24PT4-DSC is approximately 99,000 lbs.* Therefore, a*n* OS197FC TC that is based on *either the OS197 or* the OS197H TC is acceptable with any NUHOMS®-24PTH DSC *as long as* the total TC *dry and wet* payload *weights are within their respective analyzed weights listed above.*

P.3.6.2 Off-Normal Load Structural Analysis

Table P.3.6-9 shows the off-normal operating loads for which the NUHOMS® System components are designed. This section describes the design basis off-normal events for the NUHOMS® System and presents analyses which demonstrate the adequacy of the design safety features of a NUHOMS® System with the 24PTH DSC.

For an operating NUHOMS® System, off-normal events could occur during fuel loading, TC handling, trailer towing, canister transfer and other operational events. Two off-normal events are defined which bound the range of off-normal conditions. The limiting off-normal events are defined as a jammed DSC during loading or unloading from the HSM Model 102/HSM-H and the extreme ambient temperatures of -40°F (winter) and +117°F (summer). These events envelope the range of expected off-normal structural loads and temperatures acting on the DSC, TC, and HSM Model 102/HSM-H. These off-normal events are described in Section 8.1.2.

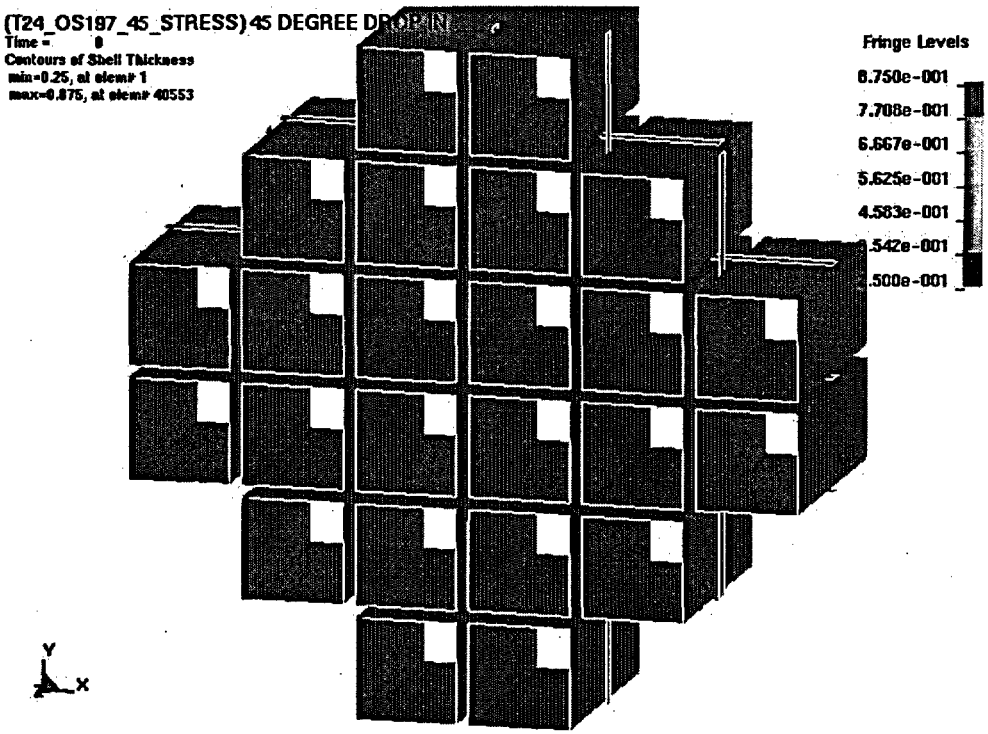

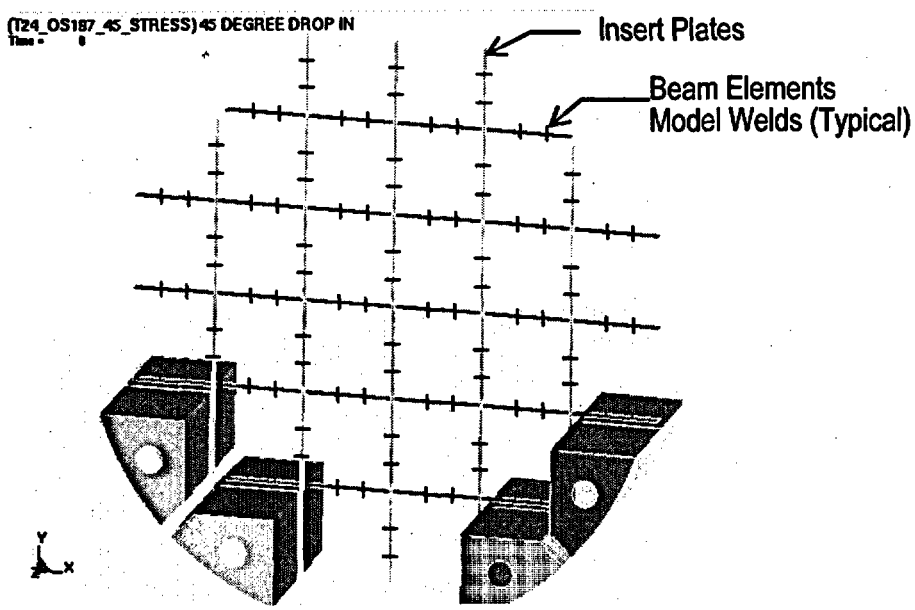

–Tubes not shown for clarity.–

Figure P.3.6-8
24PTH Basket Model Showing Fuel Compartment Tubes, Steel Insert Plates (Straps), and *Beam Elements Modeling Connection Welds*

P.3.7.4.2 24PTH DSC Shell Assembly Drop Evaluation

The shell assembly consists of the DSC shell, the shield plugs, and the top and bottom inner and outer cover plates. For the 24PTH-S-LC integral inner top and bottom forging/lead shield plugs assemblies are used. The shell assembly drop evaluation is presented in three parts:

1. DSC shell assembly horizontal drop analysis,
2. DSC shell assembly vertical drop analysis, and
3. DSC shell stability analysis.

P.3.7.4.2.1 DSC Shell Assembly Horizontal Drop Analysis

The DSC shell assembly is analyzed for the postulated horizontal side drop using the ANSYS 3-D models of the DSC shell assembly discussed in Section P.3.6.1.2. Half-symmetry (180°) models of the top end and bottom end sections of the DSC shell assembly are developed for the 24PTH-S/-L DSCs, based on the 90° models for the end drops, shown in Figure P.3.6-1 and Figure P.3.6-2. Each model includes one-half of the height of the cylindrical shell. Two 3-D models corresponding to the top and bottom segment of the shell assembly are developed for the 24PTH-S-LC, as shown in Figure P.3.6-5. Each of the DSC shell assembly components is modeled using ANSYS solid 3-D elements. The full weight of the DSC is conservatively assumed to drop directly onto a single TC rail. Elastic-plastic analyses are performed and stresses are determined for each DSC shell assembly component. The NUHOMS®-24PTH DSC shell stresses in the region of the basket assembly are also analyzed for the postulated horizontal side drop conditions. This analysis and results are presented in Section P.3.7.4.3.1.

P.3.7.4.2.2 24PTH DSC Shell Assembly Vertical Drop Analysis

The TC is assumed to be oriented vertically and dropped onto a uniform surface. The vertical TC drop evaluation conservatively assumes that the TC could be dropped onto either the top or bottom surfaces. The models shown in Figure P.3.6-1 and Figure P.3.6-2 are used for the vertical drop analysis of the 24PTH-S-/-L DSCs, and the model shown in Figure P.3.6-4 is used for the analysis of the 24PTH-S-LC DSC. No credit is taken for the energy absorbing capacity of the TC top or bottom cover plate assemblies during the drop. Therefore, the DSC is analyzed as though it is dropped on to an unyielding surface. *The end drop analysis for the 24PTH-S and 24PTH-L shell assemblies are based on linear elastic analysis. For the 24PTH-S-LC shell assembly end drop, evaluations are based on elastic-plastic analysis.* The principal components of the DSC and internals affected by the vertical drop are the DSC shell, the inner and outer top cover plates, the shield plugs, and the inner and outer bottom cover plates.

P.3.7.4.2.3 24PTH DSC Shell Assembly Stress Analysis

The ANSYS analytical models of the DSC shell assembly as described in Section P.3.6.1.2 are used to determine the drops accident stresses in the DSC shell, the inner cover plates, the outer cover plates, and the shield plugs. Equivalent static analysis is conservatively used for the drop analyses. Inertia loadings based on forces associated with the 75g deceleration (horizontal side drop), and 60g (vertical end drops) are statically applied to the models.

The 24PTH-S/24PTH-L DSC end drop models consist of 90° quarter symmetry models and include one-half of the height of the cylindrical shell. To capture the maximum stress state in the DSC assembly components, each model was analyzed for end drop loading on the opposite end (i.e., the bottom end model was analyzed for top end drop, and the top end model was analyzed for bottom end drop). In these drop orientations, the end plates are supported at the perimeter by the DSC shell. For the top and bottom end drops, the nodal locations on the impacted end are restrained in the vertical direction. Analyses show that the stresses in the DSC cover plates and shield plugs are low. These low stresses occur because for the bottom end drop, the inner and outer top cover plates are supported by the top shield plug. During a top end drop, the outer top cover plate is assumed to be supported by the unyielding impacted surface and is subjected to a uniform bearing load imposed by the DSC internals. The same is true for the DSC outer bottom cover plate and shield plug for the bottom end drop. The highest stresses occur in the DSC shell and bottom inner cover plate. The maximum stresses in the inner bottom cover plate result from the top end vertical drop condition, in which the inner bottom cover plate is supported only at the edges. The maximum DSC shell membrane stresses, which occur near the top end of the DSC shell area, result from the accelerated weight of the DSC shell and the bottom end (for top end drop case) or top end (for the bottom end drop case) assemblies.

The 24PTH-S-LC DSC end drop model consists of a full axisymmetric model of the 24PTH shell assembly. This model is used for both top end drop and bottom end drop. For the bottom end drop, the outer bottom cover plate in the 24PTH-S-LC includes an unsupported center plate inside the grapple ring support (which is welded to the bottom forging). This causes higher stresses in the outer bottom cover plate. The top shield plug consists of inner top forging encasing the lead shield plug. In the bottom end drop, the inner forging supports the lead shield plug, and to lesser extent, the outer top cover plate.

In the end drop orientations for the 24PTH-S-LC, the nodes on the impacted end are restrained in the vertical direction, representing the support provided by the TC. During a top end drop, the outer top cover plate is assumed to be supported by the unyielding impacted surface and is subjected to a uniform bearing load imposed by the DSC internals. The same is true for the DSC outer bottom cover plate for the bottom end drop. For the top end drop, the highest stresses occur at the DSC shell, the outer bottom cover plate, and the bottom forging. For the bottom end drop, the highest stresses occur at the outer bottom cover plate, and the inner top forging. *In the outer bottom cover plate (a non-pressure boundary component), very localized and limited plasticity occurs, at a location of plate thickness transition, during the bottom end drop. In this thickness transition region the plate is unsupported, and during the drop, the plate is loaded by the inertial weight of the encased lead.* Figure P.3.7-15 *shows that the plastic strains in this region are small. The calculated stresses are within Code allowables (maximum stress ratio is 0.86). The stress intensity ratios for the pressure boundary components, DSC shell and inner top and bottom cover plates/forgings, are well within Code allowables. The maximum stress intensity ratio for these components for primary membrane stress is 0.35 and for primary membrane plus bending is 0.56.*

A summary of the calculated stresses for the main components of the DSC and associated welds is provided in Table P.3.7-1 for the 24PTH-S/-L DSCs and in Table P.3.7-2 for the 24PTH-S-LC DSC.

P.3.7.4.2.4 24PTH DSC Shell Stability Analysis

The stability of the DSC shell for a postulated vertical drop impact is also evaluated. For Level D conditions, the allowable axial stress in the DSC shell is based on Appendix F of the ASME Code. The maximum axial stress in the 24PTH-S/-L DSC shell obtained from the 60g end drop analyses is 8.86 ksi. The allowable axial stress is 11.4 ksi. The corresponding maximum and allowable axial stresses for the 24PTH-S-LC DSC shell are 8.88 ksi and 9.86 ksi, respectively. Therefore, buckling of the DSC shell for a 60g vertical deceleration load does not occur.

The results of the analyses indicate the structural capacity of the NUHOMS®-24PTH basket assembly is higher than the postulated 75g side drop impact load. Thus, the 24PTH basket assembly is stable under the postulated side drop loads.

P.3.7.4.4 On-site TC Horizontal and Vertical Drop Evaluation

An analysis has been performed in Section 8.2.5.2 to evaluate the OS197 and OS197H TCs for postulated horizontal and vertical drop accidents with a static equivalent deceleration of 75g's. The evaluations for the OS197 and OS197H *TCs* are based on payload weights of *97,250* lbs and 116,000 lbs, respectively. The maximum total cask payload weight with a dry-loaded NUHOMS®-24PTH DSC is approximately 94,000 lbs. Therefore, a OS197FC that is based on *either the OS197 or* the OS197H *TC* is acceptable with any NUHOMS®-24PTH DSC *as long as* the total *TC dry* payload weight*s are within their respective analyzed weights listed above.*

P.3.7.4.5 Loss of Neutron Shield

No change to the Standardized TC with solid neutron shield presented in 8.2.5.3. For the liquid neutron shield TC, the maximum temperatures for this accident case correspond to the 40.8 kW and 117°F ambient temperature, as reported in Table P.4-13. As discussed in Section 8.2.5.3.1, this is a post-drop accident thermal condition that need not be considered in the load combination stress evaluation. Rather the peak stresses resulting from accident thermal conditions must be less than the allowable fatigue stress limit using the appropriate fatigue design curves in the ASME Code. Similar analyses of other NUHOMS® TCs have shown that fatigue is not a concern for the TC. Therefore, TC stresses need not be evaluated for post-drop accident conditions.

P.3.7.5 Lightning

No impact on the structural evaluation.

P.3.7.6 Blockage of HSM-H Air Inlet and Outlet Openings

This accident conservatively postulates the complete blockage of the HSM-H ventilation air inlet and outlet openings on the HSM-H side walls.

Since the NUHOMS® HSM-Hs are located outdoors, there is a remote probability that the ventilation air inlet and outlet vent openings could become blocked by debris. The NUHOMS® design features such as the perimeter security fence and the redundant protected location of the air inlet and outlet vent openings and the screens reduces the probability of occurrence of such an accident. Nevertheless, for this conservative generic analysis, such an accident is postulated to occur and is analyzed.

The structural consequences due to the weight of the debris blocking the air inlet and outlet vent openings are negligible and are bounded by the HSM-H loads induced for a postulated tornado (Section 8.2.2) or earthquake (Section 8.2.3).

P.3.7.11.2 DSC Fatigue Evaluation

Although the normal and off-normal internal pressures for the NUHOMS®-24PTH DSC are higher relative to the NUHOMS®-24P DSC, the range of pressure fluctuations due to seasonal temperature changes are essentially the same as those evaluated for the NUHOMS®-24P DSC. Similarly, the normal and off-normal temperature fluctuations for the NUHOMS®-24PTH DSC due to seasonal fluctuations are essentially the same as those calculated for the NUHOMS®-24P DSC. Therefore, the fatigue evaluation presented in Section 8.2.10.2 for the 24P DSC remains applicable to the NUHOMS®-24PTH DSC.

P.3.7.11.3 TC Load Combination Evaluation

There is no change to the TC load combination evaluations. Table P.3.7-15 is a summary of OS197/OS197H/OS197FC TC stresses. This table incorporates the thermal stress analysis results for these TCs loaded with a 24PTH DSC documented in P.3.6.1.5. In addition, the results of the modified top cask lid, documented in P.3.6.1.5, have been incorporated (primary stresses in Table P.3.7-15). The stress results summarized in Table P.3.7-15 use the stresses due to mechanical loads for the OS197H as summarized in Chapter 8. Allowable stresses have been adjusted for the higher temperatures associated with the TC loaded with a 24PTH DSC.

The evaluations performed in Sections 8.1 and 8.2 for the OS197 and OS197H casks are based on payloads of *97,250* lbs and 116,000 lbs, respectively. The maximum total cask payload with a dry-loaded NUHOMS®-24PTH DSC is approximately 94,000 lbs. Therefore, a OS197FC TC that is based on *either the OS197 or* the OS197H *TC* is acceptable with any NUHOMS®-24PTH DSC *as long as* the total *TC dry* payload*s are within their respective analyzed weights listed above.*

P.3.7.11.4 TC Fatigue Evaluation

No change.

P.3.7.11.5 HSM –H Load Combination Evaluations

P.3.7.11.5.1 HSM –H Concrete Component Evaluation

The required strength, U, for critical sections of concrete is calculated in accordance with the requirements of ANSI 57.9 [3.14] and Chapter 9 of ACI 349 [3.27], including the strength reduction factors defined in ACI 349, Section 9.3.

The concrete design loads are multiplied by load factors and combined to simulate the most adverse load conditions. The load combinations described in Table P.3.7-16 are used to evaluate the concrete components.

For the door anchorage, the controlling load is tornado generated differential pressure drop load. The maximum tensile force per bolt (there are four bolts that attach the door assembly to the front concrete wall of the HSM-H) is 9.0 kips. This is less than the allowable load per bolt of 10.8 kips. The concrete pull-out strength is conservatively estimated as 24 kips which is greater than the ultimate capacity of the four bolts, thus satisfying the ductility requirements of the ACI Code.

P.3.7.11.6.6 Evaluation of the HSM-H Heat Shields

The top heat shield (louvers) consists of seven panels. Each panel has two stainless steel mounting bars. The aluminum louvers are mounted on the mounting bars. Each mounting bar is suspended from the roof by two threaded rods. The natural lateral frequency of a typical rod is conservatively estimated to be 9.0 Hz. The combined axial and bending stress in the hanger rods is 34.63 ksi. The allowable axial and bending stress is 86.1 ksi.

The side heat shields consists of three panels. Each panel is suspended from the roof by two threaded rods, and supported laterally and longitudinally by four rods. The maximum axial plus bending stress in the lateral and longitudinal support rods is 83.7 ksi. The allowable axial and bending stress is 86.1 ksi.

P.3.7.11.6.7 Evaluation of the HSM-H Seismic Retainers

The seismic retainer consists of a capped tube steel embedment located within the bottom center of the round access opening of the HSM-H, and a tube steel retainer assembly that drops into the embedment cavity after 24PTH-DSC transfer is complete. The drop-in retainer extends approximately 4" above the rail to provide axial restraint of the 24PTH-DSC. The maximum seismically induced shear load in the retainer is 61 kips. The maximum shear stress in the retainer is 15.25 ksi. The allowable shear stress is 17.8 ksi.

P.3.7.11.6.8 Thermal Cycling of the HSM-H

No change.

Table P.3.7-20
Comparison of Highest Combined Shear Forces/Moments with the Capacities

Component	Load Comb. (1)	Quantity	V_I Kips/ft	V_{o1} kips/ft	V_{o2} kips/ft	M_1 kip-in/ft	M_2 kip-in/ft
Rear Wall (upper)	Comb 1c thru 6c	Computed	14.52	7.68	8.23	63.82	121 .65
		Capacity	76.8	14.5	14.5	305.9	305.9
		Ratio	**0.19**	**0.53**	**0.57**	**0.21**	**0.40**
	Comb7c	Computed	*13.03*	*11.37*	*4.20*	*131.14*	*264.5*
		Capacity	69.6	13.8	13.8	273.8	273.8
		Ratio	***0.18***	***0.82***	***0.30***	***0.48***	***0.97***
Rear Wall (Lower)	Comb 1c thru 6c	Computed	17.34	9.48	13.25	159.40	167.70
		Capacity	98.4	36.2	36.2	778.10	778.10
		Ratio	**0.18**	**0.26**	**0.37**	**0.21**	**0.22**
	Comb7c	Computed	*9.49*	*6.40*	*20.84*	*154.30*	*251.80*
		Capacity	90.10	34.30	34.30	696.30	696.3
		Ratio	***0.11***	***0.19***	***0.61***	***0.22***	***0.36***
Side Walls (Upper)	Comb 1c thru 6c	Computed	16.59	5.38	6.01	138.48	143.66
		Capacity	55.40	14.80	14.80	202.10	202.10
		Ratio	**0.30**	**0.36**	**0.41**	**0.69**	**0.71**
	Comb7c	Computed	22.37	12.08	3.10	87.24	87.76
		Capacity	50.50	14.00	14.00	180.80	180.80
		Ratio	**0.44**	**0.86**	**0.22**	**0.48**	**0.49**
Side Walls (Lower)	Comb 1c thru 6c	Computed	36.17	17.43	21.12	308.10	216.77
		Capacity	64.00	23.4	23.4	322.9	322.9
		Ratio	**0.57**	**0.75**	**0.91**	**0.96**	**0.67**
	Comb7c	Computed	19.28	21.12	15.34	97.25	180.24
		Capacity	58.70	22.2	22.2	289.0	289.0
		Ratio	**0.33**	**0.95**	**0.69**	**0.34**	**0.63**
Roof	Comb1c Thru 6c	Computed	13.18	5.87	12.38	265.53	401.25
		Capacity	177.60	59.10	59.10	2438.10	2438.10
		Ratio	**< 0.10**	**< 0.10**	**0.21**	**0.11**	**0.17**
	Comb7c	Computed	7.42	11.48	24.06	330.77	897.67
		Capacity	162.40	56.10	56.10	2181.70	2181.70
		Ratio	**< 0.10**	**0.21**	**0.43**	**0.15**	**0.41**
Front Wall (Upper)	Comb 1c thru 6c	Computed	41.82	38.86	37.00	681.10	1042.27
		Capacity	174.70	56.30	56.30	2317.20	2317.20
		Ratio	**0.24**	0.69	0.66	0.30	0.45
	Comb7c	Computed	*18.36*	*48.95*	*26.29*	*1853.0*	*1906.74*
		Capacity	159.60	53.40	53.40	2073.50	2073.50
		Ratio	***0.12***	***0.92***	***0.49***	***0.89***	***0.92***
Front Wall (Lower)	Comb1c thru 6c	Computed	29.29	30.43	37.83	1783.50	836.92
		Capacity	192.10	73.60	73.60	3042.50	3042.5
		Ratio	**0.16**	**0.42**	**0.52**	**0.59**	**0.27**
	Comb7c	Computed	*48.04*	*45.95*	*41.38*	*1908.90*	*507.22*
		Capacity	176.00	69.80	69.80	2722.40	2722.40
		Ratio	***0.27***	***0.66***	***0.59***	***0.70***	***0.19***

Note: (1) Comb 1c thru 6c includes normal thermal. Comb 7c includes accident thermal. (See Table P.3.7-16).

Table P.3.7-21
Maximum/Minimum Forces/Moments in the Rail Components in the Local System

Load Combination		F_x Kips	F_y Kips	F_z Kips	M_x kip-in	M_y kip-in	M_z Kip-in
C1S	MAX	0.0	33.0	65.2	54.8	231.1	213.7
	MIN	0.0	-41.0	-61.3	-45.2	-1146.7	-236.2
C2S	MAX	38.5	39.8	77.0	0.22	428.2	247.8
	MIN	-28.9	-39.8	-60.9	-0.32	-1137.6	-247.8
C3S	MAX	86.5	30.7	89.6	54.9	592.7	199.4
	MIN	-86.5	-38.1	-63.0	-45.2	-1422.4	-230.4
C4S	MAX	22.3	38.2	102.1	54.9	562.5	-267.6
	MIN	-22.3	-46.3	-98.3	-45.2	-1869.0	-290.2
C5S	MAX	0.	*49.6*	*82.1*	*183.7*	*264.8*	*267.3*
	MIN	0.	*-54.1*	*-80.9*	*-159.3*	*-143.4*	*-267.1*

Table P.3.7-22
Maximum/Minimum Forces/Moments in the Rail Extension Plates in the Local System

Load Combination		F_x Kips	F_y Kips	F_z Kips	M_x kip-in	M_y kip-in	M_z Kip-in
C1S	MAX	0.0	0.85	-0.25	2.7	6.8	13.8
	MIN	0.0	-4.0	-0.73	-2.7	-4.3	-45.9
C2S	MAX	40.0	2.6	-0.4	0.1	5.3	26.1
	MIN	-30.0	-2.6	-0.5	-0.1	-2.6	-26.1
C3S	MAX	80.0	0.8	-0.2	2.7	7.2	13.6
	MIN	-79.9	-3.9	-0.8	-2.8	-4.2	-44.9
C4S	MAX	38.5	1.5	-0.0	2.7	9.3	17.0
	MIN	-38.5	-4.7	-1.0	-2.8	-5.8	-53.2
C5S	MAX	0	*1.02*	*0.34*	*9.4*	*12.3*	*18.2*
	MIN	0.	*-7.6*	*-1.5*	*-9.5*	*-9.7*	*-94.7*

Table P.3.7-23
Maximum/Minimum Axial Forces in the Cross Member Components

Load Combination		Fx Kips
C1S	MAX	6.2
	MIN	5.2
C2S	MAX	8.1
	MIN	5.8
C3S	MAX	5.2
	MIN	2.6
C4S	MAX	6.2
	MIN	5.2
C5S	MAX	7.1
	MIN	5.1

Table P.3.7-24
Rail Component Results

Load Comb.	Interaction Ratio(1)	Shear Stress Ratio(2)	Stiffener Plate Stress Ratio(3)
C1S	0.35	0.64	0.16
C2S	0.58	0.83	0.00
C3S	0.57	0.89	0.18
C4S	0.50	0.92	0.15
C5S	*0.38*	*0.65*	*0.53*

Notes:

(1) Axial and bending stresses are computed using axial (F_x) and bending moment (M_y, M_z) results from Table P.3.7-21. Interaction ratios are based on appropriate equations from Chapter H of AISC [3.20]. See Tables 3.2-10 and Table P.3.7-17.

(2) Shear stresses are computed using shear forces (F_y, F_z) from Table P.3.7-21. Shear stress ratio is the computed shear stress/shear stress allowable. See Tables 3.2-10 and Table P.3.7-17.

(3) Flexural stresses in the stiffener plates are computed using torsional moment (M_x) result from Table P.3.7-21. Stiffener plate stress ratio is the bending stress in the plate/bending allowable stress. See Tables 3.2-10 and Table P.3.7-17.

Table P.3.7-25
Extension Plates and Cross Members Results

Load Comb.	Extension Plates Interaction Ratio(1)	Cross Members Stress Ratio(2)
C1S	0.77	0.25
C2S	0.77	0.32
C3S	0.71	0.20
C4S	0.60	0.25
C5S	*0.71*	*0.31*

Notes:

(1) Axial and bending stresses are computed using axial (F_x) and bending moment (M_y, M_z) results from Table P.3.7-22. Interaction ratios are based on appropriate equations from Chapter H of AISC [3.20]. See Tables 3.2-10 and Table P.3.7-17.

(2) Axial stresses in the cross members are computed using axial (F_x) force results from Table P.3.7-23. Cross member stress ratio is the axial stress in the member/axial allowable stress. See Tables 3.2-10 and Table P.3.7-17.

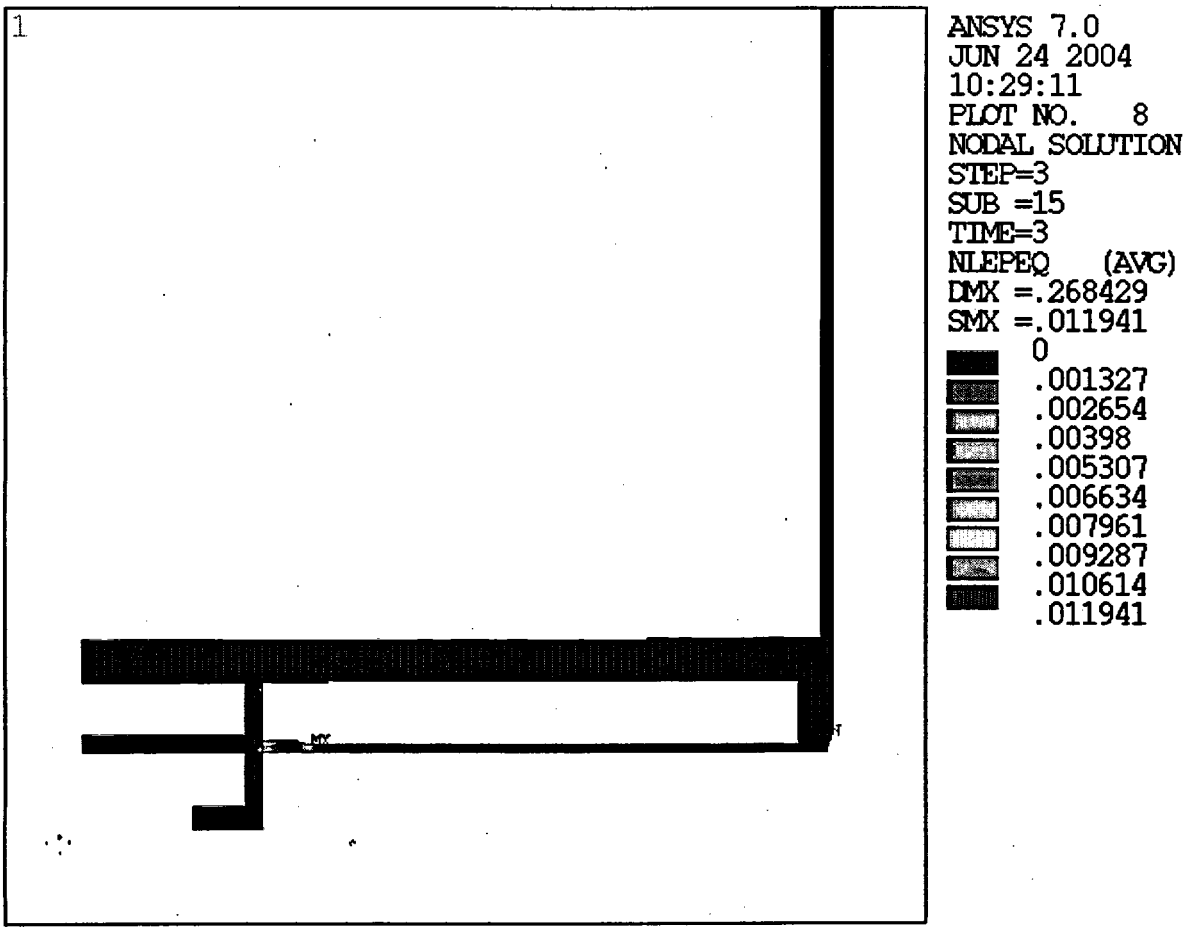

Figure P.3.7-15
24PTH-S-LC Plastic Strain Plot – 60g Bottom End Drop + 20 psi Off-Normal Pressure

16. Concrete[1]

Temperature (°F)	K (Btu/min-in-°F) [4.29]	ρ (lb_m/in^3)[1]	C_p (Btu/lb_m-°F) [4.42]	Emissivity [4.30]
70	1.597E-3	0.084	0.22	0.9
1382	7.983E-4			

(1) Conservatively, the properties used herein for the HSM-H walls, *and* roof do not include the effects of rebar. Additionally, the ISFSI pad is conservatively modeled as concrete and does not include the effects of rebar. Including the effects of rebar would otherwise increase the effective conductivity of the HSM-H concrete walls, roofs, and ISFSI pad.

17. Effective Neutron Shield Thermal Conductivity vs. Circumferential Cask Position

Angle On Cask Body	k_{eff}, Btu/min-in-°F [4.38]	
	Water-Filled	Air-Filled
0°	0.011520	0.000385
30°	0.010848	0.000393
60°	0.010933	0.000408
90°	0.010708	0.000417
120°	0.008868	0.00391
150°	0.008695	0.000322
180°	0.007403	0.000227

The effective thermal conductivity within the neutron shield is directly proportional to the thermal conductivity of water or air and exponentially proportional to the associated Rayleigh number existing in the neutron shield cavity.

The thermal conductivity and the coefficient of thermal expansion increase with increasing temperature, while the density and viscosity decrease with increasing temperature (Table A.3 from [4.26]. Therefore, the net effect of an increased heat load will be both a higher thermal conductivity and Rayleigh number. As such, the effective thermal conductivity computed for the 24 kW heat load in Reference [4.38] is conservatively less than the actual effective thermal conductivity for 40.8 kW heat load.

For the case of an air filled neutron shield, the thermal conductivity and viscosity of air increase with increasing temperature, while the density and the coefficient of thermal expansion decrease with increasing temperature. The net effect of operation at a higher temperature level will be a higher thermal conductivity, but a lower Rayleigh number for a given ΔT. Since increasing the heat load within the transfer cask will tend to increase both the operating temperature and the ΔT required to remove the heat from the cask, the lower ΔT associated with the 24 kW heat load used to compute the Reference [4.38] effective thermal properties effectively under-estimates the Rayleigh number for the 40.8 kW heat load.

The combined effect on the computed effective thermal conductivity due to operations at the proposed higher temperature level and a higher ΔT than assumed in the Reference [4.38] results in effective thermal conductivity higher than the 24 kW from Reference [4.38] Therefore, use of Reference [4.38] values for air filled neutron shield case is conservative for the 40.8 kW heat load case.

18. Borated Aluminum and Boral Thermal Conductivity [See Section P.4.3]

$$\text{Decay heat flux} = \frac{Q}{\pi D_i L} \quad \text{Btu/hr-in}^2$$

where,

Q = decay heat load (24, 31.2, or 40.8 kW)
Di = inner DSC diameter = 66.19"
L = DSC cavity length = 169.6"

To maximize the applied heat flux, the minimum cavity length of 169.6 inches which bounds the 24PTH-S and 24PTH-L or –S-LC DSCs, is used in the above equation. The calculated decay heat flux values are as follows:

Heat Load (kW/DSC)	Decay Heat flux (Btu/hr/in^2)
24	2.322
31.2	3.019
40.8	3.948

The thermal analysis of a typical HSM-H is performed for a loaded 24PTH DSC located in the interior of a multiple module array with a 24PTH DSC present in the two adjacent HSM-Hs. The HSM-H top and front surfaces are modeled as exposed to the prevailing ambient conditions in this model. The side and back surfaces are modeled as being adiabatic in order to simulate the adjacent modules.

Single/End HSM-H model

An additional model was constructed for the specific purpose of calculating the maximum concrete gradients. For this model, the thermal analysis is performed for a free standing HSM-H with the top and front, as well as the back and side surfaces exposed to the prevailing ambient conditions.

The maximum temperature gradient occurs in a single (stand-alone) or an end HSM-H wherein one or two of the HSM-H sidewalls are exposed to the cold ambient temperature. To bound the maximum temperature gradient across the HSM-H concrete walls, the associated finite element model is modified such that the three feet thick shield walls are added to the side and back walls of the HSM-H. An average gap of 0.125" is considered between the shield walls and the HSM-H module. The single/end HSM-H model simulates a single HSM-H module exposed to –40°F ambient temperature without solar heat flux. The finite element model of the single HSM-H module is depicted in Figure P.4-4.

P.4.4.5 Description of the HSM-H Blocked Vent Model

To determine the maximum temperatures of the HSM-H and the DSC shell for the blocked vent accident case, the finite element model of the HSM-H is modified to a transient model.

During the blockage of the air inlet and outlet vents in the HSM-H, there will be convection within the closed HSM-H cavity. Conservatively, no convection is considered within the HSM-H cavity

during the blocked vent condition. The analysis considers only the thermal conductivity of air within the HSM-H cavity. The mesh size of the model is increased slightly to preclude possible computer resource problems for the transient run.

The DSC basket and associated fuel assemblies for the transient case are modeled as a homogenized material with suitable effective properties as determined in Section P.4.8.3. Heat generating boundary conditions are applied uniformly on all of the elements representing the DSC contents. The amount of generated heat per unit volume of the DSC contents is calculated as follows:

$$\text{Heat generation rate} = \frac{Q}{(\pi/4\ D_i^2\ L)} \quad \text{Btu/hr-in}^3$$

where:

Q = decay heat load (24, 31.2, or 40.8 kW)
Di = inner DSC diameter = 66.19"
L = DSC cavity length = 169.6"

The heat generating rates for 40.8, 31.2, and 24 kW decay heat are shown in the table below:

Heat Load, kW/DSC	Heat Generation Rate $\left(\frac{\text{Btu}}{\text{hr-in}^3}\right)$
40.8	0.239
31.2	0.182
24	0.140

The nodes of the DSC contents are disconnected in the axial direction from the DSC shield plugs to simulate the uniform heat generation over the radial surface of the DSC.

The initial conditions for the blocked vent accident case are identical to the boundary conditions applied for the off-normal case with a 105°F daily average temperature (117°F max. daylight temperature) and maximum solar heat flux. The emissivity of the support structure is assumed to be 0.3. The finite element model utilized for the transient runs is depicted in Figure P.4-5. This model assumes the maximum decay heat load of 40.8 kW to bound the maximum temperatures within the HSM-H for the accident conditions.

P.4.4.6 Description of Cases Evaluated for the HSM-H

The HSM-H thermal analyses are performed for the design basis normal ambient air temperatures defined in Section P.4.4.1.

A summary of the cases considered for HSM-H thermal analysis is presented in Section P.4.4.3.

P.4.6.7.1 Blocked Vent Accident Evaluation

For the postulated blocked vent accident condition, the HSM-H ventilation inlet and outlet openings are assumed to be completely blocked for a 40-hour period concurrent with the extreme off-normal ambient condition of 117°F with insolation.

For conservatism, a transient thermal analysis is performed using the 3-D model developed in Section P.4.5, for HLZCs 1 and 5. HLZCs 2, 3 and 4 are bounded by the temperature results for HLZC 1. When the inlet and outlet vents are blocked, the air surrounding the DSC in the HSM-H cavity is contained (trapped) in the HSM-H cavity. The temperature difference between the hot DSC surface and the surrounding HSM-H (cooler) heat shield and concrete surfaces results in closed cavity convection. *However, closed cavity convection has been conservatively ignored. The analysis considers only the thermal conductivity of air.*

Summaries of the calculated fuel cladding and DSC component temperatures are listed in Table P.4-25 through Table P.4-28.

P.4.6.7.2 Transfer Accident Evaluation

The postulated transfer accident event consists of 24PTH DSC transfer in the OS197FC TC in a 117°F ambient environment with loss of the solar shield and the loss of liquid neutron shielding. All five HLZCs were evaluated. HLZC 1 bounded the results of HLZCs 2 and 3. The results for HLZCs 1, 4 and 5 are shown in Table P.4-25 through Table P.4-28.

P.4.6.7.3 Hypothetical Fire Accident Evaluation

For the postulated worst-case fire accident, a 300 gallon diesel fire is simulated for a NUHOMS®-24PTH DSC with a decay heat load of 40.8 kW during transfer in the TC. This accident event bounds other fire scenarios associated with loading operations and storage within the HSM-H due to the large thermal mass of the HSM-H and its vent configuration which provides protection for the DSC and its payload.

Steady state, off-normal conditions are assumed prior to the fire, which consist of a 117°F ambient temperature without a solar shield in place on the TC but with water filled neutron shield. The fire has a temperature of 1,475°F, and an emittance of 0.9 and a duration of 15 minutes based on the 300-gallon diesel fuel source and complete engulfment of the TC for the duration of the fire. This is conservative because it allows the maximum amount of heat input into the NUHOMS® system components. Subsequent to the fire, the TC is subjected to 117°F ambient conditions with maximum insolation. Note that these hypothetical fire parameters and assumptions are very conservative.

It is assumed that liquid neutron shield (water) is present throughout the 15-minute fire transient even though it is expected to be lost and replaced with air very early in the fire transient. This assumption maximizes the heat input from the fire to the canister because of the high conductivity of water compared to air. To maximize the canister temperature during the post-fire transient, it is assumed that water in neutron shield cavity is lost at the beginning of post-fire transient and replaced by air as the heat flow is now from canister to the ambient.

P.4.8 Determination of Effective Thermal Properties of the Fuel, Basket and Air Within the HSM-H Closed Cavity

This section presents the methodology and determines the effective thermal conductivity, specific heat and density for the fuels to be stored within NUHOMS®-24PTH DSC with helium backfill and vacuum for use in the analysis of the thermal performance of the NUHOMS®-24PTH DSC.

This section also determines the effective thermal conductivity, density and specific heat load of the 24PTH DSC basket for use in the transient thermal analysis in Section P.4.4 and P.4.5.

P.4.8.1 Determination of Bounding Effective Fuel Thermal Conductivity

P.4.8.1.1 Fuel Assemblies Evaluated

The fuel assemblies that are considered for storage in the NUHOMS® 24PTH DSC, including the design data for each fuel assemblies, are listed in Section P.2. This section includes calculation of the bounding properties among fuels to store in 24PTH-S or -L DSC with maximum total decay heat per DSC up to 40.8 kW. The bounding properties of B&W 15x15 fuel assemblies were calculated for thermal analysis of 24PTH-S-LC DSC with maximum total decay heat of 24 kW per DSC.

P.4.8.1.2 Summary of Thermal Properties of Materials

The thermal conductivity and specific heat values of Zircaloy, UO_2 pellets, and Helium are presented in Section P.4.2. The emissivity of Zircaloy is also presented in Section P.4.2.

P.4.8.1.3 Calculation of Fuel Axial Effective Thermal Conductivity

The axial fuel conductivity is assumed to be limited to the cladding conductivity weighted by its fractional area as required in NUREG 1536 [4.7].

$$K_{axl} = (K_{zirc})(A_{zirc}/A_{eff}) \qquad (1)$$

K_{zirc} = Conductivity of Zircaloy 4
A_{eff} = (8.90") x (8.90") = 79.21 in^2
A_{zirc} = Cross section area of Zircaloy cladding in the fuel assembly

Equation (1) is used to calculate axial effective conductivity for the fuel assembly types listed in Section P.2. The results are plotted in Figure P.4-44.

P.4.8.1.4 Calculation of Fuel Transverse Effective Thermal Conductivity

The transverse fuel effective conductivity is determined by creating a two-dimensional finite element model of the fuel assembly centered within a fuel compartment. The outer surfaces, representing the fuel compartment tube walls, are held at a constant temperature and heat generating boundary condition is applied to the fuel pellets within the model. A maximum fuel assembly temperature is

P.4.8.3 24PTH DSC Basket Effective Thermal Properties

The 24PTH DSC basket effective density, thermal conductivity and specific heat are calculated for use in the transient analyses of the 24PTH DSC in the OS197FC transfer cask and in the HSM-H. The calculation of these thermal effective properties is based on the DSC component weights.

The 24PTH DSC effective density $\rho_{eff\ DSC\ basket}$, and specific heat $c_{p\ eff\ DSC\ basket}$ are calculated as volumetric and weight average values, respectively.

The effective transverse thermal conductivity is determined by theoretical solution for conduction in an infinite cylinder with uniform heat generation [4.41]:

$$k_{eff-basket} = \frac{Q}{4\pi \cdot L \cdot (T_c - T_s)}$$

where
- Q is total heat load, W
- L is cylinder (DSC cavity) length, m,
- T_C is temperature at the cylinder center, ℃
- T_S is temperature at the cylinder surface. ℃

The effective transverse thermal conductivities of the 24PTH DSC basket $k_{eff\text{-}basket}$ are calculated for 40.8, 31.2, and 24 kW total heat loads per DSC, using the 24PTH DSC ANSYS models.

The heat generation is applied to the fuel assemblies uniformly without a peaking factor. The temperatures from 100°F to 800°F are applied uniformly to the DSC shell.

An average, $(T_s+T_c)/2$, is used as the reference temperature, for which $k_{eff\text{-}basket}$ is reported.

The criterion for determining the bounding 24PTH DSC basket effective density $\rho_{eff\ DSC\ basket}$, and specific heat $c_{p\ eff\ DSC\ basket}$ is based on the lowest value of $c_{p\ eff\ DSC\ basket}$ and $\rho_{eff\ DSC\ basket}$.

The DSC basket axial effective thermal conductivity is conservatively calculated based on axial fuel effective thermal conductivity:

$$k_{basket\ axial} = k_{fuel\ axial} \cdot A_{fuel\ cells} / A_{DSC\ internals}\ .$$

where
- $k_{basket\ axial}$ is DSC axial effective thermal conductivity,
- $k_{fuel\ axial}$ is fuel axial effective thermal conductivity,
- $A_{fuel\ cells}$ is total fuel cells cross-section area,
- $A_{DSC\ internals}$ is cross-section area within DSC shell.

The bounding radial and axial thermal conductivity values for 24PTH-S and 24PTH-L, and -S-LC DSCs are shown in Section P.4.2.

P.4.8.4 Effective Air Conductivity in the HSM-H Closed Cavity

During blockage of the inlet and outlet vents, the air within the HSM-H is trapped. The convection heat transfer under these circumstances reduces to free convection in closed cavities. *For conservatism, no convection is considered with the HSM-H cavity during blockage of the vents.*

PAGE DELETED IN ITS ENTIRETY.

PAGE DELETED IN ITS ENTIRETY.

DSC over the length of the fuel basket. The decay heat loading is simulated as a uniform heat flux applied over the 169.6-inch length of the DSC shell between the closure plugs. For conservatism, the minimum DSC length is assumed for the analysis which is the same as the ANSYS model in Section P.4.4.4.

While the fins on the side heat shields are ignored for simplicity and conservatism, the top heat shield is modeled as individual plates to accurately capture the geometry and the flow regime through the louvers.

The ability of the Fluent™ program to create unstructured computational meshes was used to concentrate the mesh density in those areas requiring greater fluid flow and/or thermal resolution and decrease the mesh density in those areas (i.e., within the concrete walls, etc.) that do not experience large gradients. The resultant unstructured mesh used for this evaluation is illustrated in Figure P.4-55. The total size of the mesh used in the modeling of the HSM-H exceeds 1,629,250 elements.

Table P.4-40 presents a comparison of the peak component temperatures obtained using the ANSYS analytical model vs. those obtained using the confirmatory analysis methodology. As seen from the table, *in* general *a* good agreement is seen between the methodologies, with the CFD based confirmatory methodology predicting peak surface temperatures on the DSC *shell and concrete base unit that are essentially equivalent to the ANSYS methodology.* The confirmatory methodology does predict a higher peak roof concrete temperature than the ANSYS analytical model by approximately *13*°F, a hotter louvered (i.e., top) heat shield temperature by approximately *9*°F, and a hotter side heat shield temperature by approximately *44*°F.

The higher side heat shield temperature is directly related to the simplification by the confirmatory analysis in ignoring the approximately 10-fold increase in convective surface area represented by the fins provide on the side shields. The higher peak temperature in the louvered heat shield is due to differences in the airflow distribution across the length and width of the heat shield and to differences in the vertical temperature profile. In keeping with its assumption of uniform flow and temperature profiles, the ANSYS analytical model analysis predicts a nearly flat temperature profile across the shield (i.e., 185.8 to 187.6°F). In contrast, the confirmatory analysis predicts a *10*°F variation across the surface of the heat shield, with an average temperature of *193*°F.

The difference in the peak temperature of the roof concrete is partly due to differences in the computed view factors between the DSC and the underside of the roof through the louvered heat shield and partially due to differences in the flow distribution within the HSM. The ANSYS analytical model assumption of a fully mixed air temperature within each fluid zones does not factor in the 'plume' of hot air rising from the centerline of the DSC.

4.34 Rohsenow, Hartnett, and Ganic, Handbook of Heat Transfer Fundamentals, 2nd edition, McGraw-Hill Publishers, 1995

4.35 David R. Lide, *CRC Handbook of Chemistry and Physics*, 83rd edition, 2002-2003, CRC Press.

4.36 SINDA/FLUINT™, Systems Improved Numerical Differencing Analyzer and Fluid Integrator, *Version 4.5, Cullimore & Ring Techno logies, Inc., Littleton, CO, 2002*

4.37 Thermal Desktop™, *Version 4.5, Cullimore & Ring Technologies, Inc., Littleton, CO, 2002*

4.38 Section M.4 of Appendix M, Revision 6 of Application for Amendment No. 5 to the NUHOMS® Certificate of Compliance No. 1004, (TAC NO. L23343).

4.39 "ASHRAE Handbook, Fundamentals" – SI Edition, 1997

4.40 White, F. M., Fluid Mechanics, 2nd Edition, McGraw-Hill, 1986.

4.41 Incropera, F. P., D. P. DeWitt, *Fundamentals of Heat and Mass Transfer*, 3rd Edition, Wiley, 1990.

4.42 Cavanaugh et al., *Guide to Thermal Properties of Concrete and Masonry Systems*, Reported by ACI Committee 122, Report # ACI 122R-02, American Concrete Institute, Detroit, MI, 2002.

4.43 Transnuclear, Inc., TN-68 Dry Storage Cask Final Safety Analysis Report, Revision 0, Hawthorne, NY, 2000 (Docket 72-1027).

4.44 FLUENT™, Version 5.6, Fluent Inc., Lebanon, NH, 2003.

4.45 ICEPAK™, Version 4.08, Fluent Inc., Lebanon, NH, 2003.

4.46 TN Calculation, NUH32PT.0414, Rev. *1*, "Validation of FLUENT™/ICEPAK™ for Convective Flow in Enclosures."

4.47 Perry, Chilton, et al, "Chemical Engineer's Handbook," 5th Edition, 1973.

Table P.4-3
HSM-H Components Normal and Off-Normal Maximum Temperatures, 31.2 kW Heat Load

Component	Maximum Temperature (°F)[3]		
	Ambient 117°F Case 5[1]	Ambient 117°F Case 5A[2]	Ambient -40°F Case 6
DSC Shell	391	401	270
Concrete	183	201	9
Top Heat Shield	173	176	8
Side Heat Shield	164	221	1
DSC Support Rail	248	254	99

Notes:
(1) The results are with fins on side heat shields.
(2) The results are without fins on side heat shields.
(3) The maximum temperatures shown are for the off-normal condition which bounds the normal condition maximum temperatures.

Table P.4-4
HSM-H Components Normal and Off-Normal Maximum Temperatures, 24 kW Heat Load

Component	Maximum Temperature (°F)[1]	
	Ambient 117°F Case 7	Ambient -40°F Case 8
DSC Shell	344	216
Concrete	168	-2
Top Heat Shield	162	0
Side Heat Shield	152	-9
DSC Support Rail	221	71

Note:

(1) The maximum temperatures shown are for the off-normal condition which bounds the normal condition maximum temperatures.

Table P.4-5
HSM-H Components Maximum Temperatures (°F), 40.8 kW Decay Heat Load, 117°F Ambient, Blocked Vent Accident (Case 9)

Component	38.5 hr Blockage
DSC Shell	*637*
Concrete[1]	*408*[1]
Top Heat Shield	*355*
Side Heat Shield	*499*
DSC Support Rail	*556*

1. The calculated temperature is above the 350°F limit given in [4.7]. Testing will be performed to document that concrete compressive strength will be greater than that assumed in the structural analyses.

Table P.4-6
Single HSM-H Components Maximum Temperatures, 40.8 kW Heat Load, -40°F Ambient, Blocked Vent Accident (Case 10)

Component	38.5 hr Blockage
DSC Shell	*577*
Concrete	*248*
Top Heat Shield	*206*
Side Heat Shield	*407*
DSC Support Rail	*484*

Table P.4-16
DSC Basket Assembly Maximum Normal Operating Component Temperatures; HLZC 4 (31.2 kW)

Operating Condition	T_{alum} (°F)	T_{poison} (°F)	T_{tube} (°F)	$T_{DSC\ shell}$ (°F)
DSC in HSM-H, 0°F ambient[1]	<565	<566	<568	<367
DSC in HSM-H, 100°F ambient[1]	<637	<638	<640	<445
DSC in OS197FC cask, 0°F ambient[3]	<680[2]	<681[2]	<682[2]	454
DSC in OS197FC cask, 100°F ambient[3]	680	681	682	475
DSC in OS197FC cask, 100°F ambient[4] (with inserts)	678	679	680	548

1) Temperatures are bounded by temperatures for HLZC 1 (Table P.4-15).
2) Temperatures are bounded by temperatures for 100°F ambient case.
3) Assumes 24PTH-S DSC without aluminum inserts in R45 transition rails.
4) Assumes 24PTH-S DSC with aluminum inserts in R45 transition rails.

Table P.4-21
DSC Basket Assembly Maximum Off-Normal Operating Component Temperatures, HLZC 1[4] (40.8 kW)

Operating Condition	T_{alum} (°F)	T_{poison} (°F)	T_{tube} (°F)	$T_{DSC\ shell}$ (°F)
DSC in HSM-H, -40°F Ambient	534	535	537	333
DSC in HSM-H, 117° F Ambient	641	642	643	448
DSC in OS197FC with sunshade, 117°F ambient[2]	<641[1]	<642[1]	<643[1]	444
DSC in OS197FC with sunshade, 117°F ambient[3]	604	605	607	480

1) Temperature is provided using bounding storage in HSM-H case with 117°F ambient.
2) Assumes 24PTH-S DSC with aluminum inserts in R45 transition rails.
3) Assumes 24PTH-S DSC *with* aluminum inserts in R45 transition rails and use of 475 cfm air circulation with external fan per Table P.4-41.
4) HLZC 1 bounds the temperatures for HLZC 2 and 3.

Table P.4-25
Fuel Cladding Accident Condition Maximum Temperatures

Heat Load Zoning	HLZC 1[2] (°F)	HLZC 4 (°F)	HLZC 5 (°F)	Limit (°F)
DSC in HSM, Blocked Vent, 117°F	*881*[1]	*<881*[2]	< 809[3] /809[4]	1058[5]
DSC in TC, loss of sun shade, neutron shield water and air circulation with fan, if used, 117°F	914	843	747	

1) Temperature at 38.5 hour of blocked vent.
2) Temperatures for HLZC 1 bound the temperatures for HLZC 2, 3, and 4.
3) Temperature for storage in HSM-H is bounded by temperature for storage in HSM Model 102.
4) Temperature for storage in HSM Model 102 at 40 hours of blocked vent.
5) ISG-11, Revision 2 [4.20]

Table P.4-26
DSC Basket Assembly Accident Maximum Component Temperatures; HLZC 1 (40.8 kW)

Operating Condition	T_{alum} (°F)	T_{poison} (°F)	T_{tube} (°F)	$T_{DSC\ shell}$ (°F)
DSC in HSM-H, Blocked Vent[1], 117°F	*828*	*829*	*830*	*637*
DSC horizontal in OS197FC loss of sun shade, neutron shield water and air circulation with fan, if used, 117°F Ambient	860	861	862	685

1) Temperature at 38.5 hour of blocked vent.

Table P.4-40
Comparison Of Peak Component Temperatures For 117°F Ambient With 40.8 kW Decay Heat Load

Component	ANSYS Analytical Model (°F)	CFD Based Confirmatory Calculation (°F)
DSC Shell	448	*452*
Base Unit Concrete	202	*201*
Roof Concrete	186	*199*
Top Heat Shield	188	*197*
Side Heat Shield	181	*225*

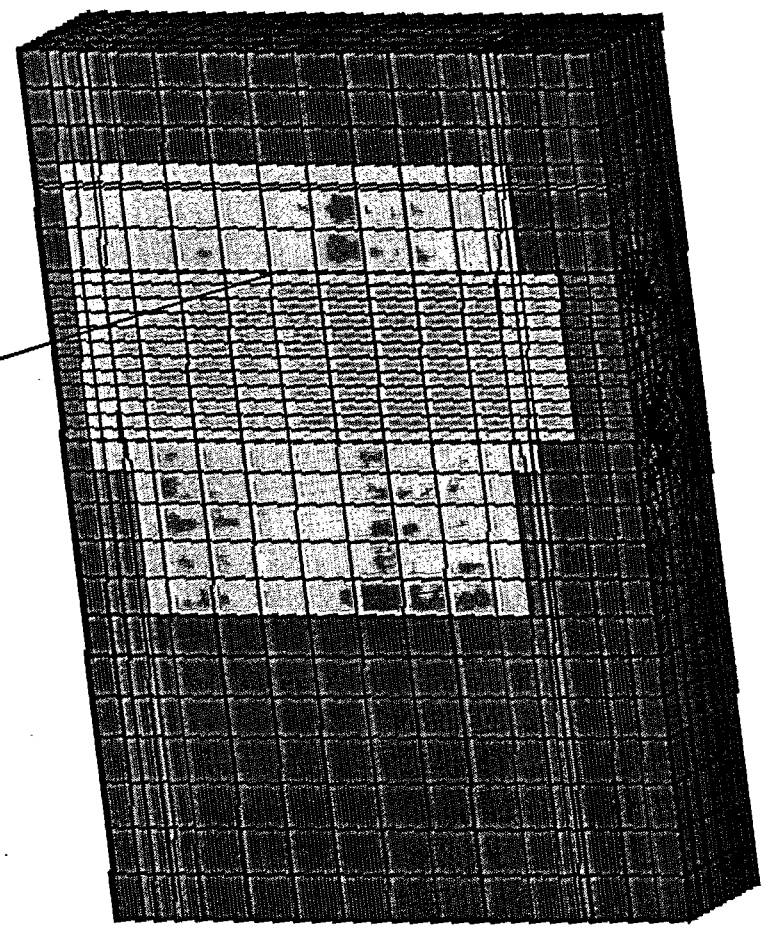

Figure P.4-5 HSM-H with 24PTH DSC Finite Element Model for Blocked Vent Analysis

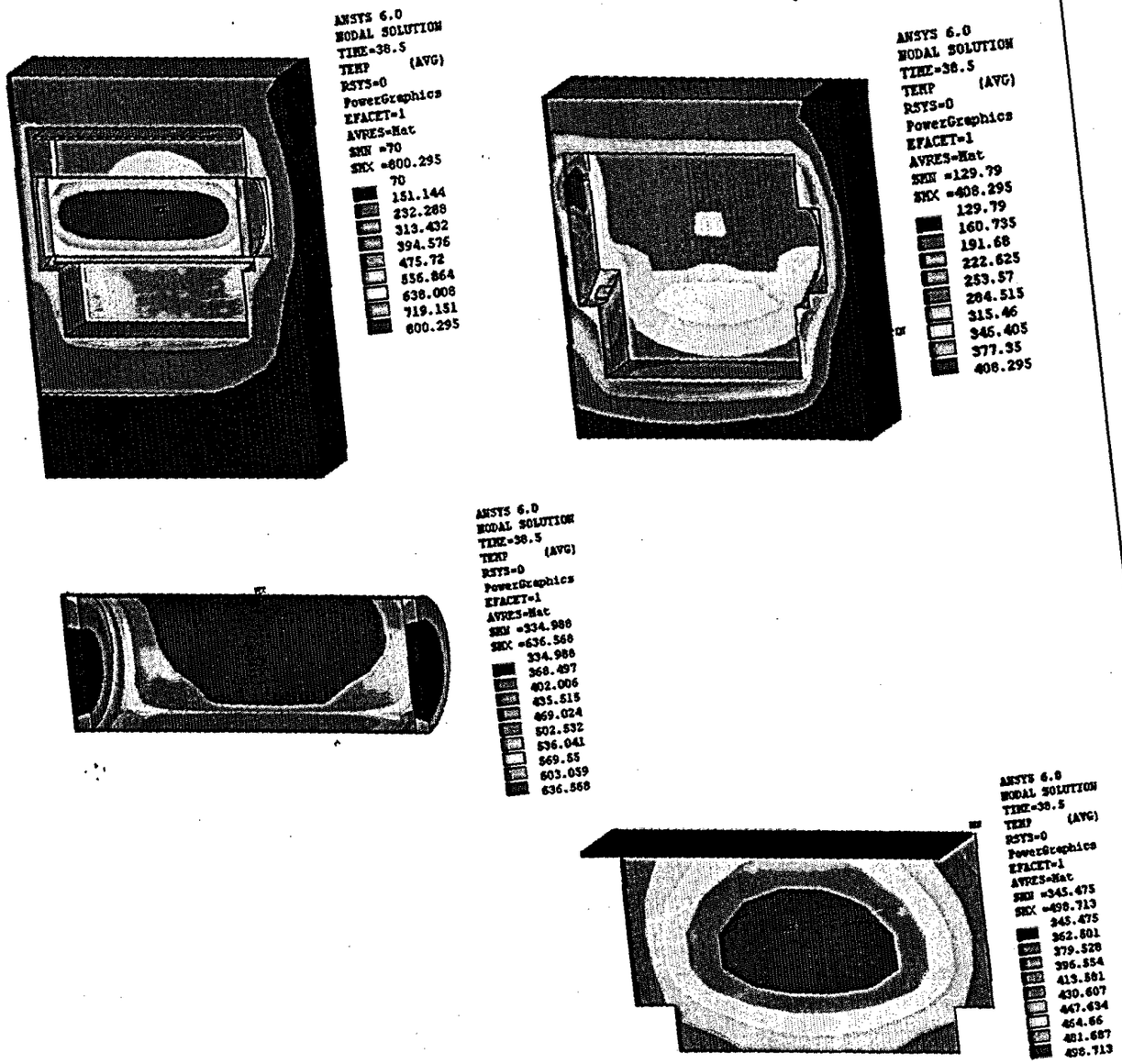

Figure P.4-14 Temperature Distribution in HSM-H and 24PTH DSC Shell Assembly, 40.8 kW heat load, at 38.5 (typical) hours of Blocked vent, 117°F ambient

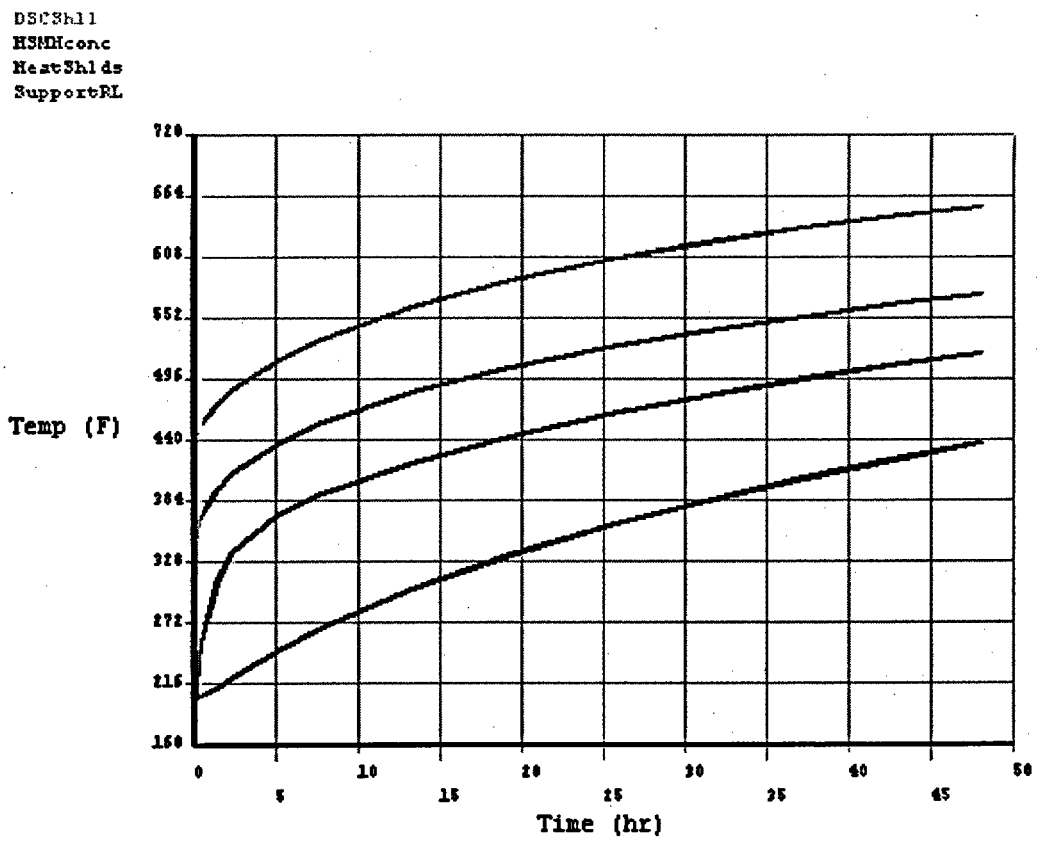

Figure P.4-15 Temperature-Time Histories of HSM-H Model Components during Blocked Vents Accident Case, 40.8 kW, 117°F Ambient

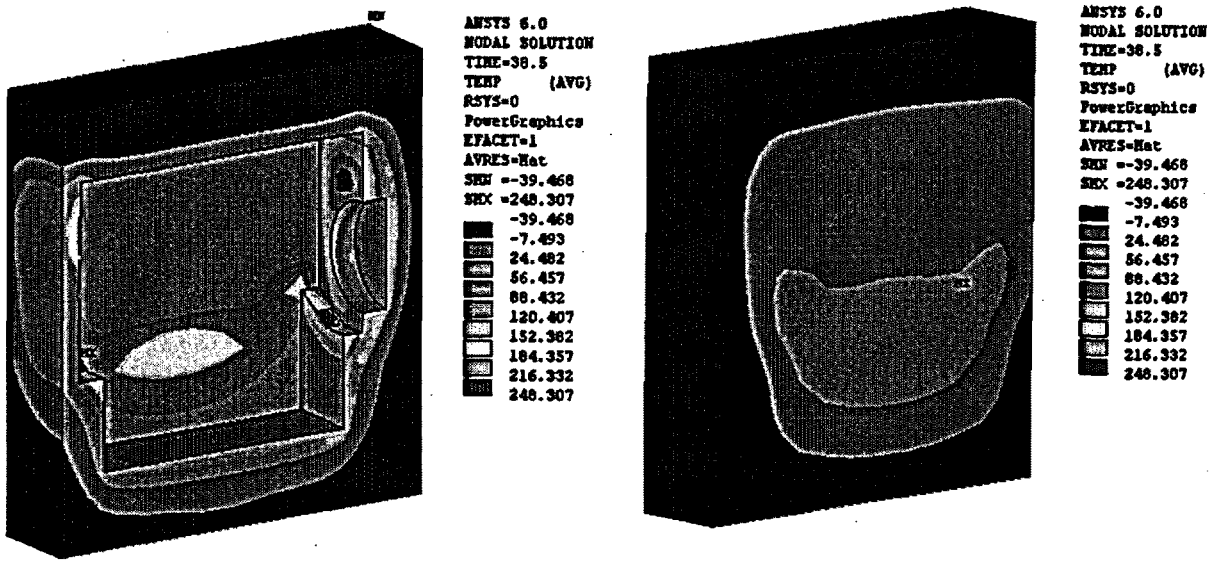

Figure P.4-17 Temperature Distribution in a Single HSM-H, 40.8 kW Heat Load, -40°F Ambient, Maximum Temperature Gradients through Concrete Walls. Blocked Vent Transient at 38.5 Hours

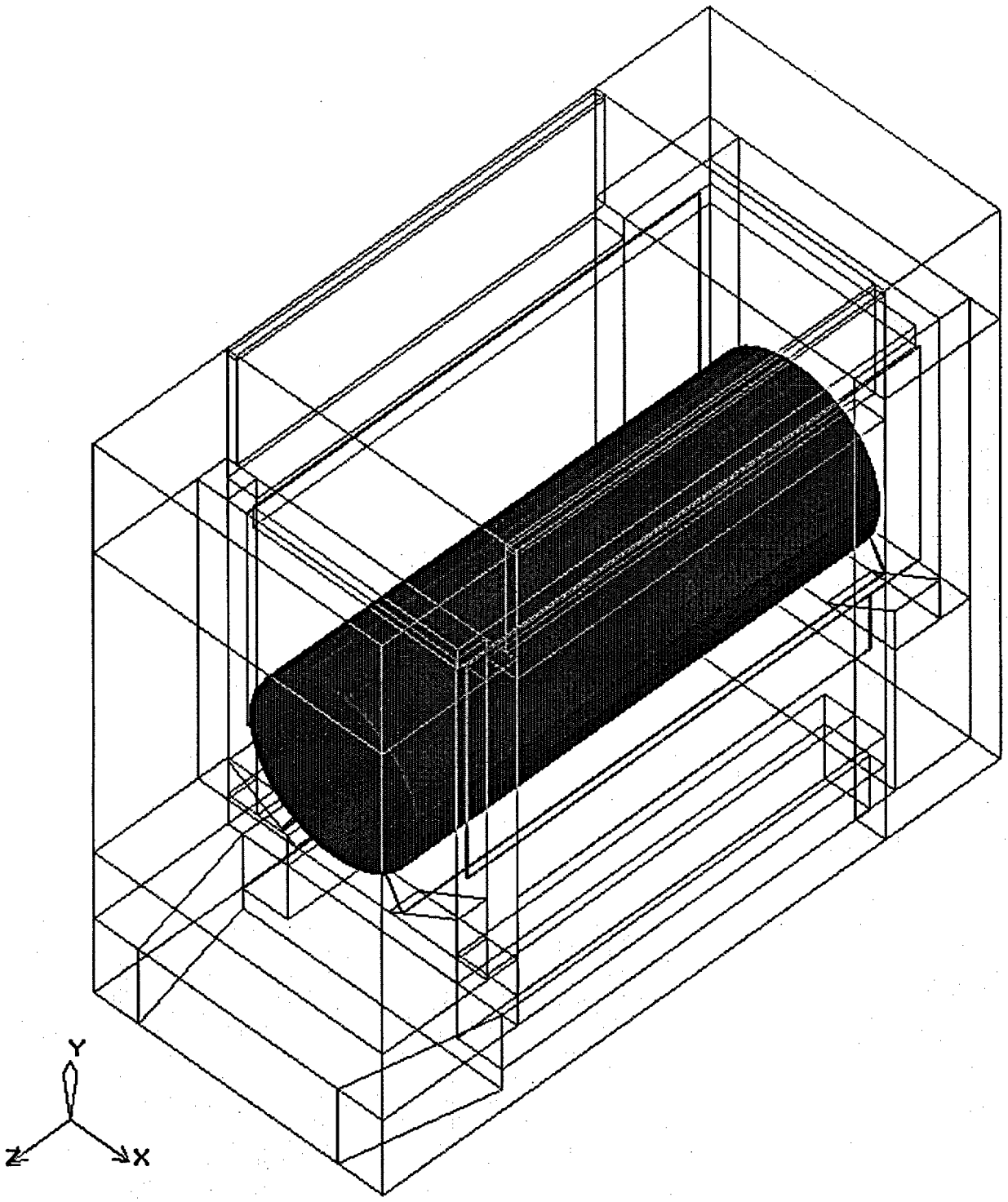

Figure P.4-54 DSC Within HSM-H

P.5.2 Source Specification

Thermal and radiological source terms are calculated with the SAS2H/ORIGEN-S modules of SCALE 4.4 [5.1] for the fuel. The SAS2H/ORIGEN-S results are used to develop the fuel qualification tables listed in Table P.2-6 through Table P.2-13 and the design-basis fuel source terms suitable for use in the shielding calculations. The thermal and radiological source terms for the CCs which are taken from Appendix J, are shown in Table P.5-12.

The B&W 15x15 assembly is the bounding fuel assembly design for shielding purposes because it has the highest initial heavy metal loading and CO-59 content of the hardware regions as compared to the 14x14, other 15x15, and 17x17 fuel assemblies which are also authorized contents of the NUHOMS®-24PTH DSC. The neutron flux during reactor operation is peaked in the in-core region of the fuel assembly and drops off rapidly outside the in-core region. Much of the fuel assembly hardware is outside of the in-core region of the fuel assembly. To account for this reduction in neutron flux, the fuel assembly is divided into four exposure "regions." The four axial regions used in the source term calculation are: the bottom (nozzle) region, the in-core region, the (gas) plenum region, and the top (nozzle) region. The B&W 15x15 fuel assembly masses for each irradiation region are listed in Table P.5-6. The light elements that make up the various materials for the various fuel assembly materials are taken from reference [5.4] and are listed in Table P.5-7. The design-basis heavy metal weight is 0.490 MTU. These masses are irradiated in the appropriate fuel assembly region in the SAS2H/ORIGEN-S models. To account for the reduction in neutron flux outside the In-Core regions neutron flux (fluence) correction factors are applied to light element composition for each region. The neutron flux correction factors which are from Reference [5.15] are given in Table P.5-8.

Evaluations of the existing data with SAS2H and the 44-group ENDF/B-V library used in the analysis are documented in References [5.11] and [5.12]. These comparisons all show generally good agreement between the calculations and measurements, and show no trend as a function of burnup in the data that would suggest that the isotopic predictions, and therefore neutron and gamma source terms, would not be in good agreement. A similar conclusion is also reached by the results documented in JAERI report [5.13]. In fact, for the case with 46,460 MWd/MTU burnup, the isotopic predictions are all within 2% of those measured. There are ongoing efforts, some of which are documented in Reference [5.10], to obtain more data for burnups above 45 GWd/MTU. There is no reason to expect that the ongoing evaluations of the higher burnup fuel will result in less favorable comparisons. *Therefore, the uncertainty in the gamma source term, and associated dose rates, is estimated to be within ±5%.*

As noted in References [5.14] and [5.10], there is no public data for the neutron component currently available that bounds a fuel burnup of up to 62 GWd/MTU. However, as documented in Reference [5.14] and confirmed in the SAS2H analysis, the total neutron source with increasing burnup is more and more dominated by spontaneous fission neutrons. Reviewing the output from the SAS2H runs, the neutron source term is due almost entirely to the spontaneous fission of Cm-244 (~*94%* of all neutrons both spontaneous fission and (α,n)). After reviewing the measured Cm-244 content compared to the Cm-244 content predicted by SAS2H and the 44-group ENDF/B-V library documented in References [5.11] and [5.12] for burnups up to 46,460 MWd/MTU, it is readily apparent that the calculated values are within ±11 % of the measured values, with most of the predicted values within ±5% of the measured. Finally, there is no

observed trend as a function of burnup in the data that would indicate that the predicted Cm-244 content is significantly different at higher burnups. *Therefore, as the CM-244 isotope accounts for more than 94% of the total neutron source term, the uncertainty in the neutron source and associated neutron dose rates is expected to be less than ±1 %.*

As documented in Reference [5.14] and as observed in preparing the fuel qualification tables, the gamma dose rate increases nearly linearly with burnup relative to the direct gamma component and the neutron dose rate increases with burnup to the fourth power. Therefore, as burnups go beyond 45 GWd/MTU, the contribution from neutron (and associated n,γ) components to the total dose rates measured on the surfaces of the DSC, TC and HSM (HSM-H and HSM Model 102) increase in relative importance to that of the gamma component. However, this increase in the importance of the neutron source term has a relatively minor effect on the area dose rates on and around the HSM as these are dominated by the gamma component as shown in Table P.5-1 and Table P.5-2. The surface dose rates on the HSM are dominated by the gamma component because the HSM is constructed of thick reinforced concrete, which is an excellent neutron shield. Therefore, even a postulated substantial increase in the neutron source term would have a relatively minor effect on the site dose rate evaluation presented in Section P.10 of the amendment application.

For the TC, the neutron source term has a relatively minor effect on the area dose rates during most of the cask handling operations, since the DSC cavity and the annulus between the TC and DSC is filled with water and most of the work is done around the top of the cask. The neutron component is of more importance on and around the TC during transfer operations but, in general, only represents a small portion of the total dose rate on the sides and top of the TC. While the neutron dose rate on the bottom of the TC is slightly higher than gammas, relatively little occupational dose is received from this area. The dose rates for the design basis fuel on the surfaces of HSM and TC are shown in Table P.5-1 through Table P.5-5. These tables show that gamma dose rates are substantially higher than neutron dose rates. Therefore, the neutron component of the dose is a relatively minor fraction of the total occupational and site boundary dose.

The occupational exposure calculations demonstrate that most of the dose received by workers during cask loading and transfer operations is due to the gammas on and around the cask. The only surface of the TC that is dominated by neutrons is at the bottom of the cask. A small fraction of the total occupational exposure is due to the doses around the bottom of the cask because very little work is performed on or around the bottom of the cask with fuel in the TC.

As discussed above, any impact of uncertainties in source terms is expected to be negligible for the 24PTH system. Therefore, isotopic depletion calculations with SAS2H for fuel burned above 45 GWd/MTU are appropriate.

The fuel qualification tables are generated based on the decay heat limits for the various heat load zoning configurations shown in Figure P.2-1 through Figure P.2-5. SAS2H is used to calculate the minimum required cooling time to the nearest 0.1 year as a function of assembly initial enrichment and burnup for each decay heat limit. These cooling times are rounded up to the nearest 0.5 year increment in the final fuel qualification tables. Because the decay heat generally increases slightly with decreasing enrichment for a given burnup, it is conservative to

assume that the required cooling time for a higher enrichment assembly is the same as that for a lower enrichment assembly with the same burnup. The required cooling time for initial enrichments that fall between any two SAS2H runs are assumed to be that of the lower enrichment case results.

Fuel qualification tables for fuel without CC are listed in Table P.2-6 through Table P.2-9. However, some assemblies will contain a CC, which adds up to 8 watts of decay heat per assembly. Therefore, an additional set of fuel qualification tables are developed, as shown in Table P.2-10 through Table P.2-13, for fuel that contains CC. The fuel qualification tables for fuel with CC have slightly longer cooling times when compared to fuel without CC.

Reconstituted and/or damaged fuel is also acceptable for the DSC payload. Reconstituted fuel may contain up to 10 solid stainless steel rods that replace fuel rods. Reconstituted fuel has a rather small effect on the dose rate such that for cooling times less than 10 years, 1 year of cooling time is added if reconstituted stainless steel rods are present. If the cooling time is greater than 10 years, no additional cooling time is needed. Additional discussion on the method used to analyze reconstituted fuel is provided in Section P.5.2.5. Damaged fuel has essentially no impact on the dose rate as the source term would not be impacted and gross axial source redistribution is not likely.

The design-basis source terms are defined as the burnup/initial enrichment/cooling time combination given in the fuel qualification tables that result in the maximum dose rate on the surface of the HSM (either type) or TC (all types). Note that for a given DSC design, the design basis HSM source will not necessarily be the same as the corresponding design basis TC source. The 1-D discrete ordinates code ANISN [5.5] and the CASK-81 22 neutron, 18 gamma-ray energy group, coupled cross-section library [5.3] is used to determine the HSM and TC dose rate for each entry in the fuel qualification tables and thereby determine the design basis source. As ANISN is a 1-D code, a single dose location must be selected for both the HSM and TC for analysis purposes. For the HSM, the roof is selected as the dose location, and for the TC the cask side is selected as the dose location. This approach, described in detail in Section P.5.2.4, is consistent with the method used to determine the fuel qualification tables for the Standardized NUHOMS® canister designs described in Section 7.2.3 and Appendix M.5. The radiological source terms generated in the SAS2H/ORIGEN-S runs are used in the ANISN evaluations to calculate the surface dose rates. The ANISN models are similar to the appropriate MCNP4C2 models for the locations of interest.

Heat load zoning configuration 2 (Figure P.2-2) produced the bounding total surface dose rate for both the HSM-H and OS197FC TC using the 24PTH-L DSC. The 24PTH-L DSC, HSM-H design-basis source terms are from fuel with 41 GWd/MTU burnup, an initial enrichment of 3.3 wt. % U-235 and 3-years cooling. The 24PTH-L DSC, OS197FC design-basis source terms are from fuel with 62 GWd/MTU burnup, an initial enrichment of 3.4 wt. % U-235 and 5.6-years cooling.

The heat load zoning configuration selected for the shielding analysis of the 24PTH-S-LC DSC bounds the actual heat load configuration shown in Figure P.2-5 because 1.5 kW fuel is placed in all 24 locations. The 24PTH-S-LC DSC, Standardized TC design-basis source terms are from fuel with 32 GWd/MTU burnup, an initial enrichment of 2.6 wt. % U-235 and 3.0-years cooling.

Table P.5-1
Summary of NUHOMS®-24PTH-L DSC in HSM-H, Maximum and Average Dose Rates, Configuration 2 (2)

Dose Rate Location	Maximum Gamma (mrem/hr)	Gamma MCNP 1σ Error	Maximum Neutron (mrem/hr)	Neutron MCNP 1σ Error	Maximum Total(1) (mrem/hr)	Total MCNP 1σ Error
HSM Roof (centerline)	*20.1*	0.038	0.5	0.018	20.6	0.037
HSM Roof Birdscreen	205.8	0.019	4.1	0.012	209.9	0.018
HSM End (Side) Shield Wall Surface	3.4	0.081	0.1	0.016	3.5	0.079
HSM Door Exterior Surface (centerline)	1.3	0.143	0.1	0.524	1.3	0.139
HSM Front Birdscreen	1232.0	0.068	5.5	0.076	1237.0	0.068

Dose Rate Location	Average (mrem/hr)	Gamma MCNP 1σ Error	Average Neutron (mrem/hr)	Neutron MCNP 1σ Error	Average Total (mrem/hr)	Total MCNP 1σ Error
HSM Roof	*20.3*	*0.011*	0.5	0.006	*20.8*	*0.011*
HSM End (Side) Shield Wall Surface	1.0	0.016	0.1	0.033	1.1	0.015
HSM Front	*32.2*	*0.047*	0.1	0.066	*32.3*	*0.047*
HSM Back Shield Wall	0.6	0.074	0.1	0.025	0.6	0.074

Notes:
(1) Gamma and Neutron dose rate peaks do not always occur at same location; therefore, the total dose rate is not always the sum of the gamma plus neutron dose rate.
(2) Dose calculated using Configuration 2 in 24PTH-L DSC bounds configurations 1, 3 and 4.

P.9.1.4 Component Tests

No change.

P.9.1.5 Shielding Integrity Tests

No change.

P.9.1.6 Thermal Acceptance Tests

The analyses to ensure that the NUHOMS®-24PTH system is capable of performing their heat transfer function are presented in Section P.4.

P.9.1.7 Poison Plate Acceptance Tests

The poison plates only serve as a neutron absorber for criticality control and as a heat conduction path. The NUHOMS®-24PTH DSC safety analyses do not rely upon their mechanical strength except in through-thickness compression. The radiation and temperature environment in the cask is not sufficiently severe to damage the aluminum matrix that retains the boron-containing particles. To assure performance of the plates' Important-to-Safety function, the only critical variables that need to be verified are thermal conductivity and B10 areal density as discussed in the following paragraphs.

P.9.1.7.1 Thermal Conductivity Testing of Poison Plates

The poison plate material shall be qualification tested to verify that the thermal conductivity equals or exceeds the values listed in Section P.4.3. Acceptance testing of the material in production may be done at only one temperature in that range to verify that the conductivity equals or exceeds the corresponding value in Section P.4.3.

Testing may be by ASTM E1225 [9.3], ASTM E1461 [9.4], or equivalent method, performed on coupons as defined in Section P.9.1.7.2.1.

P.9.1.7.2 B10 Areal Density Testing of Poison Plates

There are three poison materials qualified for the NUHOMS®-24PTH DSC basket:

- Borated aluminum,
- Boron carbide/aluminum metal matrix composites (MMCs), such as Boralyn® or Metamic®, and
- Boral®.

For each poison material, the NUHOMS®-24PTH DSC basket is configured with three alternate basket configurations, depending on the boron loadings analyzed (designated as Type A basket for low B10 loading, Type B basket for moderate B10 loading, and Type C basket for high B10 loading). A summary of the minimum poison loadings considered and the corresponding credit

taken in the criticality analysis for each poison material as a function of 24PTH DSC basket type is summarized in Table P.9-1.

The B10 areal density and uniformity of the poison plates shall be verified, based on type, using approved procedures, as follows.

P.9.1.7.2.1 Borated Aluminum Using Natural or Enriched Boron, 90% B10 Credit

Borated Aluminum Material Description

The poison plate consists of wrought aluminum containing isotopically enriched B10. Alternately, a thicker aluminum plate containing natural B10 or a blend of enriched boron and natural boron is also acceptable provided it meets the specified minimum areal B10 density. Because of the negligibly low solubility of boron in solid aluminum, the boron appears entirely as discrete second phase particles of AlB_2 in the aluminum matrix. The matrix is limited to any 1000 series aluminum, aluminum alloy 6063, or aluminum alloy 6351 so that no boron-containing phases other than AlB_2 are formed. Titanium may also be added to form TiB_2 particles, which are finer. The effect on the properties of the matrix aluminum alloy are those typically associated with a uniform fine (1-10 micron) dispersion of an inert equiaxed second phase.

The nominal wt. % boron for full thickness (0.875 inch) plates with natural boron, by NUHOMS®-24PTH DSC basket Type is given in Table P.9-2. For example, the 3.0 wt. % For Type C basket converts to a nominal areal density of B10 as follows: (2.69 g BAl/cm^3)(3.0 wt. % B)(18.5 wt. % B10)(0.875 inch)(2.54 cm/inch) = 0.0332 g B10/cm^2, which is 4% above the design minimum of 0.032 g B10/cm^2 for Type C basket. If the poison sheets are paired with aluminum sheets (see drawing NUH24PTH-1003-SAR), the boron content shall be proportionately higher, up to that needed to maintain the minimum required B10 areal density. The specified wt. % boron for partial thickness (0.125 inch) plates with enriched boron, by NUHOMS®-24PTH DSC basket Type is given in Table P.9-2. For example, the 4.2 wt. % converts to a nominal areal density of B10 as follows: (2.69 g BAl/cm^3)(4.2 wt. % B)(95 wt. % B10)(0.125 inch)(2.54 cm/inch) = 0.0341 g B10/cm^2, which is 6% above the design minimum of 0.032 g B10/cm^2 for Type C basket.

The cast ingot may be rolled, extruded, or both to the final plate dimensions.

Borated Aluminum Test Coupon and Lot Definitions

A sample taken from the plate material is a test coupon. Test coupons will be removed so that there is at least one coupon contiguous with each plate. These coupons will be used for neutron transmission and thermal conductivity testing. The minimum dimension of the coupon shall be as required for the acceptance test procedures.

A lot is defined as all the plates produced from a single cast ingot, or all the plates produced from a single heat.

Borated Aluminum Acceptance Testing, Neutronic

Effective B10 content is verified by neutron transmission testing of these coupons. The transmission through the coupons is compared with transmission through calibrated standards composed of a homogeneous boron compound without other significant poisons, for example zirconium diboride or titanium diboride. These standards are paired with aluminum shims sized to match the scattering by aluminum in the poison plates. Uniform but non-homogeneous materials such as metal matrix composites may be used for standards, provided that testing shows them to be equivalent to a homogeneous standard.

Justification for Acceptance Test Requirements, Borated Aluminum

For a specific basket type, the criticality calculations in Section P.6 use boron areal densities that are 90% of the minimum value listed in Table P.9-1. This is justified base on the information provided in Reference [9.7].

P.9.1.7.2.2 Boron carbide/aluminum metal matrix composites (MMCs)

MMC Material Description

The MMC poison plates consist of a composite of aluminum with boron carbide particulate reinforcement. The material is formed into a billet by powder metallurgical processes and either extruded, rolled, or both to final dimensions. The finished product has near-theoretical density and metallurgical bonding of the aluminum matrix particles. It is a "uniform" blend of powder particles from face to face, i.e.; it is not a "sandwich" panel.

Typical MMC processing steps consist of:

- blending of boron carbide powder with aluminum alloy powder,
- billet formed by vacuum hot pressing (*e.g.*, Boralyn®) or cold isostatic pressing followed by vacuum sintering (*e.g.*, Metamic®),
- billet extruded to intermediate or to final size,
- hot roll, cold roll and flatten as required, and
- anneal (optional).

The nominal volume % boron carbide, by NUHOMS®-24PTH DSC basket Type, is given in Table P.9-3. For example, 29 volume % boron carbide corresponds to a B10 areal density of 0.29(2.52 g/cm^3 B_4C)(0.782 gB/gB_4C)(0.185 g B10/gB)(0.125 in)(2.54 cm/in) = 0.0336 g B10/cm^2, which is 5% above the design minimum of 0.032 g B10/cm^2.

MMC Qualification Test Program

The process specifications for the Boralyn® or Metamic® have been subjected to qualification testing to demonstrate that the process results in a material that:

- has a uniform distribution of boron carbide particles in an aluminum alloy with few or none of the following: voids, oxide-coated aluminum particles, B_4C fracturing, or B_4C/aluminum reaction products,
- meets the requirements for B10 areal density and thermal conductivity, and
- will be capable of performing its Important-to-Safety functions under the thermal and radiological environment of the NUHOMS®-24PTH DSC over its 40-year lifetime.

These qualification programs consisted of:

1. Fast neutron irradiation of the material to a fluence of about $8x10^{15}$ n/cm^2 or more, with dimensional measurements, transmission electron microscopic (TEM) examination, and /or mechanical testing to evaluate differences in the as-produced and irradiated conditions.

2. Exposure to temperatures in the range of 700°F or greater for periods of 30 days or more, again with dimensional measurements, transmission electron microscopic (TEM) examination, and /or mechanical testing to evaluate differences in the as-produced and irradiated conditions.

3. Evaluation of corrosion or hydrogen generation rates.

4. Verification of uniformity of B10 distribution by neutron radioscopy or by statistical analysis of neutron transmission measurements together with quantitative metallography.

The results of these qualification test programs have been previously presented to the NRC in the license applications for the TN-68 dry storage cask [9.6], the NUHOMS® 61BT DSC (Appendix K), and the NUHOMS® MP-197 transport packaging [9.7].

The qualification testing described above demonstrated, as would be expected from the properties of aluminum and boron carbide alone, that the materials suffer insignificant damage from the levels of radiation and temperature experienced in dry storage or transport of irradiated fuel. These materials also demonstrate corrosion characteristics very similar to the aluminum matrix.

Boralyn® qualification testing was performed on a 15 volume % boron carbide / 1000 series aluminum composite, and Metamic® qualification testing was performed on 15, 31 and 40 volume % boron carbide / 6000 series aluminum composites. The boron carbide content of material produced for the NUHOMS®-24PTH DSC will not exceed the volume percent subjected to qualification testing for that material, unless it is subjected to additional testing as described in the following sections.

The production of MMC plates for use in the NUHOMS®-24PTH DSC is consistent with the process used to produce the qualification test material. Processing changes may be incorporated into the production process, only if they are reviewed and approved by the holder of an NRC-approved QA plan who is supervising fabrication, in accordance with the following criteria:

Major processing changes, such as billet formation by processes other than hot vacuum pressing or CIP/vacuum sintering, or direct rolling of the billet (elimination of extrusion) shall be subject to a complete program of qualification testing including the four areas of radiation exposure, thermal exposure, hydrogen generation / corrosion, and B10 uniformity described above for the original Boralyn® and Metamic® qualification programs. Other examples of major changes which require qualification testing are:

- *Increase of boron carbide volume % to greater than that in qualification testing; ductility decreases with increased boron carbide content, so additional testing will verify that ductility and strength requirements of the design are satisfied.*

- *Product density (% theoretical) reduced by more than 1% less than that in qualification testing; additional testing will verify that water absorption is within limits that are acceptable for draining and vacuum drying operations, and does not significantly affect the material durability or mechanical properties.*

- *Increase of particle size of B4C powder with respect to that used to produce the qualification test material. This could affect the uniformity of particle distribution, and the effectiveness of the boron's absorption of neutrons. Additional neutron transmission testing and statistical analysis will verify that the boron carbide distribution continue to meet the design requirements.*

The product and acceptance requirements shall in all cases remain within the limits specified below.

Minor processing changes that do not have an adverse effect on the particle bonding, microstructure or uniformity of the B_4C particle distribution may be accepted by engineering review without testing. Examples of such changes include reduction of B_4C content in the MMC, increased billet forming pressure, and changes in mechanical processing variables such as extrusion speed. Changes that have an uncertain or a small adverse effect on the microstructure shall be subjected to limited additional testing such as microscopic metallurgical examination in the as-built condition of the plates. Examples of such changes are increased billet forming temperature and small increases in the B_4C content (within the maximum limits listed above).

The basis for acceptance shall be that the changes do not have an adverse effect on either the durability or neutron absorption effectiveness of the material. These characteristics are determined by the bonding and uniformity of the B_4C particle distribution. The evaluation may consist of an engineering review, or it may consist of additional testing.

Bounding specification for MMCs

1. *The metal matrix composite shall consist of boron carbide powder in an aluminum alloy matrix.*

2. *The boron carbide content shall be limited to a maximum 40% by volume.*

3. *No more than 10 wt % of the boron carbide powder shall be larger than 60 microns.*

4. *The product shall be at least 98% of theoretical density.*

5. *The composite final product form shall have the tensile properties:*

Minimum yield strength, 0.2% offset:	*1.5 ksi*
Minimum ultimate strength:	*5.0 ksi*
Minimum elongation in 2 inches:	*1%*

6. *The composite final product form shall have the minimum thermal conductivity specified in Section P.4.3.*

7. *The product shall have the minimum ^{10}B areal density specified in Section P.2, Table P.2-20. Production acceptance testing for ^{10}B areal density shall be performed by comparing the attenuation of a neutron beam through the product with the neutron attenuation through standards having known ^{10}B content. Acceptance testing by any other means may be used only if benchmarked against neutron transmission testing.*

MMC Test Coupon and Lot Definitions

Coupon removal for MMC's is the same as for borated aluminum. A lot shall be defined as all plates made from a single billet, or from a group of billets, all processed from the same batch of blended powder, and compacted into billets during a single production campaign.

MMC Acceptance Testing, Neutronic

The acceptance criteria for neutron transmission testing of MMC plates and the alternate acceptance criteria in the event that a MMC coupon fails an acceptance criteria are the same as those discussed in Section P.9.1.7.2.1.

Justification for Acceptance Test Requirements, MMCs

The justification for the test requirements and 90% B10 credit for MMCs is the same as those for borated aluminum discussed in Section P.9.1.7.2.1, except that the boron carbide particles in a MMC are typically in the range of 1-25 microns.

P.9.1.7.2.3 Boral®, 75 % B10 Credit

Material Description, Boral®

Boral® consists of a core of mechanically bonded aluminum and boron carbide powders sandwiched between two outer layers of aluminum 1100, which is mechanically bonded to the core. The boron carbide particles average approximately 85 microns in diameter. The sheet is formed by filling an aluminum 1100 box with the boron carbide/aluminum powder mixture, and then hot-rolling the box. The walls of the box form the cladding, while the powder mixture forms the core of the Boral®. Additional information on the fabrication, specification, and performance of Boral® may be found in References [9.9] and [9.10].

Acceptance Testing, Neutronic

Boral® will be procured using AAR Advance Structures' standard specification for guidance [9.9]. In accordance with Section 7.3 of that specification, B10 areal density will be verified by chemical analysis or by neutron attenuation testing, using a sampling plan that will verify that the coupon meets the specified minimum values of Table P.9-1 with 95% probability at the 95% confidence level. Both neutron absorption and chemical samples are taken from roughly one square centimeter sample through the thickness of the plate.

Table P.9-1
B10 Specification for the NUHOMS®-24PTH Poison Plates

Poison Type	24PTH Basket Type	Minimum Poison Loading (B10 mg/cm^2)	% Credit Used in Criticality Analysis
Borated Aluminum Alloy/MMC	1A or 2A	7	90
	1B or 2B	15	
	1C or 2C	32	
Boral®	1A or 2A	9	75
	1B or 2B	19	
	1C or 2C	40	

Table P.9-2
Specified Boron Content Borated Aluminum (90% B10 Credit)

Basket	*Reference*	*Reference*	*Used in Section P.6, Criticality Analysis*	*Specified Minimum*
Type	*Natural Boron Content (wt. % Boron)*	*Enriched Boron Content (wt. % Boron)*	*B10 Content (g/cm^2)*	*B10 Content (g/cm^2)*
A	*0.7*	*0.9*	*0.0063*	*0.007*
B	*1.5*	*2.0*	*0.0135*	*0.015*
C	*3.0*	*4.2*	*0.0288*	*0.032*

Table P.9-3
Specified B4C Content for Metal Matrix Composites (90% B10 Credit)

Basket	*Reference*	*Used in Section P.6, Criticality Analysis*	*Specified Minimum*
Type	*Boron Carbide Content (Volume %)*	*B10 Content (g/cm^2)*	*B10 Content (g/cm^2)*
A	*6.4*	*0.0063*	*0.007*
B	*14*	*0.0135*	*0.015*
C	*29*	*0.0288*	*0.032*

P.10.2 Off-Site Dose Calculations

Calculated dose rates in the immediate vicinity of the NUHOMS®-24PTH System are presented in Section P.5, which provides a detailed description of source term configuration, analysis models and bounding dose rates. *The bounding dose rates include the contributions from the design basis fuel plus design basis CCs.* Off-site dose rates and doses are presented in this section. This evaluation determines the neutron and gamma-ray off-site dose rates including skyshine in the vicinity of the two generic ISFSI layouts containing design-basis fuel in the NUHOMS®-24PTH DSCs.

The first generic ISFSI evaluated is a 2x10 back-to-back array of HSM-Hs loaded with design-basis fuel, including *design-basis* CCs, in NUHOMS®-24PTH-L DSCs (Configuration 2 from Section P.2). The second generic layout evaluated is two 1x10 front-to-front arrays of HSM-Hs loaded with design-basis fuel, including *design-basis* CCs, in NUHOMS®-24PTH-L DSCs (Configuration 2 from Section P.2). This evaluation provides results for distances ranging from 6.1 to 600 meters from each face of the two arrays of HSMs. The 2x10 and two 1x10 analyses are also performed for the NUHOMS®-24PTH-S-LC DSCs within HSM-Model 102s filled with 24 design basis fuel *including design-basis CCs.*

The total annual exposure for each ISFSI layout as a function of distance from each face is given in Table P.10-2 and Table P.10-3 for the HSM-H and HSM-Model 102, respectively. These data are also plotted in Figure P.10-1 and Figure P.10-2 for the HSM-H and HSM-Model 102, respectively. The total annual exposure estimates assume 100% occupancy for 365 days.

The Monte Carlo computer code MCNP [10.1] calculates the dose rates at the specified locations around the arrays of HSMs. The results of this calculation provide an example of how to demonstrate compliance with the relevant radiological requirements of 10CFR20 [10.2], 10CFR72 [10.3], and 40CFR190 [10.4] for a specific site. Each site must perform specific site calculations to account for the actual layout of the HSMs and fuel source.

The assumptions used to generate the geometry of the ISFSIs for the MCNP analyses are summarized below.

- The 20 HSM-Hs in the 2x10 back-to-back array are modeled as a box enveloping the 2x10 array of HSM-Hs including the 3-foot shield walls on the two sides of the array. The 20 HSM-Model 102s in the 2x10 back-to-back array are modeled as a box enveloping the 2x10 array of HSM-Model 102s including the six inch gaps between modules and the 2-foot shield walls on the two sides of the array. MCNP starts the source particles on the surfaces of the box.
- The 20 HSM-Hs in the two 1x10 front-to-front arrays are modeled as two boxes which envelope each 1x10 array of HSM-Hs including the 3-foot shield walls on the two sides and back of each array. The 20 HSM-Model 102s in the two 1x10 front-to-front arrays are modeled as two boxes which envelope each 1x10 array of HSM-Model 102s including the six inch gaps between modules and the 2-foot shield walls on the two sides and back of each array. MCNP starts the source particles on the surfaces of one of the boxes.

The following assumptions are applicable to both the HSM-H and HSM-Model 102 analyses.

Table P.10-2
Total Annual Exposure, 24PTH-L Within HSM-H

Two 1x10 Front To Front Array

Distance (meters)	Back Total Dose (mrem)	1σ Uncertainty (mrem)	1σ Relative Uncertainty
6.1	*3069*	*7*	*0.002*
10	*2313*	*6*	*0.003*
20	*1392*	*7*	*0.005*
30	*951*	*4*	*0.005*
40	*706*	*9*	*0.013*
50	*540*	*3*	*0.006*
60	*428*	*3*	*0.007*
70	*347*	*3*	*0.010*
80	*289*	*5*	*0.017*
90	*244*	*6*	*0.026*
100	*202*	*3*	*0.012*
200	*48*	*1*	*0.020*
300	*15*	*0.5*	*0.030*
400	*5*	*0.1*	*0.028*
500	*2*	*0.06*	*0.029*
600	*0.9*	*0.05*	*0.054*

Distance (meters)	Side Total Dose (mrem)	1σ Uncertainty (mrem)	1σ Relative Uncertainty
6.1	*25063*	*40*	*0.002*
10	*12448*	*25*	*0.002*
20	*3851*	*15*	*0.004*
30	*1853*	*11*	*0.006*
40	*1112*	*6*	*0.006*
50	*752*	*6*	*0.007*
60	*549*	*6*	*0.010*
70	*407*	*3*	*0.008*
80	*325*	*3*	*0.010*
90	*260*	*3*	*0.012*
100	*209*	*2*	*0.011*
200	*45*	*1*	*0.026*
300	*13*	*0*	*0.020*
400	*4*	*0.2*	*0.040*
500	*2*	*0.05*	*0.032*
600	*0.7*	*0.02*	*0.030*

2x10 Back To Back Array

Distance (meters)	Front Total Dose (mrem)	1σ Uncertainty (mrem)	1σ Relative Uncertainty
6.1	*75419*	*60*	*0.001*
10	*45247*	*45*	*0.001*
20	*16995*	*20*	*0.001*
30	*8413*	*20*	*0.002*
40	*4861*	*14*	*0.003*
50	*3103*	*8*	*0.003*
60	*2135*	*8*	*0.004*
70	*1522*	*4*	*0.003*
80	*1145*	*8*	*0.007*
90	*884*	*6*	*0.007*
100	*687*	*3*	*0.004*
200	*114*	*1*	*0.008*
300	*33*	*1*	*0.016*
400	*11*	*0.2*	*0.018*
500	*5*	*0.5*	*0.100*
600	*2*	*0.04*	*0.024*

Distance (meters)	Side Total Dose (mrem)	1σ Uncertainty (mrem)	1σ Relative Uncertainty
6.1	*3744*	*9*	*0.002*
10	*2483*	*10*	*0.004*
20	*1294*	*5*	*0.004*
30	*865*	*5*	*0.006*
40	*636*	*4*	*0.007*
50	*483*	*6*	*0.011*
60	*379*	*4*	*0.010*
70	*306*	*3*	*0.008*
80	*251*	*2*	*0.009*
90	*208*	*2*	*0.008*
100	*174*	*1*	*0.009*
200	*40*	*1*	*0.014*
300	*12*	*0.3*	*0.026*
400	*4*	*0.1*	*0.030*
500	*2*	*0.05*	*0.031*
600	*0.6*	*0.02*	*0.036*

Table P.10-6
Summary of ISFSI Surface Activities, 24PTH-L DSC Within HSM-H

2x10 Back-To-Back Array

Source	Area (cm^2)	*Neutron Activity (neutrons/sec)*	*Gamma-Ray Activity (γ/sec)*
Roof	3,942,392.1	6.044E+07	*3.473E+10*
Front 1	1,764,538.4	6.418E+06	*2.462E+10*
Front 2	1,764,538.4	6.418E+06	*2.462E+10*
Side 1	710,398.6	1.075E+06	3.107E+08
Side 2	710,398.6	1.075E+06	3.107E+08
Total	8,892,266.1	7.542E+07	*8.460E+10*

Two 1x10 Front-To-Front Arrays

Source	Area (cm^2)	*Neutron Activity (neutrons/sec)*	*Gamma-Ray Activity (γ/sec)*
Roof	2,257,337.4	3.461E+07	*1.989E+10*
Front	1,764,538.4	6.418E+06	*2.462E+10*
Back	1,764,538.4	4.817E+05	4.305E+08
Side 1	406,760.5	6.156E+05	1.779E+08
Side 2	406,760.5	6.156E+05	1.779E+08
Total	6,599,935.2	4.274E+07	*4.530E+10*

Table P.10-7
Summary of ISFSI Surface Activities, 24PTH-S-LC DSC Within HSM-Model 102

2x10 Back-To-Back Array

Source	Area (cm^2)	*Neutron Activity (neutrons/sec)*	*Gamma-Ray Activity (γ/sec)*
Roof	3,730,366.7	1.977E+07	7.648E+10
Front 1	1,472,513.2	4.341E+07	2.911E+10
Front 2	1,472,513.2	4.341E+07	2.911E+10
Side 1	529,547.3	1.579E+06	7.277E+09
Side 2	529,547.3	1.579E+06	7.277E+09
Total	7,734,487.8	1.098E+08	1.492E+11

Two 1x10 Front-To-Front Arrays

Source	Area (cm^2)	*Neutron Activity (neutrons/sec)*	*Gamma-Ray Activity (γ/sec)*
Roof	2,061,518.5	1.093E+07	4.227E+10
Front	1,472,513.2	4.341E+07	2.911E+10
Back	1,472,513.2	4.390E+05	4.979E+08
Side 1	292,644.6	8.725E+05	4.021E+09
Side 2	292,644.6	8.725E+05	4.021E+09
Total	5,591,834.0	5.652E+07	7.991E+10

Table P.10-8
MCNP Front Detector Dose Rates for 2x10 Array, 24PTH-L DSC Within HSM-H

Distance (meters)	Gamma Dose Rate (mrem/hr)	Gamma MCNP 1σ Uncertainty	Neutron Dose Rate (mrem/hr)	Neutron MCNP 1σ Uncertainty	Total Dose Rate (mrem/hr)	Combined MCNP 1σ Uncertainty
6.1	*8.56E+00*	*8.00E-04*	5.21E-02	5.50E-03	*8.61E+00*	*0.0008*
10	*5.13E+00*	*1.00E-03*	3.41E-02	7.60E-03	*5.17E+00*	*0.0010*
20	*1.92E+00*	*1.20E-03*	1.56E-02	1.20E-02	*1.94E+00*	*0.0012*
30	*9.51E-01*	*2.40E-03*	9.06E-03	1.71E-02	*9.60E-01*	*0.0024*
40	*5.49E-01*	*2.90E-03*	5.81E-03	1.55E-02	*5.55E-01*	*0.0029*
50	*3.50E-01*	*2.60E-03*	4.30E-03	3.65E-02	*3.54E-01*	*0.0026*
60	*2.41E-01*	*4.00E-03*	2.94E-03	2.05E-02	*2.44E-01*	*0.0040*
70	*1.72E-01*	*2.90E-03*	2.15E-03	2.02E-02	*1.74E-01*	*0.0029*
80	*1.29E-01*	*7.30E-03*	1.68E-03	3.24E-02	*1.31E-01*	*0.0072*
90	*9.96E-02*	*6.60E-03*	1.31E-03	2.89E-02	*1.01E-01*	*0.0065*
100	*7.74E-02*	*4.00E-03*	1.07E-03	2.84E-02	*7.85E-02*	*0.0040*
200	*1.28E-02*	*7.70E-03*	2.26E-04	5.32E-02	*1.31E-02*	*0.0076*
300	*3.65E-03*	*1.60E-02*	7.00E-05	4.45E-02	*3.72E-03*	*0.0157*
400	*1.25E-03*	*1.87E-02*	2.68E-05	5.66E-02	*1.28E-03*	*0.0183*
500	*5.23E-04*	*1.02E-01*	1.24E-05	5.68E-02	*5.35E-04*	*0.0996*
600	*1.95E-04*	*2.49E-02*	6.41E-06	1.18E-01	*2.01E-04*	*0.0244*

Table P.10-9
MCNP Back Detector Dose Rates for the Two 1x10 Arrays, 24PTH-L DSC Within HSM-H

Distance (meters)	Gamma Dose Rate (mrem/hr)	Gamma MCNP 1σ Uncertainty	Neutron Dose Rate (mrem/hr)	Neutron MCNP 1σ Uncertainty	Total Dose Rate (mrem/hr)	Combined MCNP 1σ Uncertainty
6.1	*3.33E-01*	*0.0024*	1.74E-02	0.0104	*3.50E-01*	*0.0023*
10	*2.50E-01*	*0.0028*	1.39E-02	0.0121	*2.64E-01*	*0.0027*
20	*1.50E-01*	*0.0049*	8.68E-03	0.0152	*1.59E-01*	*0.0047*
30	*1.03E-01*	*0.0047*	5.86E-03	0.0213	*1.09E-01*	*0.0046*
40	*7.66E-02*	*0.0140*	4.04E-03	0.0179	*8.06E-02*	*0.0133*
50	*5.85E-02*	*0.0061*	3.16E-03	0.0237	*6.16E-02*	*0.0059*
60	*4.65E-02*	*0.0074*	2.34E-03	0.0255	*4.88E-02*	*0.0071*
70	*3.78E-02*	*0.0103*	1.76E-03	0.0244	*3.96E-02*	*0.0099*
80	*3.15E-02*	*0.0173*	1.46E-03	0.0332	*3.30E-02*	*0.0166*
90	*2.67E-02*	*0.0268*	1.17E-03	0.0280	*2.79E-02*	*0.0257*
100	*2.21E-02*	*0.0129*	9.07E-04	0.0275	*2.30E-02*	*0.0124*
200	*5.21E-03*	*0.0193*	2.53E-04	0.1507	*5.46E-03*	*0.0197*
300	*1.66E-03*	*0.0311*	8.16E-05	0.0697	*1.74E-03*	*0.0298*
400	*5.53E-04*	*0.0297*	3.10E-05	0.0734	*5.84E-04*	*0.0284*
500	*2.06E-04*	*0.0304*	1.32E-05	0.0865	*2.19E-04*	*0.0291*
600	*9.04E-05*	*0.0562*	7.29E-06	0.2079	*9.77E-05*	*0.0542*

Table P.10-10
MCNP Side Detector Dose Rates, 24PTH-L DSC Within HSM-H

2x10 Back-to-Back Array

Distance (meters)	Gamma Dose Rate (mrem/hr)	Gamma MCNP 1σ Uncertainty	Neutron Dose Rate (mrem/hr)	Neutron MCNP 1σ Uncertainty	Total Dose Rate (mrem/hr)	Combined MCNP 1σ Uncertainty
6.1	*4.03E-01*	*2.50E-03*	2.46E-02	9.80E-03	*4.27E-01*	*0.0024*
10	*2.67E-01*	*4.30E-03*	1.65E-02	1.17E-02	*2.83E-01*	*0.0041*
20	*1.39E-01*	*3.80E-03*	8.46E-03	2.26E-02	*1.48E-01*	*0.0038*
30	*9.35E-02*	*6.40E-03*	5.33E-03	2.60E-02	*9.88E-02*	*0.0062*
40	*6.89E-02*	*7.20E-03*	3.72E-03	2.60E-02	*7.26E-02*	*0.0070*
50	*5.25E-02*	*1.19E-02*	2.61E-03	2.43E-02	*5.51E-02*	*0.0114*
60	*4.11E-02*	*9.70E-03*	2.18E-03	8.36E-02	*4.33E-02*	*0.0101*
70	*3.34E-02*	*8.70E-03*	1.58E-03	3.02E-02	*3.49E-02*	*0.0084*
80	*2.74E-02*	*9.80E-03*	1.23E-03	2.71E-02	*2.86E-02*	*0.0095*
90	*2.28E-02*	*8.30E-03*	9.96E-04	3.06E-02	*2.38E-02*	*0.0081*
100	*1.91E-02*	*8.80E-03*	8.04E-04	3.96E-02	*1.99E-02*	*0.0086*
200	*4.34E-03*	*1.47E-02*	1.79E-04	5.12E-02	*4.52E-03*	*0.0143*
300	*1.36E-03*	*2.68E-02*	5.34E-05	2.44E-02	*1.42E-03*	*0.0258*
400	*4.60E-04*	*3.17E-02*	2.28E-05	3.64E-02	*4.82E-04*	*0.0303*
500	*1.65E-04*	*3.26E-02*	1.05E-05	6.80E-02	*1.75E-04*	*0.0309*
600	*6.39E-05*	*3.85E-02*	4.83E-06	7.33E-02	*6.87E-05*	*0.0362*

Two 1x10 Front-To-Front Arrays

Distance (meters)	Gamma Dose Rate (mrem/hr)	Gamma MCNP 1σ Uncertainty	Neutron Dose Rate (mrem/hr)	Neutron MCNP 1σ Uncertainty	Total Dose Rate (mrem/hr)	Combined MCNP 1σ Uncertainty
6.1	*2.83E+00*	*1.60E-03*	2.99E-02	1.43E-02	*2.86E+00*	*0.0016*
10	*1.40E+00*	*2.00E-03*	1.97E-02	1.30E-02	*1.42E+00*	*0.0020*
20	*4.30E-01*	*4.00E-03*	9.86E-03	2.29E-02	*4.40E-01*	*0.0039*
30	*2.06E-01*	*6.00E-03*	5.91E-03	2.06E-02	*2.12E-01*	*0.0059*
40	*1.23E-01*	*5.70E-03*	4.37E-03	4.18E-02	*1.27E-01*	*0.0057*
50	*8.27E-02*	*7.50E-03*	3.09E-03	3.50E-02	*8.58E-02*	*0.0073*
60	*6.01E-02*	*1.03E-02*	2.56E-03	7.40E-02	*6.27E-02*	*0.0103*
70	*4.47E-02*	*8.50E-03*	1.79E-03	3.69E-02	*4.64E-02*	*0.0083*
80	*3.58E-02*	*1.07E-02*	1.36E-03	3.96E-02	*3.71E-02*	*0.0104*
90	*2.85E-02*	*1.26E-02*	1.15E-03	4.37E-02	*2.97E-02*	*0.0122*
100	*2.31E-02*	*1.15E-02*	8.60E-04	2.54E-02	*2.39E-02*	*0.0111*
200	*4.96E-03*	*2.69E-02*	2.07E-04	6.44E-02	*5.16E-03*	*0.0260*
300	*1.38E-03*	*2.10E-02*	7.16E-05	6.72E-02	*1.45E-03*	*0.0202*
400	*4.83E-04*	*4.23E-02*	2.73E-05	5.16E-02	*5.10E-04*	*0.0401*
500	*1.72E-04*	*3.40E-02*	9.99E-06	3.25E-02	*1.82E-04*	*0.0322*
600	*6.92E-05*	*3.23E-02*	5.63E-06	7.12E-02	*7.48E-05*	*0.0303*

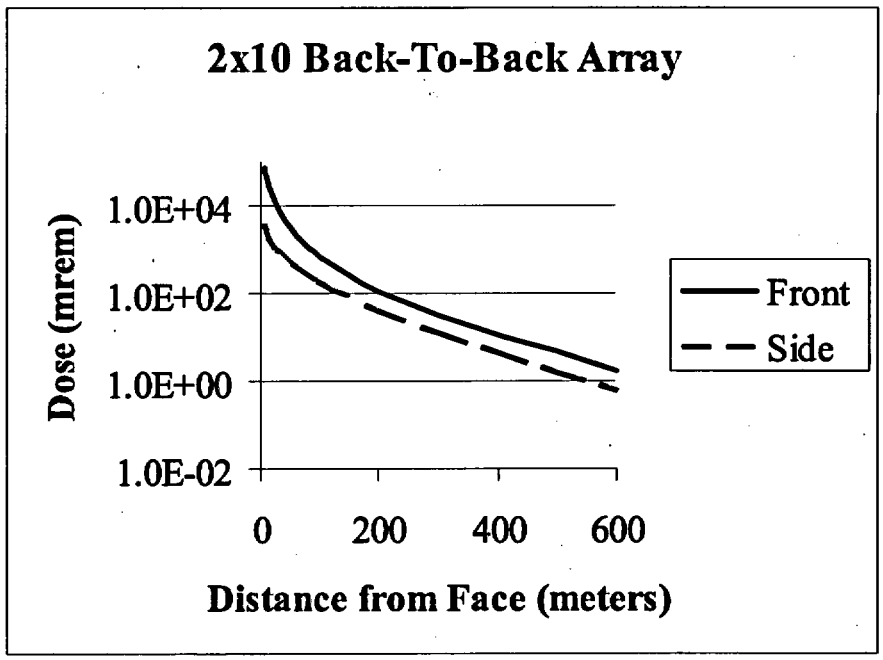

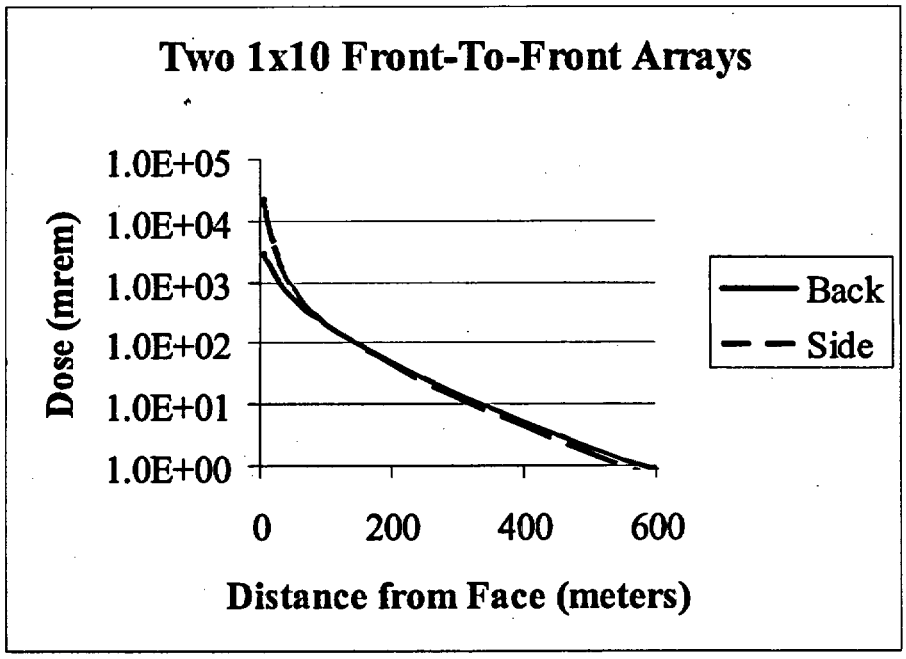

Figure P.10-1
Annual Exposure from the ISFSI as a Function of Distance, 24PTH-L DSC Within HSM-H

TRANSNUCLEAR, INC.
DOCKET NO. 72-1004
TAC NO. L23653

REQUEST FOR ADDITIONAL INFORMATION

DATED May 3, 2004

Chapter P.1 General Discussion

Question 1-1

Revise the statement on Page P.1-7, Section P.1.2.1.3, second sentence stating, "This external air circulation feature...and basket type used in the DSC is 1 A, 1 B, or 1C..." It seems that the external air circulation feature is needed if the basket type used is 2A, 2B, or 2C at maximum heat loads of 31.2 kW per DSC (See Tables on pages P.1-2 and P.3.1-2).

This information is required by the staff to assess compliance with 10 CFR 72.236(f).

Response to 1-1

SAR Section P.1.2.1.3, second paragraph has been revised to add the following sentence at the end of this paragraph: "or if the decay heat is greater than 24 kW (but not greater than 31.2 kW) and basket type used is 2A, 2B, or 2C, and specific time limits for transfer are not met".

Question 1-2

Provide the nominal thickness of major components on Drawing NUH 24PTH-1001 and NUH 24PTH-1002. The "Bill of Material" on these drawings shows only the material type/specification without relevant dimensions such as the thickness. The design details of these drawings show either a maximum or a minimum dimension. The nominal thickness of major components should be specified on the design drawing.

This information is required by the staff to assess compliance with 10 CFR 72.236(b).

Response to 1-2

Nominal thicknesses for the major components have been specified in the Parts List shown in SAR drawings NUH24PTH-1001-SAR and NUH24PTH-1002-SAR.

Question 1-3

Show that adequate radial gap has been provided between the basket assembly and the DSC cavity to accommodate differential thermal expansion and to minimize thermal stresses between components.

Drawing NUH24PTH-1002 shows the DSC outside diameter to be 67.19 inches. With 0.5 inch shell thickness, the DSC cavity inside diameter is 66.19 inches. Drawing NUH24PTH-1003 shows that the basket assembly outside diameter is 65.94 inches. This leaves a total radial gap of only 66.19-65.94 = 0.25 inch. Page P.3.4-8 states that, "In the 'radial' direction clearance is provided between the basket outer diameter and DSC cavity inside diameter, and between the poison/aluminum plates and interfacing basket components." Page P.3.4-9 states that the required radial direction clearance is 0.313 inch to insure no interferences with the R90 transition rails and a cold gap of 0.4 inch is provided. Resolve the differences between the required radial gap and the actual gap provided.

This information is required by the staff to assess compliance with 10 CFR 72.236(b).

Response to 1-3

The "radial" expansion of 0.313" calculated on page P.3.4-9 is the differential thermal expansion of the aluminum heat transfer plates at the center of the basket (item 9 on Sheet 4 of Drawing NUH24PTH-1003-SAR) which are the longest aluminum plates and therefore, the controlling component for thermal expansion. The clearance of 0.40" is the clearance provided between these plates and the inside surface of the R90 transition rails (item 2 in NUH24PTH-1003-SAR), which is obtained by subtracting the length of item 9 (60.50") from the distance between R90 rails (2 x 30.45" per View A-A of NUH24PTH-1004-SAR), i.e., 60.90-60.50=0.40". This is shown in the following figure.

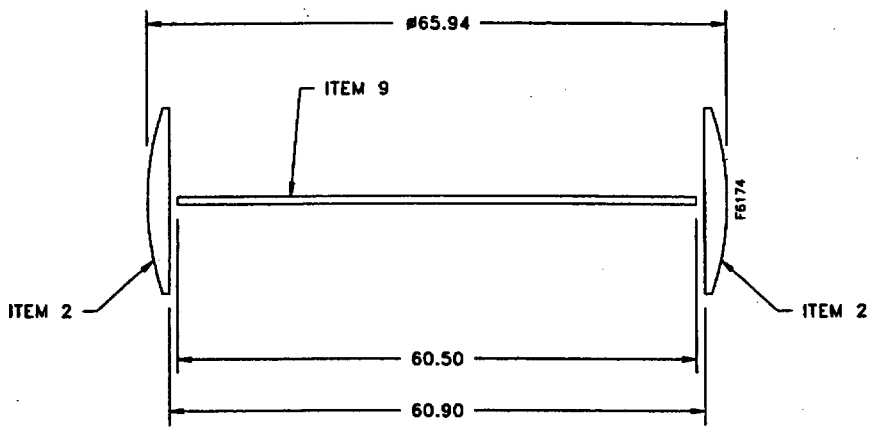

The above sketch has been added to SAR Section P.3.4.4.2 to clarify the SAR text.

As noted on Section P.3.4.4.2 (page 3.4-8), radial expansion of the basket assembly (i.e. stainless steel fuel compartment tubes welded to the insert plates) and potential interference with the DSC shell was evaluated as part of the LS-DYNA thermal stress analyses. An additional hand calculation has been added to SAR Section P.3.4.4.2 (page 3.4-9) to show that adequate gap has been provided between the basket assembly and the DSC shell cavity.

Question 1-4

Show the attachment of the Alternative Door (Drawing NUH-03-7001, Sh. 9) to the HSM-H Module main assembly.

This information is required by the staff to assess compliance with 10 CFR 72.236(b).

Response to 1-4

Drawing NUH-03-7001-SAR, has been revised to show the attachment of the Alternate Door to the HSM-H. The alternate door is attached to the front wall of the HSM-H by four L-shaped clamps located at the 45° line in each quadrant of the door, as shown in sheets 5 and 9 of revised drawing NUH-03-7001-SAR. The clamps are anchored to the concrete wall using four ¾" diameter bolts that are bolted into four 8-inch deep embedded anchors.

SAR Section P.3.1.1.2 has been revised to provide additional description of the alternate door. SAR Section P.3.7.11.6.5 has been revised to provide additional details on the HSM-H door attachment evaluations.

Question 1-5

Provide the justification for adding Note 2 to Drawing No. NUH-03-8000 per proposed Amendment No. 8. The note states, "Neutron shield relief valve set pressure of 20 psig minimum (40 psig when used with 24PTH DSC)."

This information is required by the staff to assess compliance with 10 CFR 72.11.

Response to 1-5

The 20 psig relief valve set pressure is an operational requirement in the NUHOMS® standard operating procedures. It was incorporated in the FSAR drawing as a result of previous NRC questions (previous amendment applications) regarding this relief valve set pressure. For the 24PTH the increased relief valve set pressure of 40 psig is due to the higher neutron shield temperatures/pressure requirements resulting from the higher heat load (40.8 kW vs. 24 kW). Since the neutron shield has been evaluated and shown to be acceptable for a maximum pressure of 50 psig, and for ease of operations, Note 2 of drawing NUH-03-8000-SAR has been revised to require the same set pressure for all DSCs (heat loads), as follows: "Neutron shield relief valve set pressure of 40 psig min. and 45 psig max."

Chapter P.2 Principal Design Criteria

Question 2-1

Correct the typographical error on page P.2-17 Section 2.5.1, that states, "The principal design criteria for the NUHOMS®-24PTH DSC are presented in Table P.2-17." It is noted that Table P.2-17 should have been Table P.2-18.

Response to 2-1

Typographical error corrected in SAR Section P.2.5.1. For clarification, a new paragraph has been added to SAR Section P.2.5.2 to refer to Table P.2-18 for the HSM-H principal design criteria.

Question 2-2

Revise Table P.2-18 to incorporate the different configurations of the NUHOMS®-24PTH DSC System with the maximum allowable heat load generation rate per DSC. If this is not desirable, provide a separate summary table for the different configuration of the NUHOMS®-24PTH System. The maximum heat load of the stored fuel per DSC should be included in the table for design criteria or provided in a separate summary table.

This information is required by the staff to assess compliance with 10 CFR 72.236(b) and 72.236(f).

Response to 2-2

A new table, Table P.2-21, has been added to incorporate the different configurations of the 24PTH DSC with the maximum allowable heat load per DSC.

Chapter P.3 Structural Evaluation

Question 3-1

Provide justification for the alternative to the ASME Code in Table P.3.1-2, Section NG-3352. The fusion (spot) or plug type welds between the stainless steel fuel insert plates (straps) and the stainless steel fuel compartments are qualified based on testing. To meet the 36 kips capacity requirements, the capacity of the welded connection is determined from the individual specimen test result times the number of welds on each side of the tube. The size of the fusion (spot) or plug welds and the total number of welds per each side of the tube are not shown. Furthermore, it is not clear that shearing force will be evenly shared by all spot welds. If the shearing force is not evenly shared, some spot welds may fail first and create a domino effect leading to failure of all spot welds and the welded connection.

This information is required by the staff to assess compliance with 10 CFR 72.236.

Response to 3-1

The 24PTH basket is classified as an ASME Code Subsection NG component. Due to accessibility restrictions for welding the stainless steel fuel compartment tubes to the connecting stainless steel insert plates the use of fusion type welds was selected.

Table NG-3352-1 of Subsection NG does not contain design provisions for fusion welds. As such, the use of fusion welds for the 24PTH basket is an ASME Code Alternative. Therefore, TN requires the use of pre-production qualification testing combined with production testing to demonstrate structural acceptance of these welds.

The selection of the 36 kips acceptance load criterion is based on a factored design loading. The required minimum tested capacity of the welded connection is specified at 36 kips (at room temperature). This value is based on the maximum load of 18.8 kips for the welded connection obtained from the 75g drop accident case from the finite element model of the 24PTH basket assembly, which explicitly models the welds. The 18.8 kips is obtained by summation of the tension (compression forces on the weld are conservatively ignored) and shear forces on each beam element representing each weld at the connection and combining the resulting forces in each direction by SRSS, See Section P.3.6.1.3.2 (E). The 18.8 kips is the maximum value obtained over all the welds in the finite element model for all drop orientations considered. In addition, the 18.8 kips is adjusted for test versus analysis temperature effects (conservatively using allowable at 800°F) as follows:

$$18.8\left(\frac{S_{u\,at70^\circ F}}{S_{u\,at800^\circ F}}\right)=18.8\left(\frac{75\ ksi}{62.8\ ksi}\right)=22.5\ kips$$

A test to design margin of safety of 1.6 is applied to the factored load; 22.5 x1.6=36 kips. The 1.6 factor is based on guidance from ASME Appendix F for component supports qualified by testing. The resulting test load will be further reduced by the ratio of Code minimum versus actual tensile properties of the tested material to account for actual strength of the material.

The welding process, the size of each individual fusion weld, and the number of welds in the connection is not specified in the drawing to allow flexibility to the fabricator to best meet the 36 kips load design requirement. To address any concerns about shearing forces not evenly shared, it is planned that the test will be done on the pattern of a typical insert plate-to-tube connection, not the individual weld deposit, and will be tested to failure. The fabricator must then demonstrate, through testing, that the selected weld pattern configuration meets the design requirement. In this manner concerns about uneven "sharing" of the load between individual weld deposits with potential for a domino failure of the welds are eliminated.

SAR Table P.3.1-2 has been modified to indicate that the capacity of the welded connection is determined from the test of the weld pattern of a typical insert plate-to-the tube connection, not the individual weld deposit.

Question 3-2

Provide the basis to conclude that the maximum weld loads on the welds connecting the steel insert straps and the fuel tubes listed in Table P.3.6-8 are reasonably accurate and conservative.

The application states that, "Loads on the welds connecting the steel insert straps and the fuel compartment tubes are evaluated using the beam element forces obtained from the LS-DYNA analysis." However, the weld loads as shown in Table P.3.6-8 are small when compared to the maximum stresses in the steel straps shown in Table P.3.6-7. Please provide an explanation. Clarify if steel straps and the welds are both included in the LS-DYNA analysis or if only the welds are included.

This information is required by the staff to assess compliance with 10 CFR 72.236.

Response to 3-2

The normal/off-normal condition maximum loads on the welds connecting the stainless steel insert (strap) plates to the fuel compartment tubes as listed in Table P.3.6-8 result from the finite element analysis of the basket model in which the steel basket insert plates (straps) and the insert plates (straps)-to-tube welds are explicitly modeled in the LS-DYNA stress analysis model. SAR Figure P.3.6-8 (bottom figure) has been revised to clearly show the basket insert plates (straps) and the welds (beam elements) in the LS-DYNA model (the fuel compartment tubes and some transition rails are excluded from this view for clarity). This figure is reproduced below. As shown, on each side of a fuel compartment tube, two beam elements are used to model the welds between the fuel compartment tube and the basket strap(s).

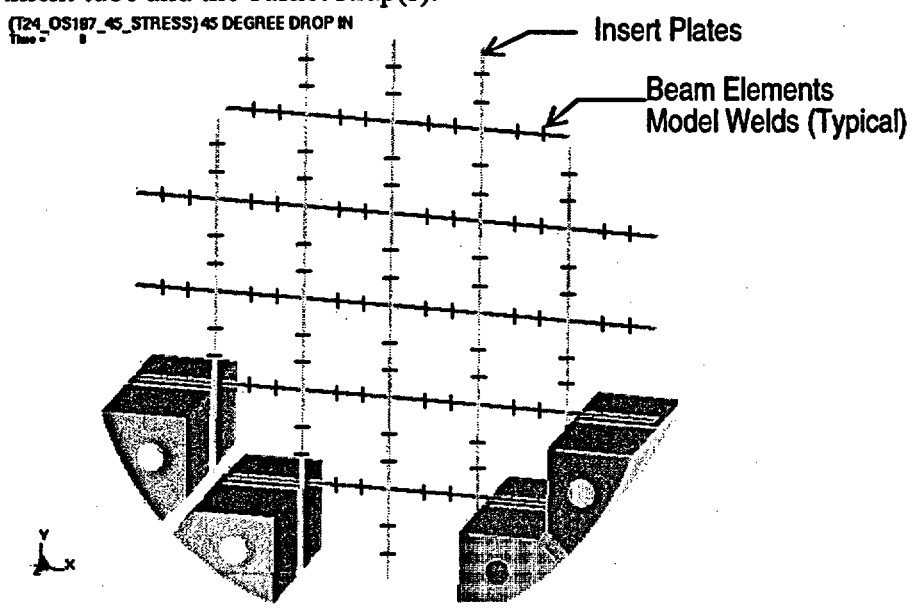

–Tubes not shown for clarity.–

Separate analyses are performed for deadweight (with the 24PTH DSC in the TC and in the HSM configurations) and for thermal conditions. The thermal stress analysis model uses the bounding temperature profile shown in SAR Figure P.3.4-2. Handling loads are conservatively estimated as twice the loads due to deadweight.

In the basket stress model, the only connections between the straps and the fuel compartment tubes are through the beam elements representing the welds. Thus, all loads which tend to cause "separation" of the tube and basket straps are directly carried by the beam elements representing the welds. This modeling approach ensures that the welds carry all possible loads. Only tension forces on the beam elements are considered in the calculation of the maximum weld load (compression forces are conservatively ignored). However, the compression forces are accounted in the calculation of the insert plate stresses. In the LS-DYNA model, contact surfaces are defined between the tube(s) and the steel strap(s) to represent the contact/bearing between these surfaces and to properly transfer the loads through adjacent basket components.

As discussed in response to question 3-1, the design of the welded connection is based on the maximum resultant weld force calculated from the beam(s) axial and shear forces obtained in each of the three orthogonal directions (for all the beam elements in the model used to represent the welds), and combined as described in Section P.3.6.1.3.2 (E). The resulting weld loads are summarized in Table P.3.6-8.

The stresses reported in Table 3.6-7 for the insert (strap) plates include the combination of primary plus secondary stresses obtained from separate analyses. This combination is conservatively done by absolute summation of the maximum primary stress with the maximum secondary (i.e. thermal) stress, regardless of location (i.e., the maximum thermal and deadweight stresses may not be at the same location or for the same insert plate).

Therefore, the normal/off-normal condition weld loads reported in Table P.3.6-8 and basket steel insert plate (strap) stresses reported in Table P.3.6-7 are reasonably accurate and conservative.

SAR Section P.3.6.1.3.1 has been revised to describe the welds and inset plates in the LS-DYNA finite element model.

Question 3-3

Describe the method to identify whether the OS197FC TC design is based on the OS197H design or the OS197 design. It was stated in Section P.3.4.3 Lifting Devices that, "The maximum critical lift weight with a NUHOMS®-24PTH DSC is approximately 215,000 lbs. Therefore, an OS197FC TC that is based on the OS197H design is acceptable with any NUHOMS®-24 DSC. An OS197FC TC that is based on the OS197 design is limited to a total critical lift weight of 208,500 lbs." It is not clear how to identify which design the OS197FC TC is based on.

This information is required by the staff to assess compliance with 10 CFR 72.236(b).

Response to 3-3

To clearly identify the OS197FC configurations, Section P.1, last sentence of 4th bullet has been modified as follows: "The OS197 TC with a modified top lid is designated as the OS197FC TC. The OS197H TC with a modified top lid is designated as the OS197HFC TC." Note that this designation is also shown in SAR drawing NUH-03-8000-SAR.

SAR Sections P.3.6.1.5, P.3.7.4.4, and P.3.7.11.3 have been revised to clarify the wet and dry payloads allowed in these TCs, as described in FSAR Revision 8.

Question 3-4

Provide an explanation for the discrepancy between Section P.3.7.4.2.1 DSC Shell Assembly Horizontal Drop Analysis and Section P.3.7.4.2.3 DSC Shell Assembly Stress Analysis. Section P.3.7.4.2.1 states that, "Elastic-Plastic analyses are performed and stresses are determined for each DSC shell assembly component." However, Section

P.3.7.4.2.3, states that, "Equivalent static linear elastic analysis is conservatively used for drop analyses." These two statements are not consistent.

This information is required by the staff to assess compliance with 10 CFR 72.236(b).

Response to 3-4

As described in Section P.3.7.4.2.1, elastic-plastic analyses are used for the horizontal accident drop evaluations of the 24PTH shell assemblies. For the vertical end drop evaluations, linear elastic analyses are used for the 24PTH-S and 24PTH-L shell assemblies and elastic-plastic analyses are used for the 24PTH-S-LC shell assembly.

The elastic-plastic analysis for the 24PTH-S-LC is performed in accordance with the provisions in NB-3225 for Level D loads. As shown in a new SAR Figure P.3.7-15, which is reproduced below, the results of the analysis indicate that plasticity is very localized and limited to a section of the outer bottom plate (a non-pressure boundary component) at a location of plate thickness transition. In this region, the plate is unsupported and during the drop the plate is loaded by the inertial weight of the encased lead. The figure below shows that the plastic strains in this region are small; similarly the calculated stresses are within Code allowables (maximum stress ratio is 0.86 (See Table P.3.7-2). The stress ratios for the pressure boundary components, DSC shell and inner top and bottom cover plates/forgings, are well within Code allowables, i.e., the maximum stress ratio for primary membrane stress is 0.35 and for primary membrane plus bending is 0.56 (See Table P.3.7-2). SAR Section P.3.7.4.2.3 has been revised to provide additional discussion of the 24PTH-S-LC end drop analysis results.

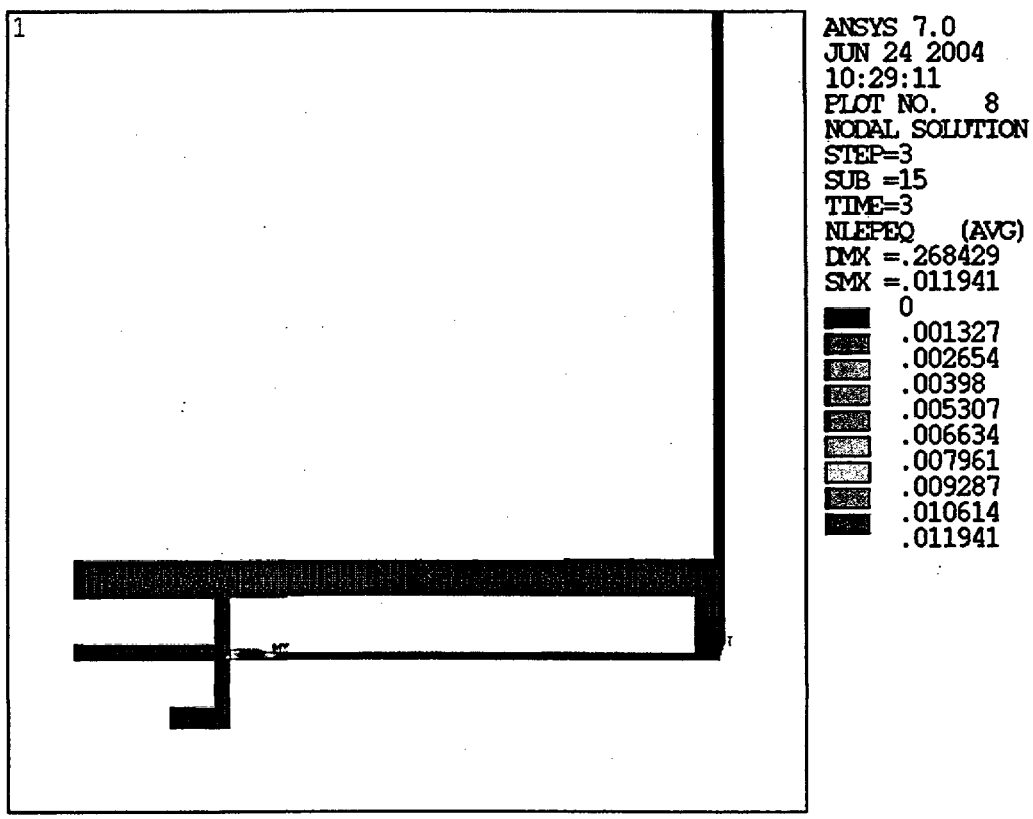

SAR Sections P.3.7.4.2.2 and P.3.7.4.2.3 have been revised to clarify the analytical approach used for the drop evaluations and to remove the noted discrepancy. A new sentence has been added in Section P.3.7.4.2.2 to indicate that the vertical end drop analyses for the 24PTH-S and 24PTH-L shell assemblies are based on equivalent static linear elastic analysis, while the vertical end drop analyses for the 24PTH-S-LC shell assembly is based on equivalent static elastic-plastic analysis. In SAR Section P.3.7.4.2.3, second paragraph, the words "linear elastic" have been deleted to remove the noted discrepancy with Section P.3.7.4.2.1. In addition, the stress-strain relationship for SA 240 Type 304 material used in the elastic-plastic analyses is now reflected in SAR Section P.3.3.1 with the addition of SAR Figure P.3.3-1.

Question 3-5

The application states that thermal effects on material stiffness (E) and yield stress (S_y) are included in the analysis (See page P.3.7-15). Provide a discussion on how temperature dependent material properties are applied to the finite element model and analysis.

This information is required by the staff to assess compliance with 10 CFR 72.236(b).

Response to 3-5

For the LS-DYNA stress analyses of the 24PTH basket assembly, temperature dependent material properties (e.g., modulus of elasticity, E, and yield stress, S_y) were applied using LS-DYNA Material Type 4 (*mat_elastic_plastic_thermal). This material type models bilinear elastic-plastic behavior and permits temperature dependent material coefficients to be defined. Properties at eight (8) temperatures were defined, from 0°F to 800°F for the stainless steel components (fuel compartment tubes, basket straps, etc) using values of E and S_y from the ASME Code as listed in Table P.3.3-1 (page P.3.3-3). For the R90 (aluminum) transition rails, properties were defined from 0°F to 600°F.

The temperature distribution shown in Figure P.3.4-2 (page P.3.4-14) was applied to the 24PTH DSC basket assembly. The material properties at the applied temperatures, from the defined material property tables, are assigned to the elements within LS-DYNA. This method of application of temperature dependent material coefficients is similar to the ANSYS type analysis.

A copy of pages from the LS-DYNA User's Manual for Material Type 4 is attached.

Chapter P.4 Thermal Evaluation

Question 4-1

Provide the basis for the use of Final Safety Analysis Report (FSAR) Section M.4.9 neutron shield effective thermal properties for transfer cask analyses at high heat loads. If necessary, update the transfer cask thermal analyses.

The FSAR Section M.4.9 effective thermal properties were computed for a heat load of 24 kW. The higher heat loads associated with this amendment may significantly affect the thermal properties.

This information is required by the staff to assess compliance with 10 CFR 72.236(f).

Response to 4-1

The effective thermal conductivity within the neutron shield of the OS197/OS197H TC were shown in FSAR Section M.4.9 to be directly proportional to the thermal conductivity (k) of water or air and exponentially proportional to the associated Rayleigh number (Ra) existing in the neutron shield cavity. This proportionality can be expressed as:

$$k_{effective} \propto k_{Air/Water} \times (Ra)^{0.333}$$

The Rayleigh number is computed from: $Ra_L = \frac{\rho^2 g_c \beta L^3 \Delta T}{\mu^2} \times Pr$, where

g_c = gravitational acceleration
ΔT = temperature difference
μ = dynamic viscosity
L = characteristic length
β = coefficient of thermal expansion
ρ = density of the fluid
Pr = Prandtl number

Although the FSAR Section M.4.9 effective thermal properties are computed for a heat load of 24 kW, the resulting values are conservative for a heat load of 40.8 kW. Examination of the thermophysical properties for water (see Table A-3 from *Principles of Heat Transfer, Frank Kreith, 3rd Edition,* SAR Reference 4.26) show that the thermal conductivity and the coefficient of thermal expansion increase with increasing temperature, while the density and viscosity decrease with increasing temperature. Therefore, the net effect of an increased heat load will be both a higher thermal conductivity and Rayleigh number (note the values in last column of Table A-3 from Reference 4.26). As such, the effective thermal conductivity computed for the 24 kW heat load will be conservatively less than the actual effective thermal conductivity existing at the 40.8 kW heat load.

For the case of an air filled neutron shield, examination of the thermophysical properties for air (see Table A-3 from Reference 4.26) show that the thermal conductivity and viscosity increase with increasing temperature, while the density and the coefficient of thermal expansion decrease with increasing temperature. The net effect of operation at a higher temperature level will be a higher thermal conductivity, but a lower Rayleigh number for a given ΔT (again, note the values in last column of Table A-3 from Reference 4.26). Since increasing the heat load within the transfer cask will tend to increase both the operating temperature and the ΔT required to remove the heat from the cask, use of the lower ΔT associated with the 24 kW heat load used to compute the FSAR Section M.4.9 effective thermal properties effectively under-estimates the Rayleigh

number for the 40.8 kW heat load by approximately the ratio of the heat loads, or 40.8/24 = 1.7.

The effect of operating at a higher temperature level can be estimated by the ratio of the quantity $\left(\frac{gB\rho^2}{\mu^2}\right)^{0.333}$. Per Table P.4-12 of the SAR, steady-state operations with an air filled neutron shield will result in a neutron shield temperature of approximately 400°F (i.e., the average of the structural shell and the outer skin of the TC [488°F +325°F]/2). Conservatively assume 500°F for the purposes of this response. From the last column of Table A-3 of Reference 4.26, $\left(\frac{gB\rho^2}{\mu^2}\right) = 0.258 \times 10^6$ at 400°F and 0.159×10^6 at 500°F. The corresponding thermal conductivity of air is 0.0212 Btu/hr-ft-F at 400°F and 0.0231 at 500°F. The combined effect on the computed effective thermal conductivity due to operations at the proposed higher temperature level and a higher ΔT than assumed in the FSAR Section M.4.9 can then be estimated via:

$$\frac{k_{effective\,@\,40.8\,kW}}{k_{effective\,@\,24\,kW}} \propto \frac{k_{Air\,at\,500F}}{k_{Air\,at\,400F}} \times \left(\frac{\Delta T_{@\,40.8\,kW}}{\Delta T_{@\,24\,kW}}\right)^{0.333} \times \frac{\left(\frac{gB\rho^2}{\mu^2}\right)^{0.333}_{at\,500F}}{\left(\frac{gB\rho^2}{\mu^2}\right)^{0.333}_{at\,400F}}$$

$$\frac{k_{effective\,@\,40.8\,kW}}{k_{effective\,@\,24\,kW}} \propto \frac{0.0231}{0.0212} \times (1.7)^{0.333} \times \frac{(0.159\times10^6)^{0.333}_{at\,500F}}{(0.258\times10^6)^{0.333}_{at\,400F}}$$

$$\frac{k_{effective\,@\,40.8\,kW}}{k_{effective\,@\,24\,kW}} \propto 1.11$$

Therefore, the effective thermal properties for the neutron shield presented in FSAR Section M.4.9 are conservative for application at the 40.8 kW heat load for both water and air filled cavities. This conclusion was also confirmed via a sensitivity analysis using the CFD model of the neutron shield cavity. SAR Section P.4.2 (17) is revised accordingly.

Question 4-2

Provide additional basis such as confirmatory calculations (using methodologies validated against similar geometries and heat loads) or test results to justify the effective thermal conductivity of air in the HSM for the blocked vent accident analysis.

The correlation used in the SAR to estimate the conductivity employs a simplified model of a cylinder within a cylinder. Validation of this model is necessary due to the significant differences between the correlation and model geometries. NUREG-1536, "Standard Review Plan for Dry Cask Storage Systems" (SRP), Section 4.V states that the staff "should assess models used by the applicant for thermal analysis."

This information is required by the staff to assess the adequacy of the cask system heat removal capacity in compliance with 10 CFR 72.236(f).

Response to 4-2

Because the design of the HSM-H is thermally more efficient than the previous HSM designs and to add conservatism in the blocked vent temperatures, the blocked vent accident analysis has been reanalyzed without credit being taken for convection within the HSM-H cavity. Only conduction in air is considered in this reanalysis. The controlling blocked vent cases corresponding to the 117°F and -40°F ambient conditions were analyzed. The results indicate that for the controlling case (117°F ambient), the HSM-H concrete maximum temperatures are not significantly affected and the DSC shell and HSM-H heat shields temperatures increase.

The ANSYS basket thermal analysis model was also reanalyzed using the revised DSC shell temperature profile with the increased temperatures for the controlling ambient temperature case (117°F).

The results indicate that the basket fuel cladding and components temperatures have increased by a maximum of 50°F. However, a review of these increased temperatures with the accident transfer case shows that the increased temperatures and pressures are bounded by the transfer accident case.

The following SAR sections/figures/tables in Chapter P.4 have been revised to incorporate the revised results: Section P.4.4.5, Section P.4.6.7.1, Section P.4.8, Section P.4.8.4, Table P.4-5, Table P.4-6, Table P.4-25, Table P.4-26, Figure P.4-5, Figure P.4-14, P.4-15, and Figure P.4-17.

There is no change to the structural evaluations of the DSC because the temperatures used in the blocked vent accident structural evaluations bound the revised temperatures. The HSM-H concrete, support steel structure, and heat shield have been evaluated to address the differences in temperature distribution/temperature gradients as appropriate for the affected HSM-H components. Appropriate sections in Chapter P.3 (Table P.3.4-2, and Tables P.3.7-20 thru P.3.7-25) have been revised to incorporate the changes to the HSM-H structural evaluations.

Question 4-3

Clarify the disposition of the fuel for the blower's redundant power supply on the transfer cask skid.

Additional fuel must be accounted for in the fire accident analysis. In addition, SRP Section 4.V.4.a requires staff to verify that the model used in the thermal evaluation is clearly described.

The information is required by the staff to assess compliance with 10 CFR 72.236(f).

Response to 4-3

The total fuel inventory of 300 gallons specified in Section P.11.2.10.1 is the basis for the fire accident evaluations and includes contributions from all fire sources, including the fuel for the redundant blowers. Thus the total fuel inventory remains unchanged.

Question 4-4

Describe how applicable ANSYS Class 3 error reports for Version 6.0 have been addressed regarding the thermal analyses.

For example, two error reports, 2002-9 (edge convection and flux loads) and 2002-11 R1 (film coefficients), describe situations that could lead to significant errors in ANSYS thermal models.

This information is required by the staff to assess compliance with 10 CFR 72.236(f).

Response to 4-4

In accordance with TN QA procedures, all ANSYS class 3 error notices are evaluated and processed. The ANSYS Version 6.0 has been used only for the thermal analysis of the HSM-H. All other thermal evaluations of the 24PTH DSC have been performed with ANSYS Version 7.0.

TN has evaluated the two error reports mentioned above by the Staff for their applicability to the thermal analysis of the 24PTH HSM-H. The following is a brief discussion of the results of this evaluation.

<u>Evaluation of ANSYS Version 6.0 errors on 24PTH analyses</u>

Error Report 2002-9 states that the edge convection and flux loads for SHELL57 and SHELL157 elements are erroneously applied on a per unit area basis, not the unit length, as documented.

The HSM-H thermal analysis model uses SHELL57 elements to model the web of the DSC support rails. The free convection boundary conditions are applied only on one face of these elements. No convection load is applied on the edges on the SHELL57 elements. SHELL57 elements were also used to create the super element MATRIX50 and were unselected prior to solve the model. Therefore, Error 2002-9 does not have any impact on the thermal analysis of the HSM-H model for NUHOMS®-24PTH System.

Error 2002-11 R1 states that when a table array is used to specify temperature-dependent film coefficients on the SURF151 or SURF152 elements, the resulting thermal analysis is incorrect

SURF151 elements are not used in the HSM-H model. SURF152 elements are only used to apply the insolence as a constant heat flux load. Therefore, Error 2002-11 R1 does not have any impact on the thermal analysis of the HSM-H model.

Based on TN's evaluation of ANSYS Error Reports 2002-09 and 2002-11R1, it is concluded that these error reports do not have any impact on the thermal analysis of the 24PTH system.

Question 4-5

Provide details of why component temperatures are bounded as addressed in Table P.4-15, footnote 2, Table P.4-16, footnote 1, and Table P.4-21, footnote 1.

It is not clear from the text and corresponding footnotes why these temperatures are bounded.

This information is required by the staff to assess compliance with 10 CFR 72.236(f).

Response to 4-5

Footnote 2 in SAR Table P.4-15 states that the maximum component temperatures for the normal (T_{amb} = 100°F) transfer conditions are bounded by the off-normal (T_{amb} = 117°F) storage case because the maximum shell temperature for the off-normal storage case is higher (445 °F vs 448 °F, from SAR Table P.4-21).

Footnote 1 in SAR Table P.4-16 has a typographical error. The note has been revised to read: *"Temperatures are bounded by temperatures for HLZC 1 (Table P.4-15)"*. This note is to indicate that the maximum component temperatures for the normal (T_{amb} = 0°F and T_{amb} = 100°F) storage conditions for HLZC 4 (31.2 kW) are bounded by the corresponding normal conditions shown in Table P.4-15 for HLZC with higher DSC heat load of 40.8 kW.

Footnote 1 in SAR Table P.4-21 states that the maximum component temperatures for the off normal T_{amb} = 117°F transfer conditions (for 24PTH basket with aluminum inserts in R45 transition rails) are bounded by the off-normal T_{amb} = 117°F storage conditions, because the maximum shell temperatures for off-normal storage case is higher (444°F vs 448°F). In addition, in footnote 3 an editorial correction to change the word "without" to "with" has been made.

Question 4-6

Correct apparent inconsistencies in Tables P.4-3 and P.4-4.

The titles of these tables state that "Normal and Off-normal" cases are presented. The actual tables only present results for Off-normal cases.

This information is required by the staff to assess compliance with 10 CFR 72.11.

Response to 4-6

A footnote has been added to SAR Tables P.4-3 (Footnote 3) and P.4-4 (Footnote 1) to state that the temperature results shown in this table are for the off-normal condition, which bounds the normal condition temperatures.

Chapter P.5 Shielding Evaluation

Question 5-1

Provide the following information regarding source term estimates:

(a) Specify in Section P.5.2, numerically, the expected error in source term estimates for actinides and fission products important to radiological protection (e.g., Cs-134 and Cm-244), and source term estimates for actinides and fission products important for total decay heat for the high burnup fuels requested in the amendment.

(b) Justify why high burnup source term uncertainties are not applied in the new shielding and thermal analyses.

This amendment requests a significant increase in radiological and thermal source terms. Calculation uncertainties in the source term methodology may now have a greater impact on doses and cask temperatures, with respect to radiological and thermal safety margins present in the currently approved design. A sensitivity analysis may be a method to illustrate the effect of uncertainties on radiological and thermal safety margins.

This information regarding the source term and shielding analysis is needed to determine compliance with 10 CFR 72.236(d) and (f).

Response to 5-1

(a) As stated in Section P.5.2 of the SAR there is no data currently available for fuels with burnups greater than ≈ 47 GWd/MTU and up to 62 GWd/MTU. However, the expected uncertainty in the neutron source is provided as ± 11% based on measured data comparisons for Cm-244 to SAS2H predictions using the 44-group ENDF/BV data for burnups up to 46,460 MWd/MTU. The SAR text in Section P.5.2 also provides justification for using the Cm-244 isotope as it accounts for more than 94% (See the correction provided in response to RAI 5-3) of the neutron source predicted by the SAS2H calculation. In addition, TN also reviewed the results from SAS2H predictions versus measurements documented in NUREG/CR-6798 "Isotopic Analysis of High-Burnup PWR Spent Fuel Samples From the Takahama-3 Reactor" for burnups of 47,030 and 47,250 MWd/MTU. While the methodology used to perform the depletion calculations using SAS2H were different than those used for the "generic" depletion analysis to support the SAR amendment, again the results are also well within the ± 11% range. Section P.5.2 also provides discussion concerning the relative importance of the neutron dose on total dose rates, occupational and public exposures demonstrating that the neutron component has a relatively insignificant effect on these doses.

SAR Section P.5.2 is revised to clarify that the ± 11% is the estimated uncertainty in the neutron source term and resulting dose rates.

For the gamma source term, Section P.5.2 is revised to provide an estimated uncertainty of ± 5% for the gamma source and resulting dose rates and the basis. NUREG/CR-6798 also draws the following conclusion based on its comparison of the Takahama-3 data to predictions made using SAS2H: "The analysis results for the standard fuel (4.11 wt%

enrichment rods SF95 and SF97 indicate extremely good agreement with the code predictions ..."). As noted above, the methodology used for fuel pins burned to just over 47,000 MWd/MTU is different than the methodology used to generate the "generic" source term analysis for the SAR amendment. However, once again the codes show good agreement with the measured values. As stated in Section P.5.2 the gamma source term increases linearly with Burnup and there is no reason to suspect that this is not the case at the higher burnups. Therefore the estimated uncertainty of ± 5% is reasonable for the higher burnup cases also. The decay heat predictions are proportional to the gamma source terms, therefore, the uncertainty and conclusions for the gamma source is also applicable to the decay heat source terms.

(b) Based on the discussions above, the uncertainty in the neutron, gamma and thermal source terms are similar to those for fuels with burnups less than <45,000 MWd/MTU. In addition, as documented in TN's response to RAI # 5.2 for Amendment # 5 to COC 1004, TAC No. L23343, dated February 2002, the codes and methodologies used to calculate the dose rates on and around the NUHOMS® system are conservative when compared to the actual measured values. Therefore, no additional conservatism is required. Finally, the Technical Specifications (1.2.11b/1.2.11c and 1.2.7c/1.2.7d) require that the dose rate measurements be performed on and around the transfer cask and HSM during and following loading operations to verify that specified dose limits are met. If at anytime, these specified dose limits are exceeded an evaluation has to be performed to determine the reasons, and any effect on public exposure prior to proceeding with fuel loading operations.

Question 5-2

Demonstrate that gamma doses from energies above 3.0 MeV are insignificant for cooling times less than 5 years.

This information regarding the source term and shielding analysis is needed to determine compliance with 10 CFR 72.236(d).

Response to 5-2

Using the response functions provided in the SAR Table P.5-17 and P.5-18 for the TC and HSM respectively and the design basis source terms provided in the SAR Table P.5-10 and P.5-11, the following table is generated to show the fraction of the total dose from each gamma energy group for the design basis 3 year cooled fuels at two different burnups and enrichments. As shown in the evaluation, the contribution from energies above 3.0 MeV is less than 1.5% of the total contribution from all the energies. Considering the control components and end fittings this contribution is even less. These results are similar for the other Burnup/initial enrichment combinations shown in the fuel qualification tables with cooling times less than 5 years.

41GWd/MTU, 3.3 wt. % U-235, 3 year cooled

CASK-81 Energy Group	E_{upper} (MeV)	E_{mean} (MeV)	Source from Table P.5-10 (g/s/asbly)	TC Response Function from Table P.5-17	Response Function "Dose Rate"	Relative Contribution to total dose rate	HSM-H Response Function from Table P.5-18	Response Function "Dose Rate"	Relative Contribution to total dose rate
23	10	9	2.227E+05	4.91E-11	1.09E-05	0.000	3.06E-11	6.815E-06	0.000
24	8	7.25	1.049E+06	6.06E-11	6.36E-05	0.000	2.10E-11	2.203E-05	0.000
25	6.5	5.75	5.346E+06	6.43E-11	3.44E-04	0.000	1.18E-11	6.308E-05	0.000
26	5	4.5	1.332E+07	6.07E-11	8.09E-04	0.000	5.49E-12	7.313E-05	0.000
27	4	3.5	4.290E+10	5.05E-11	2.17E+00	0.002	2.18E-12	9.352E-02	0.013
28	3	2.75	3.473E+11	3.50E-11	1.22E+01	0.012	6.95E-13	2.414E-01	0.033
29	2.5	2.25	1.371E+13	2.12E-11	2.91E+02	0.297	2.44E-13	3.345E+00	0.456
30	2	1.83	4.527E+12	9.89E-12	4.48E+01	0.046	6.86E-14	3.106E-01	0.042
31	1.66	1.495	1.033E+14	3.69E-12	3.81E+02	0.390	1.85E-14	1.911E+00	0.260
32	1.33	1.165	3.130E+14	6.78E-13	2.12E+02	0.217	3.24E-15	1.014E+00	0.138
33	1	0.9	6.585E+14	4.54E-14	2.99E+01	0.031	3.67E-16	2.417E-01	0.033
34	0.8	0.7	3.430E+15	1.19E-15	4.08E+00	0.004	5.15E-17	1.766E-01	0.024
35	0.6	0.5	1.722E+15	1.39E-17	2.39E-02	0.000	3.69E-18	6.354E-03	0.001
36	0.4	0.35	1.713E+14	3.14E-18	5.38E-04	0.000	6.69E-20	1.146E-05	0.000
37	0.3	0.25	2.281E+14	9.11E-22	2.08E-07	0.000	3.16E-21	7.208E-07	0.000
38	0.2	0.15	8.340E+14	8.85E-30	7.38E-15	0.000	2.67E-23	2.227E-08	0.000
39	0.1	0.075	9.470E+14	8.27E-41	7.83E-26	0.000	1.32E-34	1.250E-19	0.000
40	0.05	0.025	4.275E+15	0.00E+00	0.00E+00	0.000	0.00E+00	0.000E+00	0.000
			1.270E+16	3.557E-10	9.771E+02	1.000	7.210E-11	7.341E+00	1.000

32GWd/MTU, 2.6 wt. % U-235, 3 year cooled

CASK-81 Energy Group	E_{upper} (MeV)	E_{mean} (MeV)	Source from Table P.5-11 (g/s/asbly)	TC Response Function from Table P.5-17	Response Function "Dose Rate"	Relative Contribution to total dose rate	HSM-H Response Function from Table P.5-18	Response Function "Dose Rate"	Relative Contribution to total dose rate
23	10	9	1.206E+05	4.91E-11	5.92E-06	0.000	3.06E-11	3.690E-06	0.000
24	8	7.25	5.681E+05	6.06E-11	3.44E-05	0.000	2.10E-11	1.193E-05	0.000
25	6.5	5.75	2.900E+06	6.43E-11	1.86E-04	0.000	1.18E-11	3.422E-05	0.000
26	5	4.5	7.220E+06	6.07E-11	4.38E-04	0.000	5.49E-12	3.964E-05	0.000
27	4	3.5	3.370E+10	5.05E-11	1.70E+00	0.002	2.18E-12	7.347E-02	0.013
28	3	2.75	2.730E+11	3.50E-11	9.56E+00	0.013	6.95E-13	1.897E-01	0.033
29	2.5	2.25	1.070E+13	2.12E-11	2.27E+02	0.299	2.44E-13	2.611E+00	0.458
30	2	1.83	3.550E+12	9.89E-12	3.51E+01	0.046	6.86E-14	2.435E-01	0.043
31	1.66	1.495	7.970E+13	3.69E-12	2.94E+02	0.388	1.85E-14	1.474E+00	0.259
32	1.33	1.165	2.480E+14	6.78E-13	1.68E+02	0.222	3.24E-15	8.035E-01	0.141
33	1	0.9	4.490E+14	4.54E-14	2.04E+01	0.027	3.67E-16	1.648E-01	0.029
34	0.8	0.7	2.530E+15	1.19E-15	3.01E+00	0.004	5.15E-17	1.303E-01	0.023
35	0.6	0.5	1.220E+15	1.39E-17	1.70E-02	0.000	3.69E-18	4.502E-03	0.001
36	0.4	0.35	1.340E+14	3.14E-18	4.21E-04	0.000	6.69E-20	8.965E-06	0.000
37	0.3	0.25	1.770E+14	9.11E-22	1.61E-07	0.000	3.16E-21	5.593E-07	0.000
38	0.2	0.15	6.460E+14	8.85E-30	5.72E-15	0.000	2.67E-23	1.725E-08	0.000
39	0.1	0.075	7.360E+14	8.27E-41	6.09E-26	0.000	1.32E-34	9.715E-20	0.000
40	0.05	0.025	3.320E+15	0.00E+00	0.00E+00	0.000	0.00E+00	0.000E+00	0.000
			9.554E+15	3.557E-10	7.589E+02	1.000	7.210E-11	5.695E+00	1.000

Question 5-3

Provide the following information regarding the neutron source spectrum used in the shielding analysis:

(a) Confirm that ^{244}Cm accounts for the majority of the total neutron source for the new high burnup fuel, and for the fuel with cooling times less than 5 years.

(b) Clarify if there are any additional uncertainties in the neutron source spectrum with respect to the source term evaluation for fuel cooled less than 5 years.

This information regarding the source term and shielding analysis is needed to determine compliance with 10 CFR 72.236(d).

Response to 5-3

(a) TN reviewed a sampling of the output files with high burnups and a range of burnups with short (<5 year) cooling times and confirmed that ^{244}Cm account for the vast majority of the neutron source for all cases. By way of example the breakdown of the neutron source for the three Design Basis fuel source terms given in Tables P.5-9, P.5-10 and P.5-11 is provided below. As demonstrated in the Table below, ^{244}Cm contributes well over 90% of the total neutron source for all cases.

Description	62 GWd/MTU, 3.4 wt. % U-235 and 5.6 year cooled (Table P.5-9)	41 GWd/MTU, 3.3 wt. % U-235 and 3 year cooled (Table P.5-10)	32 GWd/MTU, 2.6 wt. % U-235 and 3 year cooled (Table P.5-11)
Total Neutron Source (n/s/assembly)	1.67E+09	3.87E+08	2.10E+08
Source from Cm-244	1.57E+09	3.72E+08	2.02E+08
% Cm-244	94	96	96

TN has corrected the typo in Section P.5.2 that stated that ~ 98% of the neutrons are from Cm-244. The 98% should have been 94%.

(b) As demonstrated above more than 94% of the neutron source is from the 244Cm for fuels with short cooling times (3 years) as well as long cooling times (>5 years), therefore no additional uncertainty is required for the shorter cooling times. In addition, as noted in response to RAI 5-1, the neutron source has a minor effect on occupational and public exposures.

Chapter P.10 Radiation Protection

Question 10-1

Clarify whether the evaluation of off-site dose estimates includes the contribution from bounding non-fuel hardware. If not, revise Section P.10 to specify how a general licensee

should incorporate non-fuel hardware contributions into its site-specific evaluations under 10 CFR 72.21 2.

This information regarding the source term and shielding analysis is needed to determine compliance with 10 CFR 72.236(d).

Response to 10-1

The off-site dose estimates provided in Section P.10 incorporate the contribution from the bounding non-fuel hardware as the surface dose rates used for the analysis include the contribution from the control components (CCs or non-fuel hardware). The HSM surface dose rates are taken from Tables P.5-1 and P.5-2. These tables report the average surface dose rate for the HSM-H with its design-basis fuel plus design-basis CCs for the NUHOMS®-24PTH-L and HSM Model 102 with its design-basis fuel plus design-basis CCs for the NUHOMS®-24PTH-S-LC, respectively.

The first and second paragraphs of Section P.10.2 are revised to explicitly state that the contributions from the design-basis control components (CCs or non-fuel hardware) are included in the site dose source terms.

TN has discovered an oversight in the surface average HSM-H dose rates reported in Section P.5. The MCNP tally for the surface average calculation inadvertently did not cover the vents. Therefore, the surface average dose rate did not include the contribution from the vents. Tables P.5-1 and P.5-2 have been corrected and the site dose calculations for the HSM-H have been revised to incorporate the contribution from the vents in the results (See Tables P.10-2, P.10-6, P.10-8, P.10-9, P.10-10, and Figure P.10-1).

Chapter P.12 Technical Specifications

Question 12-1

Technical Specification 1.2.16 states that: "The determination of horizontal acceleration acting at the center of gravity (CG) of the loaded TC must be based on a peak horizontal ground acceleration at the site, but shall not exceed 0.25g." Chapter P.2, Section P.2.2.3 Seismic Design, stated that: "The seismic design criteria for the HSM-H is consistent with the criteria set forth in Section 3.2.3, with the exception that the NRC Regulatory Guide 1.60 response spectra is anchored to a maximum ground acceleration of 0.30g (instead of 0.25g) for the horizontal components..." Provide the basis for the different seismic design criteria used for the design of HSM-H system and the TC.

This information is required by the staff to assess compliance with 10 CFR 72.236(b).

Response to 12-1

The HSM-H design is more robust seismically and was evaluated to the seismic criteria stated in Section P.2.2.3 (0.3g horizontal and 0.2g vertical seismic accelerations). However, the Technical Specifications limits of 0.25g horizontal and 0.17g vertical in Section 1.1.1 (3), page A-2 are still applicable to the 24PTH system, including the HSM-H.

Question 12-2

Clarify the meaning of the term "cask" in Tech Spec 1.2.16, under "Action." Does the term "cask" mean a loaded TC? Explain the significance of the "cask weight." What will happen if the cask weight is less than 190 kips?

This information is required by the staff to assess compliance with 10 CFR 72.236(b).

Response to 12-2

The term "cask" means a loaded TC containing a DSC with fuel assemblies. The sentence: *"... and determine if the cask weight is less than 190 kips."* has been deleted from the proposed TS.

ATTACHMENT

LS-DYNA USER'S MANUAL INSTRUCTIONS FOR MATERIAL TYPE 4

*MAT_ELASTIC_PLASTIC_THERMAL

This is Material Type 4. Temperature dependent material coefficients can be defined. A maximum of eight temperatures with the corresponding data can be defined. A minimum of two points is needed. When this material type is used it is neccessary to define nodal temperatures by activating a coupled analysis or by using another option to define the temperatures such as *LOAD_THERMAL_LOAD_CURVE, or *LOAD_THERMAL_VARIABLE.

Card Format

Card 1

	1	2	3	4	5	6	7	8
Variable	MID	RO						
Type	I	F						

Card 2

Variable	T1	T2	T3	T4	T5	T6	T7	T8
Type	F	F	F	F	F	F	F	F

Card 3

Variable	E1	E2	E3	E4	E5	E6	E7	E8
Type	F	F	F	F	F	F	F	F

Card 4

Variable	PR1	PR2	PR3	PR4	PR5	PR6	PR7	PR8
Type	F	F	F	F	F	F	F	F

Card Format (no defaults are assumed)

Card 5

Variable	ALPHA1	ALPHA2	ALPHA3	ALPHA4	ALPHA5	ALPHA6	ALPHA7	ALPHA8
Type	F	F	F	F	F	F	F	F

Card 6

	1	2	3	4	5	6	7	8
Variable	SIGY1	SIGY2	SIGY3	SIGY4	SIGY5	SIGY6	SIGY7	SIGY8
Type	F	F	F	F	F	F	F	F

Card 7

Variable	ETAN1	ETAN2	ETAN3	ETAN4	ETAN5	ETAN6	ETAN7	ETAN8
Type	F	F	F	F	F	F	F	F

VARIABLE	DESCRIPTION
MID	Material identification. A unique number must be chosen.
RO	Mass density.
TI	Temperatures. The minimum is 2, the maximum is 8.
EI	Corresponding Young's moduli at temperature TI.
PRI	Corresponding Poisson's ratios.
ALPHAI	Corresponding coefficients of thermal expansion.
SIGYI	Corresponding yield stresses.
ETANI	Corresponding plastic hardening moduli.

Remarks:

At least two temperatures and their corresponding material properties must be defined. The analysis will be terminated if a material temperature falls outside the range defined in the input. If a thermoelastic material is considered, do not define SIGY and ETAN. The coefficient of thermal expansion is defined as the instanteous value. Thus, the thermal strain rate becomes:

$$\dot{\varepsilon}_{ij}^{T} = \alpha \dot{T} \delta_{ij}$$

*MAT_SOIL_AND_FOAM

This is Material Type 5. This is a very simple model and works in some ways like a fluid. It should be used only in situations when soils and foams are confined within a structure or when geometric boundaries are present.

Card Format

Card 1

	1	2	3	4	5	6	7	8
Variable	MID	RO	G	BULK	A0	A1	A2	PC
Type	I	F	F	F	F	F	F	F

Card 2

Variable	VCR	REF						
Type	F	F						

Card 3

Variable	EPS1	EPS2	EPS3	EPS4	EPS5	EPS6	EPS7	EPS8
Type	F	F	F	F	F	F	F	F

Card 4

Variable	EPS9	EPS10						
Type	F	F						